Department for Environment Food & Rural Affairs

Department for Energy Security & Net Zero

Department for Science, Innovation, & Technology

Met Office Hadley Centre

Environment Agency

Augmenting UKCP Local (2.2km) projections by down-scaling global models from CMIP5

November 2024

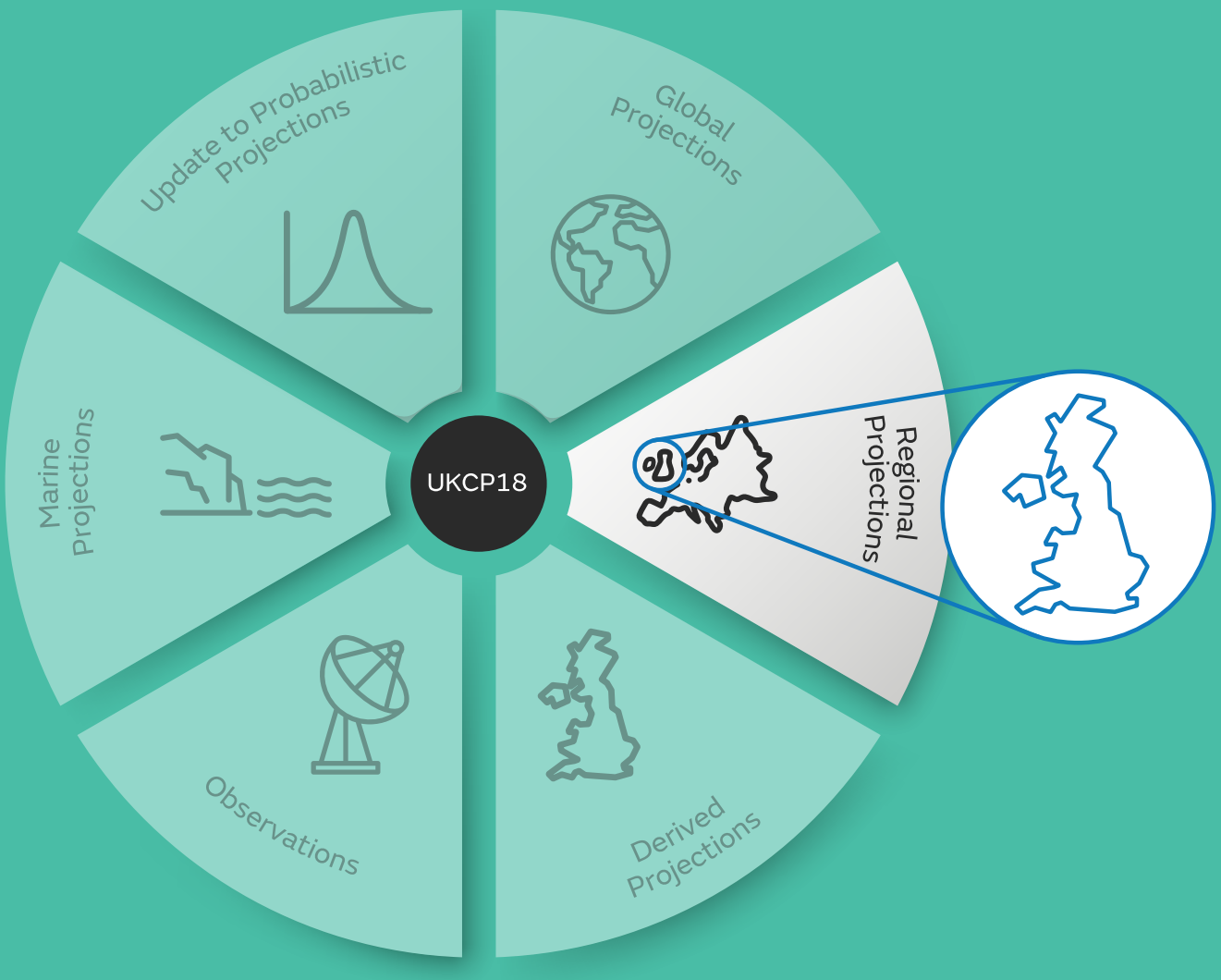

Chris Short and Lizzie Kendon

Version 1.0

Executive summary

This report describes a new addition to the set of UKCP Local climate projections included in UKCP18. UKCP Local consists of an ensemble of 12 "convection-permitting" simulations over a region covering the UK (the model grid length is 2.2 km over the UK), run for five consecutive 20-year time periods spanning 1980 – 2080 (Kendon et al. 2021, 2023b) under a high emissions scenario (RCP8.5; Moss et al. 2010). This rich dataset is particularly useful for examining how changes in extreme weather manifest through time, at fine spatial and temporal scales (e.g. Kendon et al. 2023a).

Boundary conditions for each member of the 2.2 km convection-permitting model (CPM) ensemble are provided by a member of a regional climate model (RCM) ensemble that covers Europe (with a grid length of 12 km), in turn nested inside a member of a global climate model (GCM) ensemble. The global ensemble is based on the Met Office Hadley Centre climate model, with different members created by applying perturbations to parameters in the numerical schemes used in the model to represent key physical processes (e.g. atmospheric convection). The RCM ensemble is known as UKCP Regional and the GCM ensemble forms one component of UKCP Global, along with 13 other GCMs selected from the fifth phase of the Coupled Model Intercomparison Project (CMIP5; Taylor et al. 2012), referred to as the CMIP5-13 (Murphy et al. 2018).

A key limitation of UKCP Local is that a single GCM provides the boundary conditions for the CPM (via the RCM). Future projections for the UK from the Met Office global model can be notably different to those from other international GCMs. For example, the Met Office model typically projects a greater future increase in temperature and decrease in precipitation in summer compared to the other CMIP5-13 GCMs. Given that the CPM has no access to information from these alternative global models, the UKCP Local projections will sample a narrower uncertainty range than other UKCP18 products (such as UKCP Probabilistic and UKCP Global).

Here we take a first step towards expanding the range of future outcomes sampled by UKCP Local by nesting the CPM (via the RCM) inside four different GCMs selected from CMIP5, referred to as the CMIP5-4. The CMIP5-4 models are ACCESS1-3, MPI-ESM-LR, MRI-CGCM3 and IPSL-CM5A-MR[1], chosen based on their ability to represent key features of the climate of the North Atlantic-European region and the diversity of their future projections for the UK, especially in summer.

A new set of UKCP Local and UKCP Regional projections with boundary conditions provided by the CMIP5-4 models have been produced for the same five consecutive 20-year time periods as before, again under RCP8.5. For consistency with the existing projections, the configurations of the RCM and CPM have been kept as similar as possible to those used previously (Murphy et al. 2018, Kendon et al. 2021). The only notable difference is the treatment of aerosols, although this is likely to have less of an impact for the UK compared to central Europe, for example.

[1] ACCESS1-3, MRI-CGCM3 and IPSL-CM5A-MR are all in the CMIP5-13 included in UKCP Global. We did intend to down-scale MPI-ESM-MR, which is also in the CMIP5-13, but the necessary driving data was not available at the time, so we opted to use the MPI-ESM-LR model instead. This is not in the CMIP5-13, but it does perform very similarly to the MR version (McSweeney et al. 2018).

Present-day performance of the CMIP5-driven regional models

- A requirement for successful down-scaling is that a regional model does not deviate too much from its driving model (i.e. the model providing boundary conditions) on large scales. Using a representative set of weather patterns for the UK and surrounding European area, we have checked how well the large-scale circulation of each CMIP5-4 GCM is preserved by its nested RCM. There is a very good correspondence in the day-to-day sequence of weather patterns in winter (more than 80% of days match), with less of an agreement in summer (at least 60% of days match), which is expected since the large-scale flow is weaker in this season. Overall, we are satisfied that the RCM simulations are adequately constrained by their boundary conditions, despite the large pan-European domain. Large-scale consistency between the CPMs and their driving RCMs has not been examined as this step is no different from that in existing UKCP Local simulations.
- The ability of the new CMIP5-driven CPM (and RCM) simulations to reproduce key aspects of the present-day climate has been assessed using observational data, focussing on temperature and precipitation across a range of timescales (soil moisture and snow have also been briefly considered). The main result is that biases in the regional models driven by CMIP5-4 GCMs are mostly comparable to those in the existing UKCP Local and UKCP Regional simulations (Figure 1), and thus their projections are considered equally as plausible. However, there are a few cases where the CMIP5-driven regional models have considerably larger biases than found in the UKCP18 regional ensembles, with implications for the reliability of their projections. These are as follows:
    - In winter, the CPM and RCM driven by MRI-CGCM3 significantly over-estimate precipitation across the UK (especially the RCM), with large biases generated by the down-scaling step itself. Future changes in winter precipitation from these models are thus considered unreliable.
    - Excessive winter precipitation in the MRI-CGCM3-driven models contributes to more snow on the ground in Scotland than in any other model. Consistent with this, there are significant cold biases in winter mean temperatures and the temperature of cold winter days in Scotland, although there are some members of the existing UKCP18 regional ensembles with similarly large biases. The CPM driven by MRI-CGCM3 over-estimates the number of cold spells too. On balance we advise caution if using projections for winter temperatures from the MRI-CGCM3-driven models for Scotland as we have lower confidence in them.
    - The regional models driven by IPSL-CM5A-MR also have some significant wet biases in winter precipitation, especially over England. However, these biases are largely inherited from the IPSL-CM5A-MR GCM itself, which has already been included in UKCP Global as part of the CMIP5-13. We recommend caution if using winter precipitation projections from the CPM and RCM driven by IPSL-CM5A-MR as we have less confidence in them.
    - In summer, the regional models driven by MPI-ESM-LR significantly over-estimate precipitation across the UK, and these biases are generated by the down-scaling step. Future changes in summer precipitation from these models are thus considered unreliable.

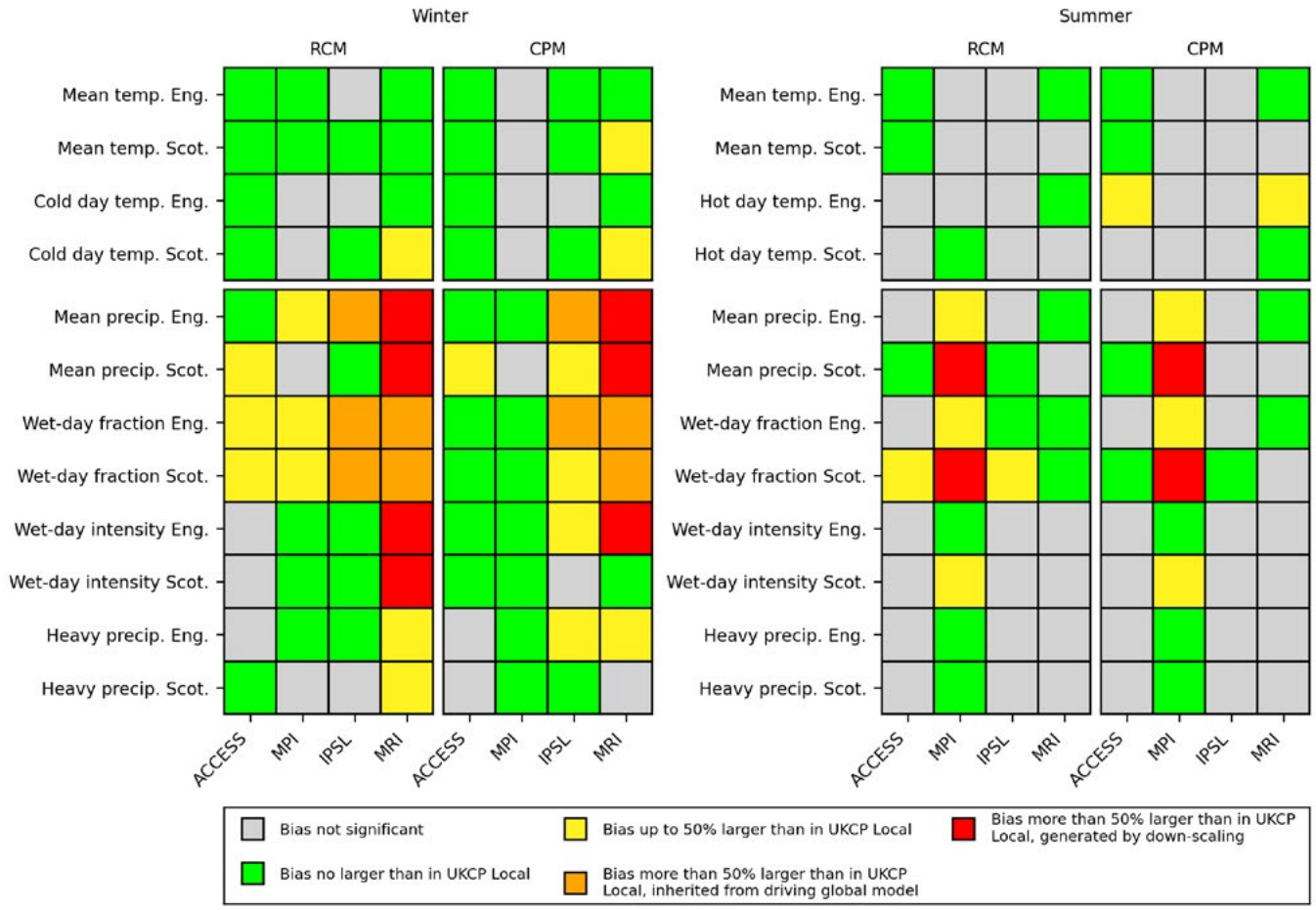

Figure 1. Summary of present-day biases in the CMIP5-driven regional models in winter (left panels) and summer (right panels), for a selection of regionally averaged temperature and precipitation metrics.

Climate change projections from the CMIP5-driven regional models

- The fully transient nature of both the new and existing UKCP Local and UKCP Regional simulations allows future changes to be defined using a specific level of global warming, instead of a fixed future period as was done in previous UKCP Local reports (Kendon et al. 2019, 2021, 2023b). Here a global warming level of 3ºC above pre-industrial is adopted. This way of framing projections is somewhat independent of emissions scenario and climate sensitivity (the equilibrium response to a doubling of CO_2), relevant here because the Met Office Hadley Centre global model has a considerably higher climate sensitivity than the CMIP5-4 GCMs chosen for down-scaling.

- Future changes in precipitation and temperature in the CMIP5-driven regional models largely follow those in their parent GCMs, with differences between the responses of parent and nested models being comparable to those between members of the existing UKCP18 ensembles. This suggests the down-scaling of alternative GCMs is behaving as desired, allowing us to sample different regions of the space of possible future changes with the UKCP18 regional models. There are several noteworthy future outcomes from the new CMIP5-driven regional model projections (Figure 2), which we believe are plausible, based on our assessment of present-day biases:

    - In summer, the regional models driven by IPSL-CM5A-MR and MRI-CGCM3 project less of a future increase in temperature than any member of the existing UKCP Local and UKCP Regional ensembles, across the UK. The models driven by ACCESS1-3 and MPI-ESM-LR also offer low-end outcomes with responses lying close to the lower bound of the range of responses from the UKCP18 ensembles.

- The MRI-CGCM3-driven models also project little future change in summer mean precipitation across the UK – as do the IPSL-CM5A-MR-driven models over Scotland - whereas the existing UKCP18 regional ensembles favour a substantial future decrease.

- In winter, future increases in precipitation over England (especially in the south) are considerably larger in the ACCESS1-3-driven models than in any member of the existing UKCP Local and UKCP Regional ensembles. Increases can be ~50% locally. Such an outcome would have impactful consequences in terms of river flows and flood risk. The CPM driven by ACCESS1-3 also projects a greater future intensification of hourly precipitation extremes in winter than any member of UKCP Local.

- At the other end of the scale, the regional models driven by MPI-ESM-LR project a decrease in winter mean precipitation over Scotland whereas most UKCP18 regional ensemble members project future increases.

- Future increases in winter mean temperature and the temperature of cold winter days in the models driven by ACCESS1-3, MPI-ESM-LR and IPSL-CM5A-MR are also smaller than in most members of the existing UKCP Local and UKCP Regional ensembles, offering new low-end outcomes in some cases.

- The range of future changes in UK-average winter and summer mean temperature and precipitation from the original and new augmented UKCP Regional and UKCP Local ensembles are compared in Tables 1 and 2.

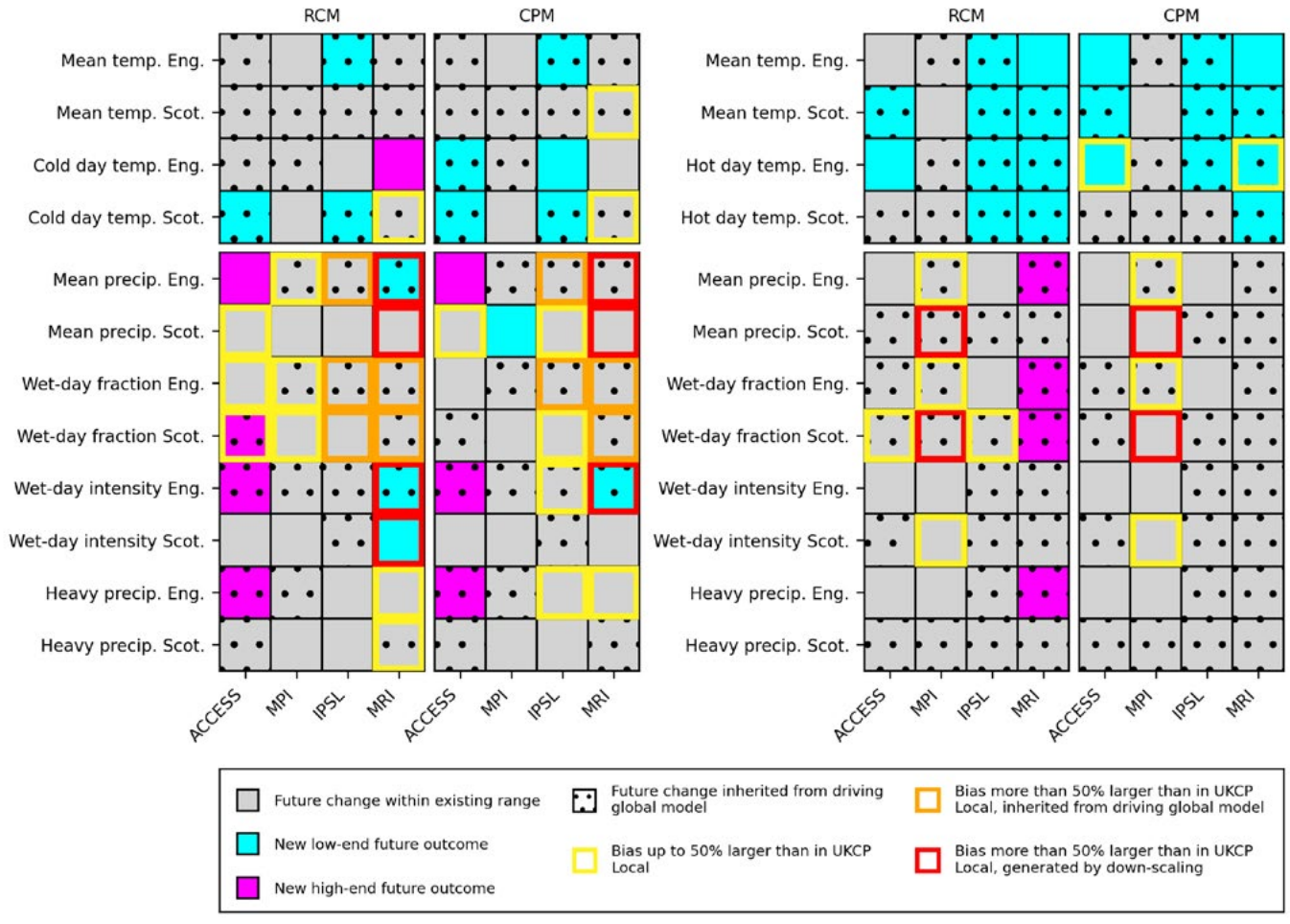

Figure 2. Summary of future changes in regionally averaged temperature and precipitation metrics from the CMIP5-driven regional models, for winter (left panels) and summer (right panels). Future changes are defined as differences between a 21-year future period, centred on the year when the global mean surface temperature reaches 3ºC above pre-industrial, and the baseline period (1980 – 2000).

	UKCP Regional	Augmented UKCP Regional
Winter mean temperature [ºC]	1.1, 2.0, 2.4	1.0, 1.7, 2.4
Summer mean temperature [ºC]	2.5, 2.8, 3.2	2.0, 2.7, 3.2
Winter mean precipitation [%]	0.9, 5.5, 13.2	-3.0, 5.1, 14.9
Summer mean precipitation [%]	-26.5, -13.6, -7.6	-26.5, -13.6, 0.5

Table 1. Comparison of future changes in UK-average winter and summer mean temperature and precipitation in the original UKCP Regional ensemble (12 members) and the augmented UKCP Regional ensemble with four additional members driven by CMIP5 GCMs (16 members in total). Future changes are defined as differences between a 21-year future period, centred on the year when the global mean surface temperature reaches 3ºC above pre-industrial, and the baseline period (1980 – 2000). For each variable low, central and high estimates are presented, corresponding to the second lowest, median and second highest response across the ensemble.

	UKCP Local	Augmented UKCP Local
Winter mean temperature [ºC]	1.2, 2.1, 2.5	1.1, 1.8, 2.5
Summer mean temperature [ºC]	2.5, 2.8, 3.2	1.9, 2.6, 3.2
Winter mean precipitation [%]	4.7, 13.9, 19.2	3.6, 11.9, 19.2
Summer mean precipitation [%]	-29.6, -13.9, -4.2	-29.6, -13.9, -3.2

Table 2. Same as Table 1 but for UKCP Local.

In summary, we have demonstrated that it is possible to successfully down-scale other international GCMs from CMIP5 with the UKCP18 CPM and RCM, providing an effective means of sampling a wider range of potential future outcomes for the UK. Augmenting UKCP Local with the new CMIP5-driven projections (giving a total of 16 simulations) promises to be particularly useful for assessments of future risks relating to changes in extreme weather at local and hourly timescales.

Using CMIP5 GCMs to drive the UKCP18 CPM (via the RCM) represents an important step forward in capability. However, it should be emphasised that, even with the new additions, the UKCP Local projections will still under-estimate uncertainties in future changes, for several reasons. First, the number of alternative GCMs we have been able to down-scale is small. Second, as in the original UKCP Local projections, uncertainty in the representation of physical processes within the CPM itself is not accounted for. Third, projections have been produced for a single emissions scenario (RCP8.5) only. Finally, no information from other CPM simulations covering the UK has been included. These are all avenues that could potentially be explored in any future update of, or addition to, UKCP Local. Therefore, we re-iterate the recommendation that, where possible, UKCP Local should be used in conjunction with other products from UKCP18 that provide a more comprehensive sampling of uncertainties (such as UKCP Probabilistic, UKCP Global and UKCP Regional).

1 Introduction

One component of the UKCP18 national climate projections is UKCP Local, an ensemble of 12 simulations at 2.2 km grid spacing over the UK. These simulations are termed “convection-permitting” because the resolution is high enough for convective storms to be (partially) resolved by the model. Initially, projections were produced for three timeslices (1980-2000, 2020-2040 and 2060-2080), released in September 2019 (Kendon at al. 2019, Kendon et al. 2021), with the remaining timeslices (2000-2020 and 2040-2060) run subsequently and released in March 2023 (Kendon et al. 2023b). These can be stitched together to produce the first ensemble of long (100-year) national climate scenarios at a resolution comparable to weather forecast models, allowing us estimate uncertainties in the future changes of local extremes and how changes manifest through time (Kendon et al 2023a). This is valuable information for conducting risk assessments and preparing effective adaptation strategies.

While undoubtedly a significant step forward in capability, the main limitation of UKCP Local is that it is likely to provide an under-estimate of uncertainties in the future changes of extremes, for several reasons. First, projections were produced for a single emissions scenario only, the high emissions scenario RCP8.5 (Moss et al. 2010). Second, each member of the 2.2 km ensemble is one-way nested inside a member of a 12 km pan-European regional model ensemble (UKCP Regional; Murphy et al. 2018), in turn nested inside a member of a 60 km global model ensemble (one component of UKCP Global; Murphy et al. 2018). The global ensemble is based on the Met Office Hadley Centre climate model, HadGEM3-GC305, with different members created by perturbing uncertain parameters in the model physics schemes. It was not possible to apply the same perturbations in the convection-permitting model (CPM) because it uses a different set of parametrisation schemes to the global model (note that the 12 km model is just a high-resolution version of the global model run over a limited area so the same parameter perturbations could be applied in this model). Therefore, the CPM ensemble samples uncertainty in the driving model physics and uncertainty in the large-scale forcing (i.e. natural variability) via its boundary conditions, but it does not sample uncertainty in the representation of physical processes within the 2.2 km model itself. Third, by down-scaling a perturbed physics ensemble (PPE) based on a single global model, there is no sampling of structural uncertainty (i.e. uncertainty due to different global model architectures including the parametrisation of physical processes) inherent to UKCP Local (or UKCP Regional either). This is an important point since HadGEM3-GC305 has a relatively high climate sensitivity (Andrews et al. 2019), and in some cases future changes are markedly different compared to other international climate models. For example, the majority of ensemble members project larger increases in summer mean temperature, and larger decreases in summer precipitation, over England than the 13 CMIP5 models included in UKCP Global (see Figure 5.1 in Kendon et al. 2021). These future changes are largely preserved upon down-scaling to convective scales, motivating the need to down-scale multiple global models with different structure. Finally, there is no sampling of structural uncertainty in either UKCP Regional or UKCP Local themselves which, in principle, could be addressed by incorporating data from other regional climate simulations that cover the UK from the EURO-CORDEX (Jacob et al. 2014, Barnes et al. 2022), CORDEX-FPS (Coppola et al. 2018) or Horizon 2020 EUCP (Hewitt and Lowe 2018) projects.

In this work we down-scale a selection of other global climate models from CMIP5 with UKCP Local (via UKCP Regional), thus sampling the effects of structural uncertainty in the driving model for the first time. The inclusion of multi-model information within the UKCP18 regional model projections promises to be particularly helpful for assessments of future risks relating to extremes. Note that we make no attempt to incorporate other sources of uncertainty here, including emissions scenario (again, we assume the RCP8.5 emissions pathway), uncertainties in the 2.2 km model physics, and structural uncertainties in the regional models themselves. These are all avenues that could potentially be explored in any future update of, or addition to, UKCP18.

2 Methodology

2.1 Selection of CMIP5 models to down-scale

The global climate projections included in UKCP18 consisted of a 15-member PPE of global climate simulations with the HadGEM3-GC305 model, augmented by 13 models selected from CMIP5 (the CMIP5-13) to add sampling of diversity of model structure. The CMIP5-13 models were selected by using a mixture of quantitative and qualitative assessment criteria to filter out models performing poorly over Europe, whilst simultaneously capturing the widest possible range of future changes (McSweeney et al. 2018).

Of the CMIP5-13 models, not all can be down-scaled with the UKCP18 regional models. Some lack the necessary driving data to make lateral boundary conditions (LBCs), others have a model top that lies below that of the UKCP18 RCM (40 km above sea level). These constraints rule out seven of the CMIP5-13. Of the remaining six, two of them (CanESM2 and HadGEM2-ES) predict similarly large future increases in surface temperature and decreases in precipitation over the UK in summer as HadGEM3-GC305; see the lower left panel of Figure 3. Therefore, we rule out these two models on diversity grounds. This leaves four models: ACCESS1-3, IPSL-CM5A-MR, MPI-ESM-MR and MRI-CGCM3, all of which yield different climate change responses for the UK in summer than HadGEM3-GC305. For example, the IPSL-CM5A-MR model predicts a much smaller temperature increase in summer, and the MRI-CGCM3 model predicts a slight increase in summer precipitation. These four CMIP5 models were thus chosen for down-scaling.

However, data from the MPI-ESM-MR model was not accessible at the time of this work, so we decided to use the MPI-ESM-LR model instead. The LR version is not part of the CMIP5-13 set of models, but it is similar to the MR version, with fewer vertical levels and lower horizontal resolution in the ocean being the key differences. MPI-ESM-LR passes all the performance criteria used to select the CMIP5-13, with similar present-day performance to the MR version (McSweeney et al. 2018), and gives similar projections to MPI-ESM-MR for the UK in all seasons except winter where the LR version predicts considerably more warming (Figure 3). The final set of CMIP5 models chosen for down-scaling in this work is thus:

- ACCESS1-3
- IPSL-CM5A-MR
- MPI-ESM-LR
- MRI-CGCM3

Hereafter we refer to this subset of CMIP5 models as CMIP5-4.

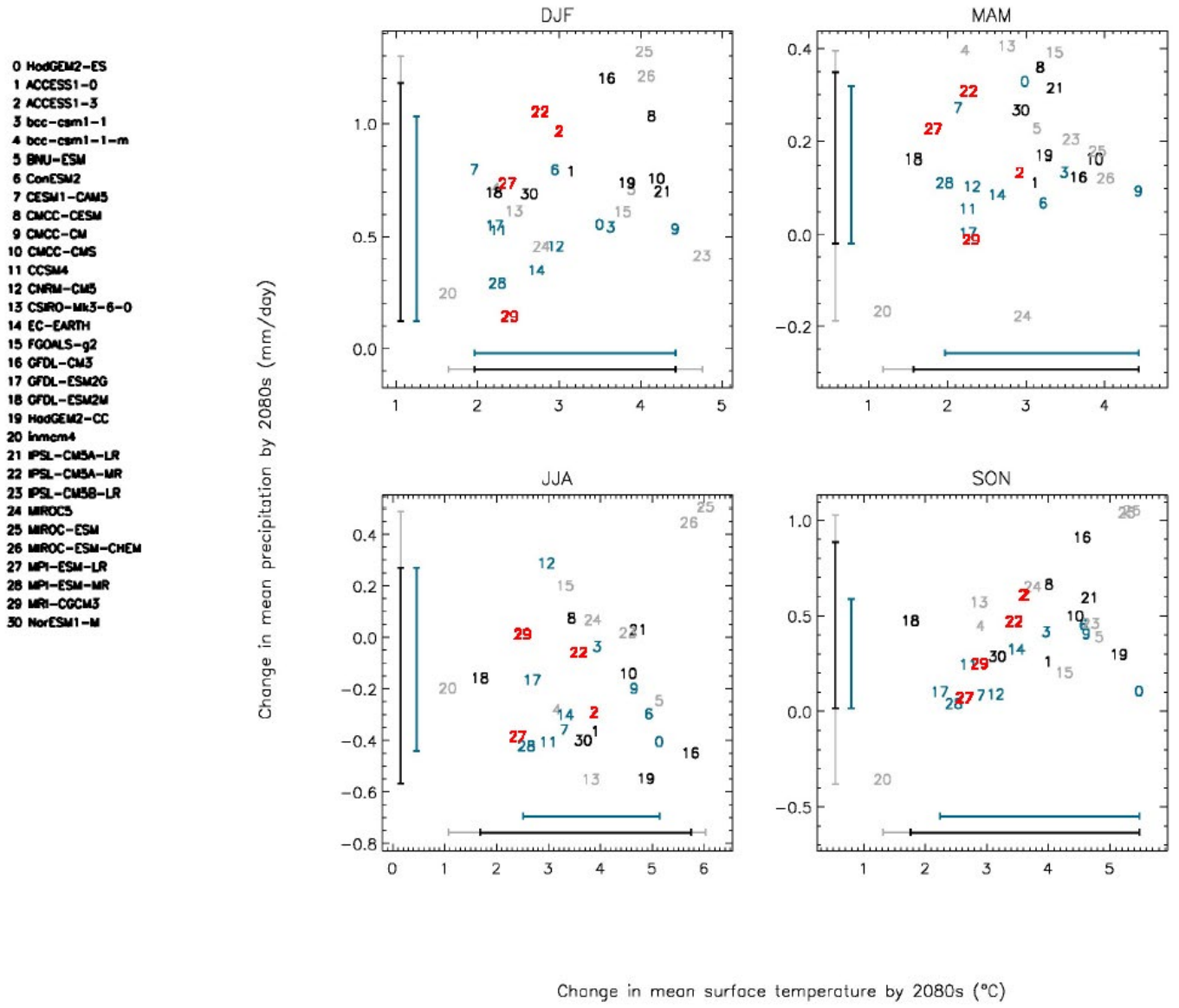

Figure 3. UK-mean future changes in seasonal mean temperature and precipitation under RCP8.5 in CMIP5 global models. Future changes are defined as the difference between fixed future (2070 – 2100) and baseline (1961 – 1990) periods. Models included in the CMIP5-13 subset are shown in blue, with models that were rejected on performance grounds shown in grey, and the four CMIP5 models chosen for down-scaling here are highlighted in red. Reproduced from McSweeney et al. (2018).

2.2 Naming conventions

All the climate models used in this report are listed in Table 3, and abbreviations used to refer to them hereafter are defined.

Model	Abbreviation	Description/notes
HadGEM3-GC305	HadGEM	Global model configuration used in UKCP18.
HadGEM3-GC305 PPE	HadGEM-PPE	15-member perturbed parameter ensemble produced with the HadGEM3-GC305 global model. Only the 12 members down-scaled with regional models in UKCP18 are used here. Model grid length is 60 km. One component of UKCP Global in Murphy et al. (2018).
HadGEM3-GC305 PPE standard member	HadGEM-STD	Single member of the HadGEM3-GC305 PPE with no parameter perturbations applied.
ACCESS1-3	ACCESS	Global models from CMIP5 chosen for down-scaling with UKCP18 regional models. Only a single member is down-scaled here (r1i1p1).
IPSL-CM5A-MR	IPSL	
MPI-ESM-LR	MPI	
MRI-CGCM3	MRI	
HadREM3-GA705	RCM	Regional model configuration used in UKCP18. Science settings match those in HadGEM3-GC305.
HadREM3-GA705 PPE	RCM-PPE	12-member perturbed parameter ensemble produced with the HadREM3-GA705 model. Driven by 12 members of the HadGEM3-GC305 PPE. Model grid length is 12 km. Referred to as UKCP Regional in Murphy et al. (2018).
HadREM3-GA705 PPE standard member	RCM-STD	Single member of the HadREM3-GA705 PPE with no parameter perturbations applied, driven by the standard (unperturbed) member of HadGEM3-GC305 PPE.
HadREM3-GA705 driven by ACCESS1-3	RCM-ACCESS	Standard (unperturbed) member of the HadREM3-GA705 PPE driven by each CMIP5-4 global model.
HadREM3-GA705 driven by IPSL-CM5A-MR	RCM-IPSL	
HadREM3-GA705 driven by MPI-ESM-LR	RCM-MPI	
HadREM3-GA705 driven by MRI-CGCM3	RCM-MRI	
HadREM3-RA11M	CPM	Convection-permitting regional model configuration used in UKCP18.
HadREM3-RA11M PPE	CPM-PPE	12-member ensemble produced with the HadREM3-RA11M model. Driven by 12 members of the HadREM3-GA705 PPE. No parameter perturbations applied in the CPM. Model grid length is 2.2 km. Referred to as UKCP Local in Kendon et al. (2021).
HadREM3-RA11M PPE standard member	CPM-STD	Single member of the HadREM3-RA11M ensemble driven by the standard (unperturbed) member of HadREM3-GA705 PPE.
HadREM3-RA11M driven by ACCESS1-3	CPM-ACCESS	Single member of the HadREM3-RA11M ensemble nested inside the standard (unperturbed) member of the HadREM3-GA705 PPE, driven by each CMIP5-4 global model.
HadREM3-RA11M driven by IPSL-CM5A-MR	CPM-IPSL	
HadREM3-RA11M driven by MPI-ESM-LR	CPM-MPI	
HadREM3-RA11M driven by MRI-CGCM3	CPM-MRI	

Table 3. Summary of all the models used in this report and the abbreviations used to refer to them.

2.3 Key characteristics of the CMIP5-4 global models

The four CMIP5 models chosen for down-scaling span a wide range of resolutions, all substantially coarser than HadGEM3-GC305; see Table 4. It follows that a key difference between the various models will be their representation of orography, illustrated by Figure 4. This is worth bearing in mind when evaluating model performance in the following sections as elevation differences will have an impact on both temperature and precipitation.

Model	Longitudinal grid spacing	Latitudinal grid spacing
MPI	1.875°	1.8°
IPSL	2.5°	1.25°
ACCESS	1.875°	1.25°
MRI	1.125°	1.1°
HadGEM	0.83°	0.56°
RCM	0.11°	0.11°
CPM	0.02°	0.02°

Table 4. Horizontal grid spacings of the various models used in this report, arranged in order of decreasing grid-box area (i.e. increasing resolution).

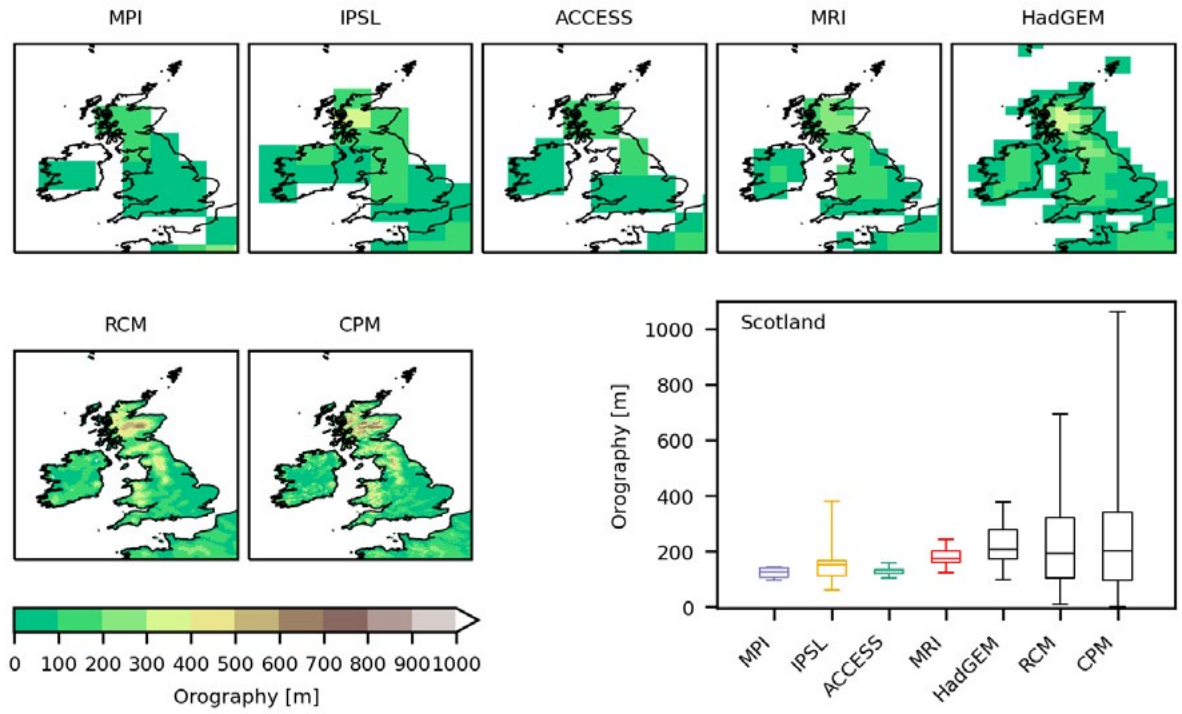

Figure 4. Representation of orography in the models used in this report, on their native spatial grids, for grid-boxes where the land fraction is greater than 50%. Models are ordered by increasing resolution as in Table 4. In the bottom right plot, the distribution of terrain heights in Scotland is shown by the box-and-whiskers: the box extends from the lower to the upper quartiles of the data, with the median shown by the solid horizontal line, and the whiskers show the full range of the data.

A key control on UK climate is the low-level prevailing winds from the west/southwest. Figure 5 shows seasonal mean biases in the 850 hPa circulation in the CMIP5-4 models, along with HadGEM-STD. In winter, the flow in ACCESS is too zonal across the UK, MPI and IPSL shift the region of strongest flow to the south, and MRI has excessively strong flow across the UK, as flagged in McSweeney et al. (2018). In summer, the low-level circulation is weaker, and the models generally perform better. The MPI model still tends to shift the peak flow too far south, but the significant biases seen in IPSL and MRI in winter are no longer evident.

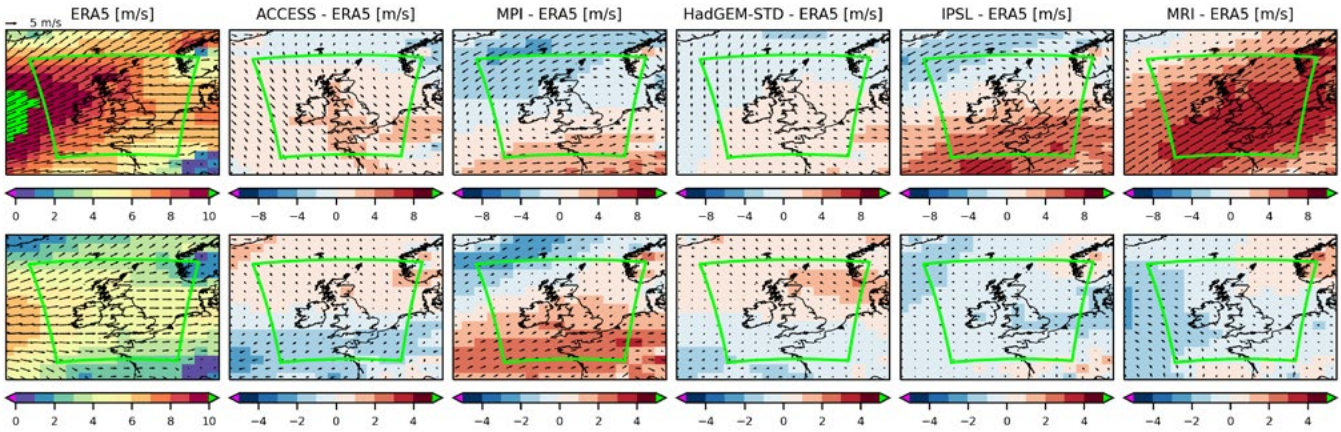

Figure 5. Seasonal mean biases in 850 hPa winds in the CMIP5-4 and HadGEM-STD global models, relative to ERA5 reanalysis (Hersbach et al. 2020), for the baseline period (1980 – 2000). The top row is for winter and the bottom row is for summer. All data has been regridded onto a common n96 grid with spacings of 1.875º and 1.25º in the longitudinal and latitudinal directions, respectively. The boundary of the CPM domain is shown for reference (green line).

Aside from circulation, another important influence on UK climate is local sea surface temperatures (SSTs; e.g. Fereday and Knight 2023). Figure 6 shows seasonal mean SST biases in the CMIP5-4 models, along with HadGEM-STD. The latter has the smallest overall SST biases, because flux adjustments are applied to the ocean surface layer in this model (Yamazaki et al. 2021). The ACCESS and MPI models tend to have a warm bias in SSTs around the UK, especially in winter, whereas IPSL and MRI display a cool bias, particularly the MRI model in winter (SST biases in these models were flagged in McSweeney et al. 2018). It is important to remember that the global model SST patterns in Figure 6 will be inherited by nested regional models since daily mean SSTs are prescribed as a lower boundary condition.

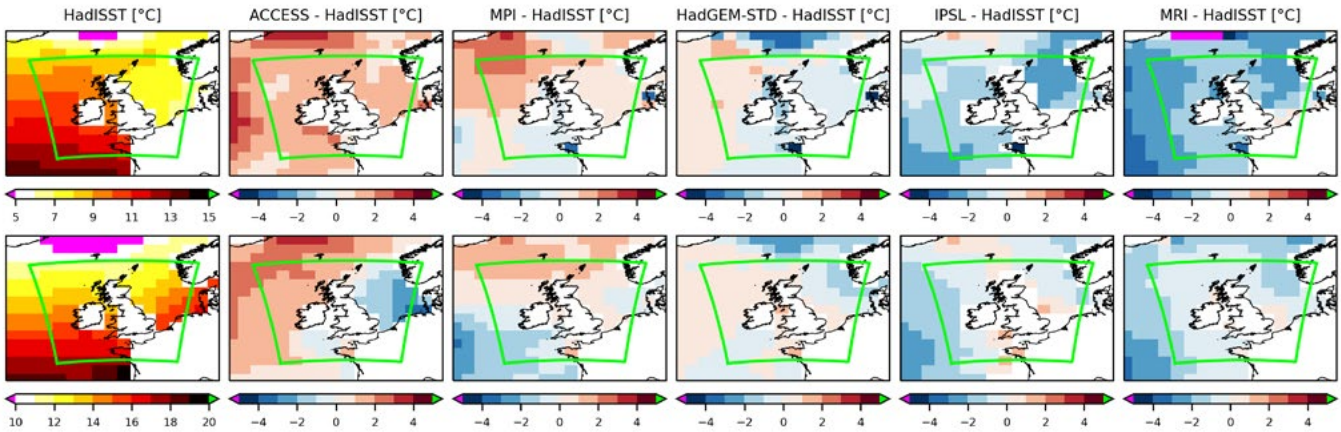

Figure 6. Seasonal mean SST biases in the CMIP5-4 and HadGEM-STD global models, relative to HadISST observations (Rayner et al. 2003), for the baseline period (1980 – 2000). The top row is for winter and the bottom row is for summer. All data has been regridded onto a common n96 grid with spacings of 1.875º and 1.25º in the longitudinal and latitudinal directions, respectively. The boundary of the CPM domain is shown for reference (green line).

Figure 7 shows biases in near-surface air temperature over the UK. In winter, biases in the CMIP5-4 models tend to follow the SST biases shown in Figure 6, with ACCESS being too warm across the UK and MRI too cold. Model biases are typically smaller in summer, apart from IPSL, which is too warm across England despite surrounding SSTs being slightly too low. Note that ACCESS still exhibits a strong warm bias across the UK in summer.

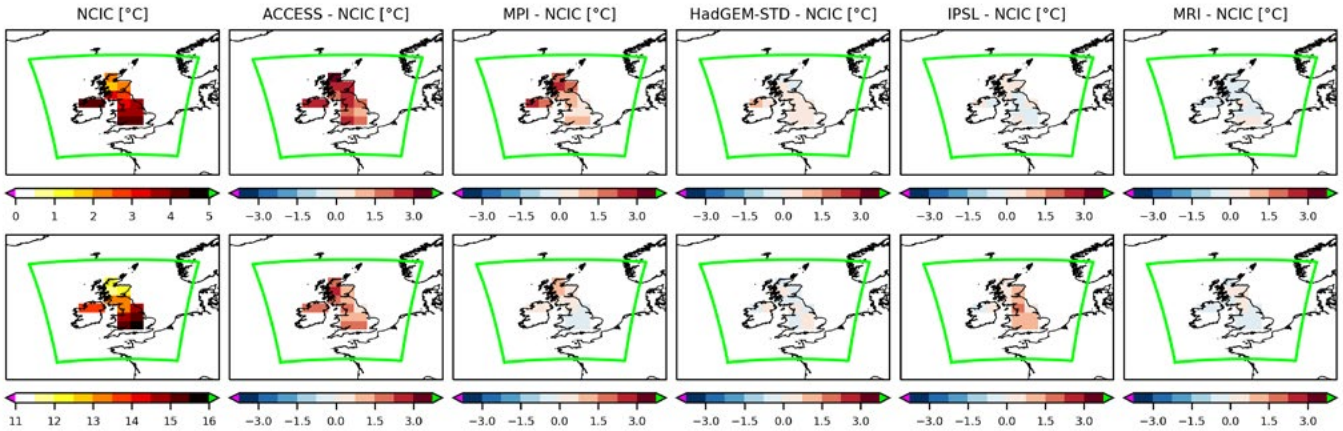

Figure 7. Seasonal mean biases in air temperature at 1.5m in the CMIP5-4 and HadGEM-STD global models, relative to NCIC observations (Perry et al. 2009), for the baseline period (1980 – 2000). The top row is for winter and the bottom row is for summer. All data has been regridded onto a common n96 grid with spacings of 1.875º and 1.25º in the longitudinal and latitudinal directions, respectively. The boundary of the CPM domain is shown for reference (green line).

Finally, model precipitation biases are presented in Figure 8. In winter all models produce too much rainfall over southeastern England, particularly IPSL and MRI. The ACCESS and MPI models have a notable dry bias over Scotland, and the western half of the UK more generally. Biases are smaller in summer in all models.

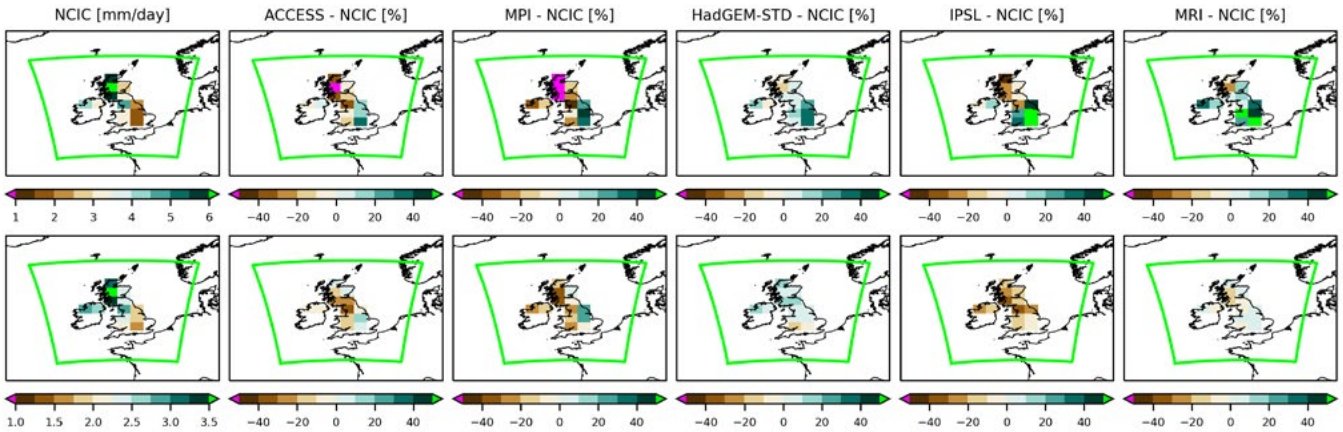

Figure 8. Seasonal mean biases in precipitation in the CMIP5-4 and HadGEM-STD global models, relative to NCIC observations (Perry et al. 2009), for the baseline period (1980 – 2000). The top row is for winter and the bottom row is for summer. All data has been regridded onto a common n96 grid with spacings of 1.875º and 1.25º in the longitudinal and latitudinal directions, respectively. The boundary of the CPM domain is shown for reference (green line).

2.4 **Regional model set-up**

Regional models are configured to be as similar as possible to those in UKCP18, with the 2.2 km CPM nested inside the 12 km RCM; see Figure 9 for a reminder of the model domains. These models are described in detail in previous reports (Kendon et al. 2019, 2021). The main difference here is that the CMIP5-4 global models are used to provide (6-hourly) LBCs for the RCM, and daily mean SSTs and sea-ice extent for both the RCM and CPM, rather than HadGEM-PPE.

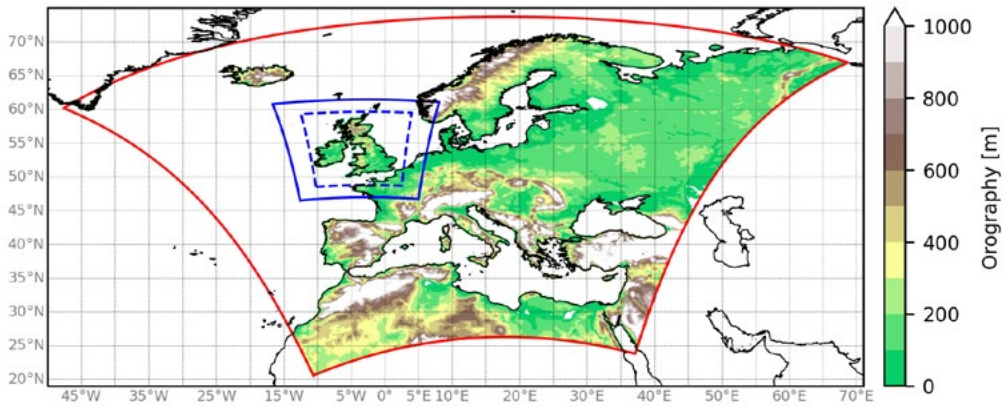

Figure 9. Domains and orography of the UKCP18 regional models. The solid red line shows the boundary of the pan-European 12 km RCM, and the solid blue line shows the boundary of the CPM nested inside this. The CPM is a variable resolution model, with a fixed grid length of 2.2 km in the region marked by the dashed blue line, stretching to 4 km outside of this.

The science configuration of the RCM and CPM mirrors that of the standard member of the respective UKCP Regional and Local ensembles released previously (Murphy et al. 2018, Kendon et al. 2019, 2021). The Unified Model (UM) version was upgraded though, from UM10.6 to UM10.9 and UM12.0 for the RCM and CPM, respectively. This was done to gain access to new code to implement a 365-day calendar in the UM, required for down-scaling IPSL (the other three CMIP5-4 GCMs employ a standard Gregorian calendar already supported by the UM). Tests were run to make sure the UM version upgrade did not systematically affect model evolution.

All ancillary files (land-sea mask, orography, land use, etc) are the same as used previously, apart from SSTs and sea-ice, which come from the driving global model (i.e. from a CMIP5 GCM in this work), and those for the Easy Aerosol scheme (Voigt et al. 2014) that is used to approximate aerosol effects in the regional models.

It was decided to use the same land-sea mask in the CMIP5-driven RCMs and CPMs as in the existing UKCP18 regional models for consistency. However, this did lead to complications when generating SST ancillaries for RCM-IPSL and CPM-IPSL, because part of the Irish Sea, English Channel and the Red Sea are not represented as sea points in the land-sea mask of IPSL. By default, the ancillary generation code generates SSTs in these regions by using a spiral search algorithm to fill in SST data from the nearest available sea points, which led to unrealistically sharp SST gradients. To remedy this, we applied inverse-distance-weighted (IDW) interpolation (with power parameter, p=2) to smoothly fill in the missing SSTs for each region before the ancillary files for the RCM and CPM were created.

Similar problems were encountered in RCM-ACCESS because the Black Sea is not represented in the land-sea mask of ACCESS. The default ancillary generation procedure then gives markedly different SSTs in the eastern and western halves of the Black Sea. In reality there is more of a north-south gradient in SSTs in the Black Sea. Using daily observed SSTs from the Reynolds et al. (2002) dataset for the period 1982-2000, we computed the scaling factor required to reproduce the zonal-mean SST at each latitude in the Black Sea from the SST at a reference point in the northeast Aegean Sea, chosen to match the location of the closest sea point to the Black Sea in ACCESS. An average scaling factor was computed for each month, varying with latitude across the Black Sea. On any given day, we generate a zonal-mean SST pattern for the Black Sea by applying the observationally derived scaling factor for the appropriate month to the SST value at the grid box in ACCESS corresponding to the reference point. These new SSTs are then used to replace the erroneous SSTs in the original ancillary file. The same procedure is followed in both present-day and future simulations. Using SST ancillary files for the other CMIP5-driven RCMs and RCM-STD, we have checked that the monthly-mean scaling factors in the models are not very sensitive to the choice of time-period, justifying this approach.

The Easy Aerosol scheme requires time series of aerosol optical properties and cloud droplet number concentration as input, but these are not available from the CMIP5-4 models. Instead, we prescribe aerosol properties in the regional models using standard forcing datasets that were developed for CMIP6, based on the MACv2-SP parametrisation of the radiative effects of anthropogenic aerosols (Stevens et al. 2017, Fiedler et al. 2019). Note this was the approach adopted in the pair of RCM and CPM simulations driven by ERA-Interim in UKCP18. This means that aerosol forcing will be the same across all the CMIP5-driven regional models, but different to that in their parent GCMs (and also the original UKCP18 regional model runs driven by HadGEM-PPE). The effect this has on regional climate projections will depend on the CMIP5 model being down-scaled: if the GCM did not represent aerosol-cloud interactions (e.g. MPI), then using MACv2-SP will lead to more of a cooling due to aerosol effects in the present-day, and thus enhanced future warming, and vice versa when down-scaling GCMs (such as ACCESS) that did include aerosol indirect effects (B. Booth, pers. comm.). However, we expect the impact of any difference in aerosol forcing between MACv2-SP and the driving GCM to be relatively small over the UK (compared to central Europe, for example), because aerosol effects in the GCM will influence SSTs which are then prescribed as a lower boundary condition in the regional model, and SSTs exert a strong control on air temperatures over the UK.

Note that an error was found in the code for producing the Easy Aerosol ancillary files for the cloud droplet number concentration. To generate these files, scaling factors from the standard CMIP6 forcing datasets described in Stevens et al. (2017; for the historical period) and Fiedler et al. (2019; for the RCP8.5 scenario) are applied to a pre-industrial model climatology (constructed using data from a low resolution, atmosphere-only global climate simulation with pre-industrial forcing for the period 1988-2009). The ancillary generation code assumed the first month in the pre-industrial climatology was January, whereas it was in fact August. This error was rectified for the CMIP5-driven runs presented here, but will have affected the regional model runs driven by ERA-Interim in UKCP18 (not RCM-PPE and CPM-PPE though).

The generation of boundary conditions for RCM-ACCESS also required special attention, because the top of the ACCESS model is 39 km above sea level, 1 km lower than the model top of the regional models. Rather than use a different vertical level set in this particular RCM, and thus lose consistency between models, it was decided to interpolate driving data from ACCESS onto the regional model level set with linear extrapolation beyond the model top.

As in UKCP18, regional model projections were produced for five sequential 21-year time-slices spanning 1979-2080, discarding the first year of each time-slice as model spin-up (mainly to allow the land surface to reach equilibrium). The RCP8.5 emissions scenario is followed from 2005 onwards. The time-slices can then be stitched together to generate a set of fully transient projections (noting that there will be discontinuities at the boundaries between time-slices that must be avoided when analysing events that span the break points). The calendar of the driving CMIP5 GCM was also adopted in the nested regional models (IPSL uses a 365-day calendar, all the others use a Gregorian calendar).

Note that, since the release of UKCP18, it has been noticed that there are instances of high rainfall in the 2.2km CPM data that have physically unrealistic spatial characteristics, manifesting as linear features aligned with the model grid. These features are the result of non-conservative behaviour inherent to the semi-Lagrangian advection scheme used in the UM. The frequency of these events could affect estimates of present-day extreme rainfall and future changes[2]. Removing these spurious features from the raw CPM data in post-processing is challenging. One way of reducing their impact is to regrid the 2.2 km data onto a coarser grid since the regridding has a smoothing effect. For this reason, data from the CMIP5-driven CPMs will be regridded onto a 5 km grid (using the Ordnance Survey National Grid reference system; OSGB) before release; the raw 2.2 km data will not be available to users. Throughout this report we therefore only use CPM data that has been regridded onto this 5 km grid (unless we are comparing with lower-resolution models in which case we regrid onto the coarsest resolution grid).

2.5 Computing future changes

Previous UKCP18 science reports (Murphy et al. 2018, Kendon et al. 2019, 2021, 2023b) defined future changes as the difference between a fixed future time period (2060-2080) and the baseline period (1980-2000). However, the rate of increase of global mean surface temperature varies considerably across the different CMIP5-4 models, hence we choose to define future changes using a specific level of global warming instead (following Hanlon et al. 2021). The advantage of this is that it allows us to frame projections in a way that is essentially independent of climate sensitivity and emissions scenario. Note that the UK's Fourth Climate Change Risk Assessment (CCRA4) will employ a similar approach[3]. We select a global warming level of 3ºC above pre-industrial temperatures since this is the maximum that all GCMs attain before 2080 (the endpoint of the nested regional simulations), thus enabling us to maximise signal-to-noise.

To compute future changes, we adopt a similar approach to Hanlon et al. (2021). For each GCM, a timeseries of annual mean global mean temperature is produced, smoothed with a 21-year rolling mean. This is converted to a timeseries of global mean temperature anomalies by subtracting off the average global mean temperature for the baseline period (1980-2000) in the GCM. Since the observed warming from the pre-industrial period (defined here as 1850-1900) to the baseline period is 0.51ºC (from HadCRUT4; Morice et al. 2012), the year when the global mean temperature anomaly reaches 2.49ºC is used to define a global warming level of 3ºC relative to pre-industrial. Once this year has been identified from the timeseries of temperature anomalies, the 21-year period centred on this year (i.e. 10 years either side) is used as the future period for computing changes in metrics relative to the fixed baseline period.

[2] See https://www.metoffice.gov.uk/binaries/content/assets/metofficegovuk/pdf/research/ukcp/ukcp18_guidance_extreme_rainfall.pdf for more information.

[3] See https://www.theccc.org.uk/publication/proposed-methodology-for-the-ccra4-advice/?chapter=3-proposed-methodological-approach-for-ccra4-ia#3-3-future-climate-change.

The future periods for each GCM simulation are listed in Table 5, along with estimates of their effective climate sensitivity (EffCS).

Global model	EffCS [K]	Future period
MPI	3.63	2057 - 2077
IPSL	4.12	2044 - 2064
ACCESS	3.53	2045 - 2065
MRI	2.60	2062 - 2080
HadGEM-STD	5.34	2038 - 2058
HadGEM-PPE r001i1p01113	5.00	2035 - 2055
HadGEM-PPE r001i1p01554	4.96	2041 - 2061
HadGEM-PPE r001i1p01649	5.35	2037 - 2057
HadGEM-PPE r001i1p01843	4.87	2040 - 2060
HadGEM-PPE r001i1p01935	4.41	2042 - 2062
HadGEM-PPE r001i1p02123	5.34	2033 - 2053
HadGEM-PPE r001i1p02242	5.05	2039 - 2059
HadGEM-PPE r001i1p02305	4.81	2038 - 2058
HadGEM-PPE r001i1p02335	5.58	2042 - 2062
HadGEM-PPE r001i1p02491	4.88	2038 - 2058
HadGEM-PPE r001i1p02868	5.10	2042 - 2062

Table 5. Definition of 21-year future periods for each GCM, based on when the global mean temperature reaches 3°C above pre-industrial. Note that MRI only reaches the 3°C global warming level in 2072, hence a shorter 19-year future period must be adopted for this model since the model integration ends in 2080. Effective climate sensitivity (EffCS) values for the CMIP5 GCMs are taken from Schlund et al. (2020).

Note the large spread in times when a global warming level of 3°C above pre-industrial is attained in the various models, with the fastest warming member of HadGEM-PPE reaching this point approximately 30 years before the MRI model. In general, the high climate sensitivity and thus warming rate of HadGEM-PPE means a global warming level of 3°C above pre-industrial is reached around the middle of the 21st century, well before the fixed future period 2060 – 2080 used in previous analyses. This could lead to substantial differences in projections in some cases.

Although the future period is chosen to be centred around the year when the global mean surface temperature reaches 3°C above pre-industrial, the level of warming attained at the regional scale can be quite different. This is worth bearing in mind when interpreting model projections in subsequent sections. To illustrate this, Figure 10 shows future changes in SSTs around the UK projected by the CMIP5-4 GCMs and HadGEM-STD. Of the CMIP5-4 GCMS, IPSL has the highest climate sensitivity and is the fastest warming (Table 5), and it displays the smallest future increases in seasonal mean SST of all the GCMs, approximately 0.8°C in winter and 1.3°C in summer (averaged over the green box in Figure 10). The corresponding increases in UK-average near-surface temperature are 0.9°C in winter and 2.1°C in summer, notably less than 2.49°C (the warming relative to the baseline period for a global warming level of 3°C above pre-industrial). For the other CMIP5-4 GCMs, future increases in seasonal mean SST, averaged over the green box in Figure 10, happen to be proportional to model climate sensitivity, although there is no particular reason for such a relationship to exist.

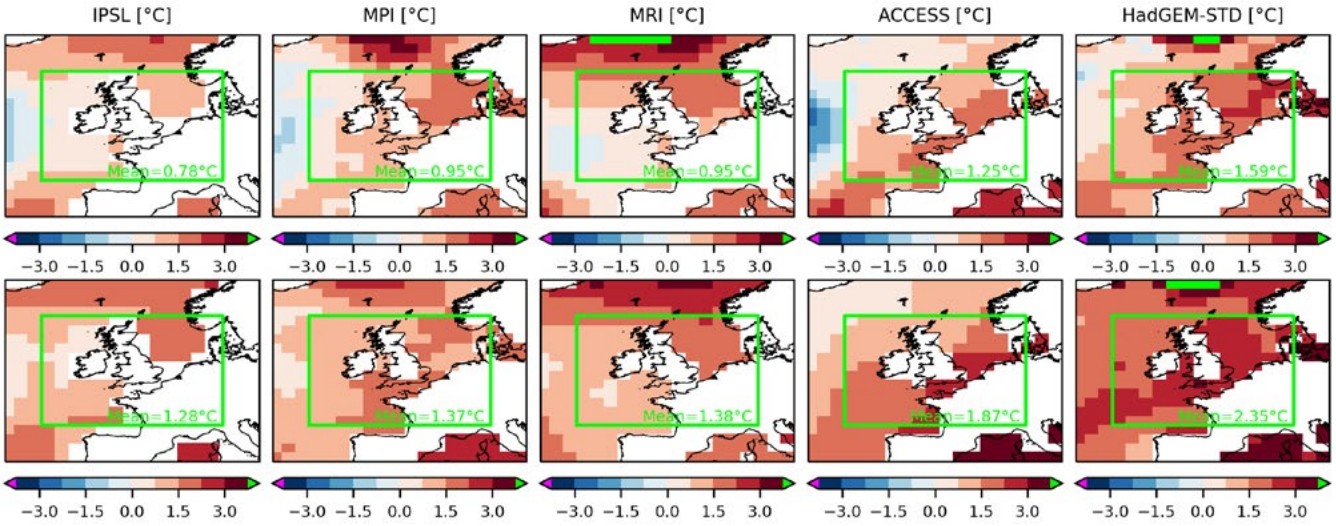

Figure 10. Future changes in seasonal mean SSTs in the CMIP5-4 and HadGEM-STD global models, for winter (top row) and summer (bottom row). Future changes are defined as the difference between a 21-year future period, centred on the year when the global mean surface temperature reaches 3ºC above pre-industrial (see Table 5), and baseline period (1980 – 2000). All data has been regridded onto a common n96 grid with spacings of 1.875º and 1.25º in the longitudinal and latitudinal directions, respectively. The green box indicates a region where SSTs exert a strong influence on UK climate (Fereday and Knight 2023) and the models are ordered from left to right by increasing future change in seasonal mean SST averaged over this box, as indicated by the green text annotation.

As a final comment, recall that one of the main reasons for choosing to down-scale the CMIP5-4 set of GCMs was to sample different future summer outcomes than available from HadGEM-PPE. Technical considerations aside, the choice of models to down-scale was largely based on attempting to maximise the diversity in future summer outcomes in Figure 3. In this figure, future changes are defined as the difference between the fixed time periods 2070-2100 and 1961-1990 and thus include the different temperature responses of the models. By defining the future period using a global warming level of 3ºC above pre-industrial, there is no guarantee that the range of summer projections from the CMIP5-4 models seen in Figure 3 will be preserved. However, as we shall see, the CMIP5-4 models (apart from ACCESS) still tend to project less of a future increase in temperature and decrease in precipitation in summer over the UK than members of HadGEM-PPE, supporting our approach (e.g. Figure 15 below).

2.6 Computing metrics and significance testing

In what follows, we assess the performance of the CMIP5-driven regional models over the baseline period by computing biases relative to observational data for a selection of metrics related to temperature and precipitation (Section 3).

The first step is to regrid all model data and corresponding observations onto a common grid. If GCMs, RCMs and CPMs are to be compared, the grid used is an n96 grid with spacings of 1.875º and 1.25º in the longitudinal and latitudinal directions, respectively (this is the same resolution as the ACCESS GCM; Table 4). When comparing just RCMs and CPMs, the CPM data is regridded onto the 12 km grid of the RCM. If only CPMs are being considered, the CPM data is regridded onto a 5km OSGB grid (as discussed at the end of Section 2.4).

Once all model and observational data has been averaged onto a common grid, any metric of interest (e.g. the 1st percentile across all days that lie within a particular season) is computed at each grid box, then the

observations are subtracted from the model to give the bias in the metric. Biases at the regional level are computed in the same way, but with an additional step of area-weighted averaging the model and observational data over the region of interest before their difference is calculated.

To test whether a bias is significant compared to natural variability, we use bootstrap resampling. Bootstrap samples are generated by randomly selecting 20 seasonal blocks of model data (monthly, daily or hourly data, depending on the metric) from the baseline period, allowing replacement. Resampling is done in seasonal blocks to allow for temporal correlation within each season. For each bootstrap sample, the bias in the desired metric is computed as described above. This process is repeated 1000 times to build up a distribution of values for the bias, and a 95% confidence interval is constructed from the 2.5th and 97.5th percentiles of this distribution. If zero does not lie in this confidence interval, this implies the model bias is significant (at the 95% level).

We also examine future changes in the same set of metrics (Section 5), which are computed in a similar way to model biases. Starting with model data on a common grid, the desired metric is computed at each grid box for the baseline and future periods separately and, if required, area-weighted averaging is applied to calculate regional averages. The baseline value is then subtracted from the future value to give the future change in the metric.

To assess whether future changes are significantly different from zero, the block bootstrap resampling approach described above is applied separately to data from the baseline and future periods. Note that the same random sequence of seasonal blocks is selected from both the present-day and future data to account for any non-stationarity within each time period. For each pair of present-day and future bootstrap samples, the future change in the desired metric is computed as described above, building up a distribution of 1000 estimates of the future change in the metric. If zero does not lie between the 2.5th and 97.5th percentiles of this distribution, then the future change is deemed significant (at the 95% level).

Note that we do not apply any kind of bias adjustment to model data here as our main aim is to characterise the biases of the new CMIP5-driven regional models, and any implications this may have for the plausibility of their projections. However, we recognise that some users may wish to apply bias adjustment for their specific applications, noting that such methods usually come with strong caveats. More information on bias adjustment methods and when to use them can be found in Fung (2018).

3 Results

3.1 Large-scale consistency with driving model

3.1.1 Present-day circulation patterns

It is well known that nested regional models can modify the large-scale circulation inherited from their driving model via their boundary conditions, especially if the domain size is large (e.g. Jones et al. 1995, Leduc and Laprise 2009). This can be the result of internal variability of the model, errors introduced by the LBC process (e.g. spatial and temporal interpolation), large changes in resolution (e.g. Matte et al. 2017), a very different representation of orography and coastlines (e.g. Antic et al. 2006), as well as fundamental differences in their dynamics and physics schemes.

If the large-scale circulation is altered too much by the nested regional model (which would violate the fundamental assumption of the one-way nesting approach to regional modelling), this could induce differences in climate change projections between the regional model and its driving GCM. From the perspective of this work, this could lead to an undesirable loss of diversity in the down-scaled projections. In what follows we assess to what extent each RCM remains broadly consistent with its driving GCM on large scales, using the weather pattern approach, a popular means of characterizing the large-scale circulation (e.g. Sanchez-Gomez et al. 2009, Dawson et al. 2012, Fabiano et al. 2020, Pope et al. 2022). Note that we focus on the RCM since we expect the CPM to follow its driving RCM more closely because (i) the CPM domain is much smaller than the RCM domain and thus more strongly constrained by its LBCs, and (ii) both the RCM and CPM are based on the UM, although there are differences in the parametrisation schemes used. In addition, the step from RCM to CPM is no different from that in the original set of UKCP Local simulations already released.

A set of weather patterns appropriate for the UK and surrounding European area was developed by Neal et al. (2016). These were generated by applying a clustering algorithm to group daily pressure at mean sea level (PMSL) anomalies for the North Atlantic-European region (30W-20E, 35N-70N) from the EMULATE dataset (Ansell et al. 2006) into a set of 30 clusters, each corresponding to a distinct circulation type. The number of clusters was decided upon with the aid of operational meteorologists. These patterns were then further grouped into a set of eight clusters, providing a broader indication of the atmospheric circulation. This reduced set of weather patterns is shown in Figure 11 and briefly described in Table 6; it is these circulation types that we adopt for our analysis.

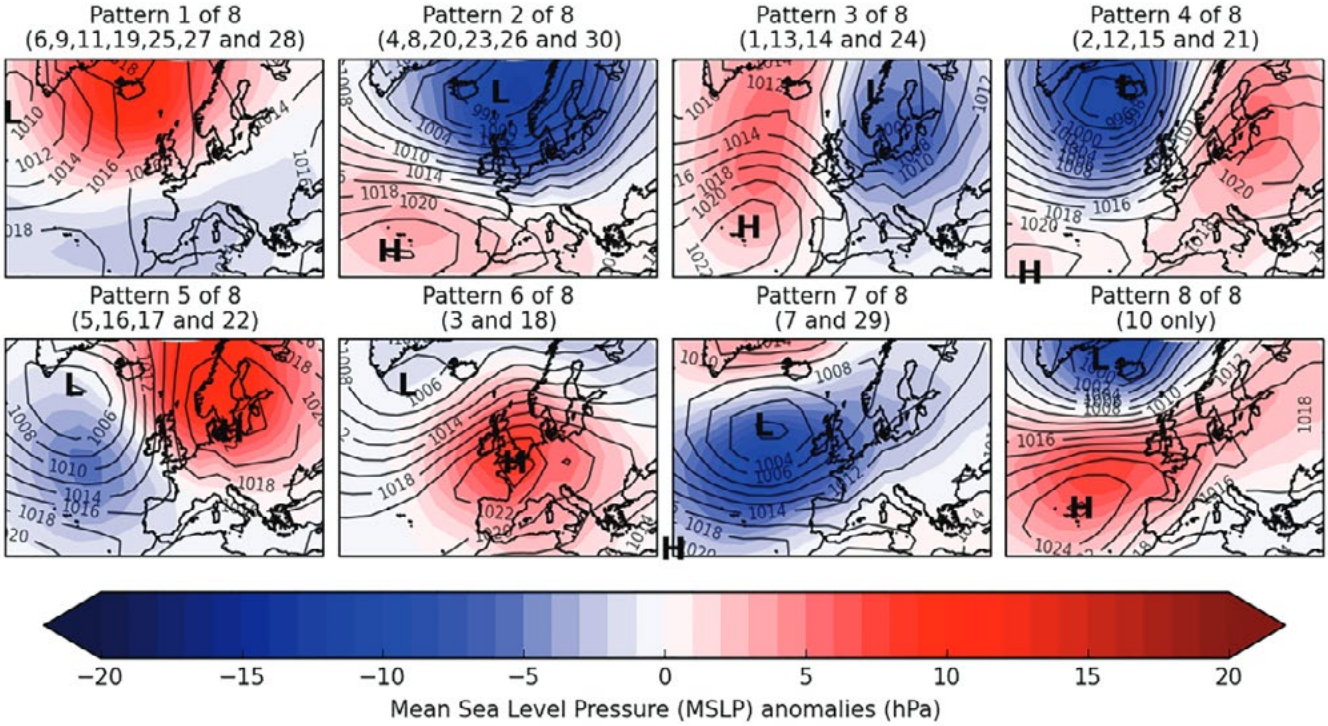

Figure 11. Set of eight weather patterns used in this analysis. Reproduced from Neal et al. (2016).

Table 1. Descriptions of the eight weather patterns and percentage occurrences from the European and North Atlantic Daily to Multi-decadal Climate Variability (EMULATE) MSLP (EMSLP) data (1850–2003). Pattern names and descriptions are relevant to the UK.

Weather pattern	Description	Percentage occurrence (1 dp)
1. NAO–	All sub-patterns going into this type in general have positive MSLP anomalies to the north of the UK and negative MSLP anomalies to the south of the UK, resulting in a negative NAO pattern.	21.2
2. NAO+	All sub-patterns going into this type in general have negative MSLP anomalies to the north of the UK and positive MSLP anomalies to the south of the UK, resulting in a zonal (positive NAO) pattern.	17.8
3. Northwesterly	All sub-patterns going into this type in general have negative MSLP anomalies to the northeast of the UK and positive MSLP anomalies to the southwest of the UK, resulting in a north-westerly flow. Sub-patterns going into this type vary between being cyclonic and anticyclonic, but the direction of flow is the same.	15.0
4. Southwesterly	All sub-patterns going into this type in general have negative MSLP anomalies to the northwest of the UK and positive MSLP anomalies to the southeast of the UK, resulting in a southwesterly flow. Sub-patterns going into this type vary between being cyclonic and anticyclonic but the direction of flow is the same.	14.8
5. Scandinavian high	All sub-patterns going into this type in general have negative MSLP anomalies to the west of the UK and positive MSLP anomalies to the east of the UK, resulting in a south to south easterly flow. Most sub-patterns in this type are anticyclonic.	12.4
6. High pressure centred over UK.	Both sub-patterns going into this type have positive MSLP anomalies over the UK and to the south of the UK, with weak negative MSLP anomalies to the north of the UK. This results in an anticyclonic westerly or southwesterly flow.	7.9
7. Low close to UK	Both sub-patterns going into this type extend a trough over the UK. Negative MSLP anomalies are centred just to the west of the UK resulting in a cyclonic southwesterly flow.	6.5
8. Azores high	Only one pattern goes into this type which shows an anticyclonic westerly flow over the UK, with an Azores high extension.	4.3

MSLP, mean sea level pressure; NAO, North Atlantic Oscillation

Table 6. Description of the set of eight weather patterns used in this analysis. Reproduced from Neal et al. (2016).

For each GCM and RCM, we assign each day in the historical period (1980-2000) to one of the eight weather patterns as follows. First, we regrid the daily mean PMSL field onto the 5º x 5º grid of the EMULATE dataset. Note that some regions of the EMULATE domain lie outside that of the RCM (13 out of 88 grid points, corresponding to ~15% of the domain, mainly in the southwest corner, see Figure 12 below). We fill in these regions using data from the driving GCM. A daily PMSL anomaly is then computed by subtracting off the mean PMSL for the corresponding day of the year, averaged over the full historical period. The area-weighted mean squared difference between the daily PMSL anomaly and each weather pattern is computed, then the day is assigned to the weather pattern which minimises this metric. This does not necessarily mean there is a good correspondence between the model PMSL anomaly and the weather pattern it is associated with; on any given day, the PMSL anomaly is more likely to be some mixture of multiple weather patterns (although not a simple linear combination since the weather patterns are not an orthogonal basis).

Note that Pope et al. (2022) used a much longer period (1900-1999) to compute the daily PMSL climatology in their analysis, possible because they were using UKCP18 global model data. We cannot do this here since the RCM simulations only start in 1980. To provide an indication of the robustness of our results, we have repeated the analysis using the period 1980-2020 to generate the climatology from the RCMs instead. The key points reported below remain unchanged, supporting our approach.

Since the weather patterns are defined as anomalies in PMSL, any difference in mean PMSL between an RCM and its driving GCM is not accounted for. Therefore, we examine seasonal mean differences in PMSL before considering weather patterns; see Figure 12.

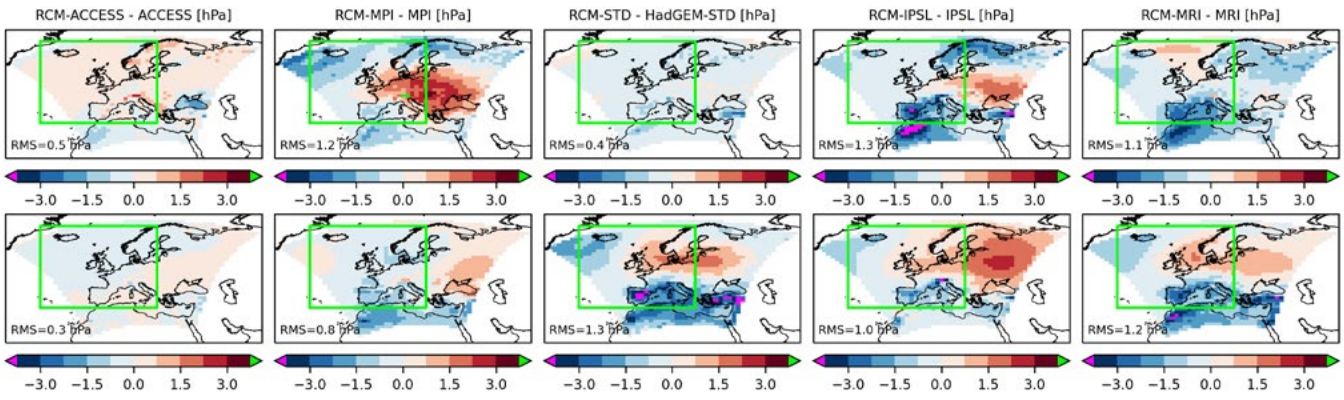

Figure 12. Differences in seasonal mean PMSL between RCMs and their driving GCMs, for the baseline period (1980 – 2000). The root-mean-square (RMS) difference across the RCM domain is also indicated in each panel. The top row is for winter and the bottom row is for summer. All data has been regridded onto a common n96 grid with spacings of 1.875º and 1.25º in the longitudinal and latitudinal directions, respectively. The boundary of the EMULATE dataset used to construct weather patterns is highlighted by the green box.

Overall, there is a good degree of consistency between RCMs and their driving models, with domain-wide root-mean-square (RMS) differences in PMSL being at most 1.3 hPa. Differences between the CMIP5-driven RCMs and their driving models are larger than those between RCM-STD and GCM-STD. One might expect this since the change in horizontal resolution is greater, and the model physics and dynamics schemes are different. Note that RCM-ACCESS deviates less from its driving model than any other CMIP5-driven RCM, despite there being more of a resolution change than for RCM-MRI. Given that ACCESS is also based on the UM, this could possibly indicate that physics differences have more of an impact on the large-scale circulation than changes in horizontal resolution, but this would require further investigation. In RCM-MPI,

RCM-IPSL and RCM-MRI there can be large differences (~5 hPa) in some regions, depending on the season. However, over the EMULATE domain used to construct the weather patterns for the UK, these RCMs tend to agree well with their driving GCMs, except in the southeast (e.g. over Spain and the Mediterranean Sea) where PMSL values are typically considerably lower in the RCMs.

Moving on to consider weather patterns, Figure 13 shows the frequency of occurrence of each pattern in the various GCMs, and how this distribution differs in their nested RCMs.

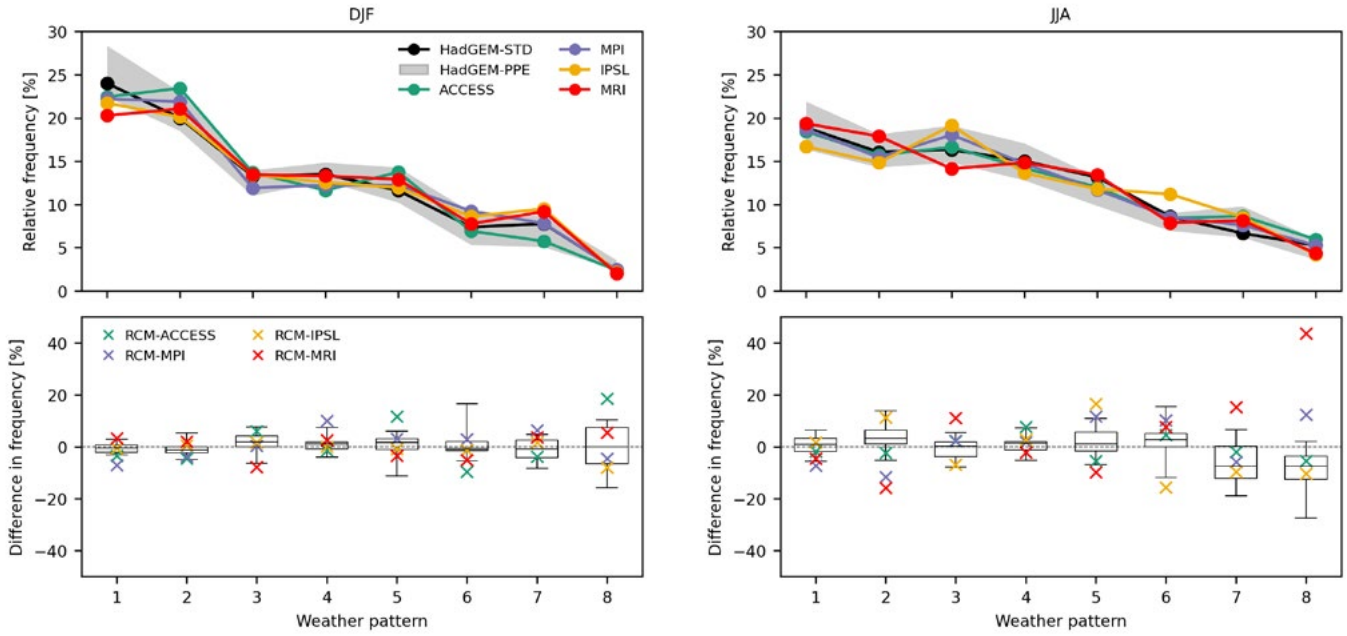

Figure 13. Frequency of occurrence of each of the eight weather patterns in the CMIP5-4 GCMs in winter (top left) and summer (top right). The standard member and range of the HadGEM-PPE is also shown for comparison. Plots on the bottom row show the relative difference in frequency of each weather pattern between the CMIP5-driven RCMs and their driving global models. In these plots, the RCM-PPE distribution is shown by the box-and-whiskers: the box extends from the lower to the upper quartiles of the data, with the median shown by the solid horizontal line, and the whiskers show the full range of the data.

The global models all show a general pattern of decreasing frequency with increasing weather pattern number, with patterns 1 and 2 being dominant in winter. The CMIP5-4 GCMs typically lie within the HadGEM-PPE spread, with a few exceptions (e.g. IPSL has more days associated with weather pattern 6 in summer than any other model).

The distribution of weather patterns in the CMIP5-driven RCMs is broadly similar to that in their driving GCMs, with absolute differences in the frequencies of weather patterns being comparable to those between members of RCM-PPE and HadGEM-PPE (which can be thought of as the ideal down-scaling set-up because HadREM3-GA705 is simply a high-resolution version of HadGEM3-GC305). There are a small number of cases where differences are larger than any in RCM-PPE, such as weather pattern 8 occurring approximately 40% more often in summer in RCM-MRI than MRI (although it should be noted there are only a small number of days assigned to this weather pattern overall).

To assess the day-to-day correspondence of large-scale circulation between each CMIP5-4 GCM and its nested RCM, in Figure 14 we show the fraction of days where the RCM weather pattern is the same as its driving model.

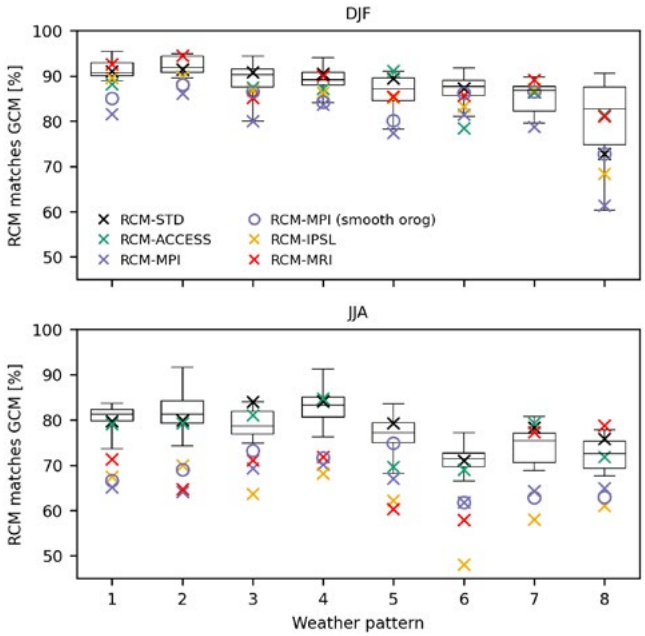

Figure 14. Fraction of days where the weather pattern in each CMIP5-driven RCM matches that of its driving GCM, in winter (top panel) and summer (bottom panel). In these plots, the RCM-PPE distribution is shown by the box-and-whiskers: the box extends from the lower to the upper quartiles of the data, with the median shown by the solid horizontal line, and the whiskers show the full range of the data. Note that the experiment RCM-MPI (smooth orog) is a sensitivity test where RCM-MPI has been re-run using the smoother orography of its parent GCM.

In winter there is clearly very good agreement between the CMIP5-driven RCMs and their parent GCMs, with all models except RCM-MPI consistently lying within the RCM-PPE spread (apart from RCM-ACCESS for weather pattern 6). Recall from Table 4 that the resolution change is largest when down-scaling the MPI model. If we re-run RCM-MPI using the smoother orography of the MPI GCM we find an increase in the day-to-day correspondence between the RCM and GCM for all weather patterns, indicating that the different representation of orography is an important factor in modifying the large-scale circulation inherited from the GCM.

In summer, there is less correspondence between RCMs and their driving GCMs, for all model pairings. This is to be expected since the large-scale flow is weaker in this season and thus the LBCs exert less of an influence. Except for RCM-ACCESS, the CMIP5-driven RCMs all deviate more from their driving GCM than any member of RCM-PPE.

Note that all regional models tend to diverge most from their driving model on summer days when the GCM is in weather pattern 6, especially RCM-IPSL, where the RCM only matches the GCM ~50% of the time. Weather pattern 6 corresponds to high pressure centred over the UK, i.e. a blocking situation. Blocking patterns can be almost stationary, in which case one might expect the RCM to begin to deviate from its driving GCM (the study of Jury et al. 2019 suggests that RCMs typically under-estimate the number of blocking days over Europe compared to their boundary conditions). Otherwise, the RCMs are able to reproduce the large-scale circulation of their driving GCM on ~60% or more of summer days.

In spring and autumn, the fraction of days where the weather pattern is the same in the RCM and its parent model typically lies between that of summer and winter, so overall we are satisfied that the RCM simulations are reasonably well constrained by their boundary conditions, despite the large pan-European domain.

So far, we have only considered the impact of down-scaling on the large-scale circulation in the historical period. In the future, it is possible that an RCM may not follow its driving model as closely, if the storm track

were to weaken for example. To investigate this, we have repeated our analysis for the future period (corresponding to a global warming level of 3ºC above pre-industrial), using the same set of weather patterns (we are assuming these patterns will still provide a good characterisation of the large-scale circulation in the future, which may not be the case, but is often assumed, e.g. Fabiano et al. 2021, Pope et al. 2022). Table 7 compares the overall fraction of days where the RCM weather pattern matches that of its driving GCM, in the historical and future periods. From this preliminary analysis, there is no evidence for any substantial future change in large-scale consistency between RCMs and their driving global models.

	DJF		JJA	
	Historical	Future	Historical	Future
RCM-MPI	0.81	0.83	0.66	0.70
RCM-IPSL	0.87	0.88	0.63	0.68
RCM-ACCESS	0.88	0.91	0.78	0.78
RCM-MRI	0.90	0.89	0.68	0.71
RCM-STD	0.89	0.90	0.80	0.81

Table 7. Fraction of days when the weather pattern in the RCMs matches that of its driving GCM, in the baseline (1980-2000) and future periods. The future period is defined as the 21-year period centred on the year when the global mean surface temperature reaches 3ºC above pre-industrial (see Table 5).

3.1.2 **Projected changes**

We now move on to examine whether large-scale future changes projected by the CMIP5-4 global models are broadly preserved upon down-scaling with the RCM and CPM. This is crucial since the main motivation for down-scaling these alternative GCMs is to sample a more diverse range of possible outcomes than captured by HadGEM-PPE (e.g. for England in summer).

Figure 15 shows seasonal mean changes in temperature and precipitation for the CMIP5-4 GCMs and their nested regional models, along with projected changes from HadGEM-PPE, RCM-PPE and CPM-PPE.

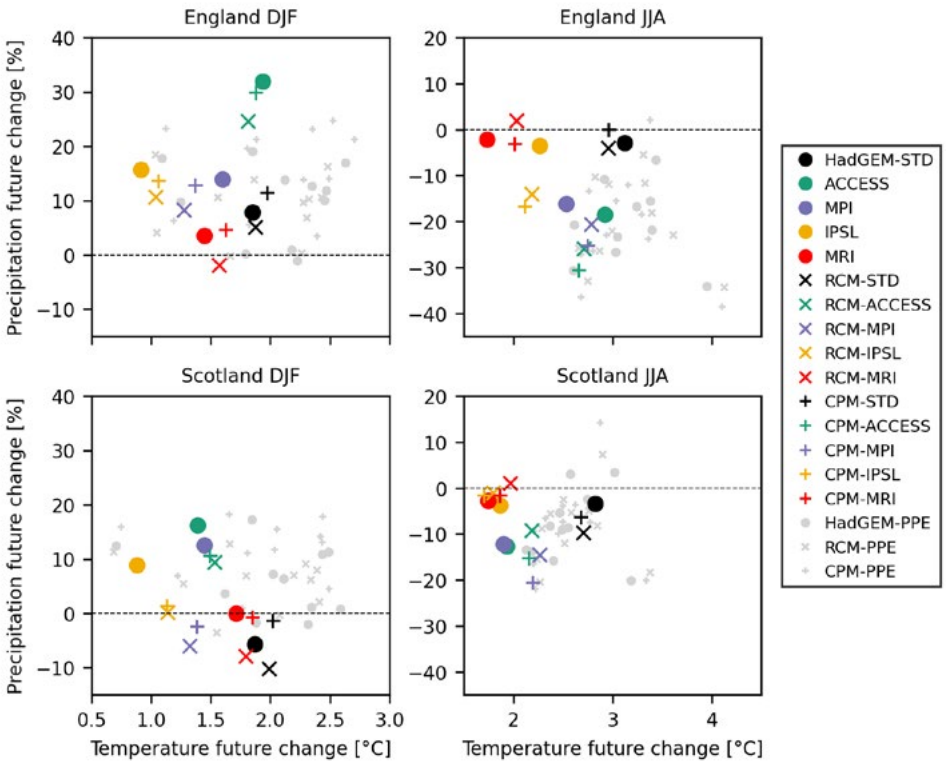

Figure 15. Scatterplots of future changes in seasonal mean air temperature at 1.5m and precipitation. Future changes are defined as differences between a 21-year future period, centred on the year when the global mean surface temperature reaches 3ºC above pre-industrial (see Table 5), and the baseline period (1980 – 2000). All data has been regridded onto a common n96 grid with spacings of 1.875º and 1.25º in the longitudinal and latitudinal directions, respectively.

The key point to take from Figure 15 is that the CMIP5-driven RCMs and CPMs mostly lie close to their parent GCMs, with differences in future changes between parent and nested models being comparable to those between members of HadGEM-PPE and RCM-PPE, and RCM-PPE and CPM-PPE, respectively. This suggests the down-scaling is generally behaving as desired, allowing us to sample different regions of the space of future changes with the new regional model runs. For example, the RCMs and CPMs driven by MRI and IPSL show much smaller increases in temperature and decreases in precipitation in summer than most members of RCM-PPE and CPM-PPE, and the regional models driven by ACCESS suggest larger increases in winter precipitation over England than any other model. Note there are occasional cases where a large difference is seen between the response of a GCM and its nested RCM, such as future changes in winter precipitation over Scotland in the MPI model. These findings will be discussed in more detail in Section 5.

3.2 Evaluation of present-day performance

3.2.1 Seasonal mean performance

Climatological biases in temperature and precipitation in the CMIP5-driven RCMs and their nested CPMs are assessed in this section.

Figures 16 and 17 show biases in near-surface air temperature in winter and summer, respectively. In these figures, and the similar ones in Sections 3.2.2 and 3.2.3, models are ordered according to the seasonal mean SST bias in their driving GCM, from most positive to most negative (Figure 6). This is done to reflect the importance of local SSTs for modulating the climate of the UK.

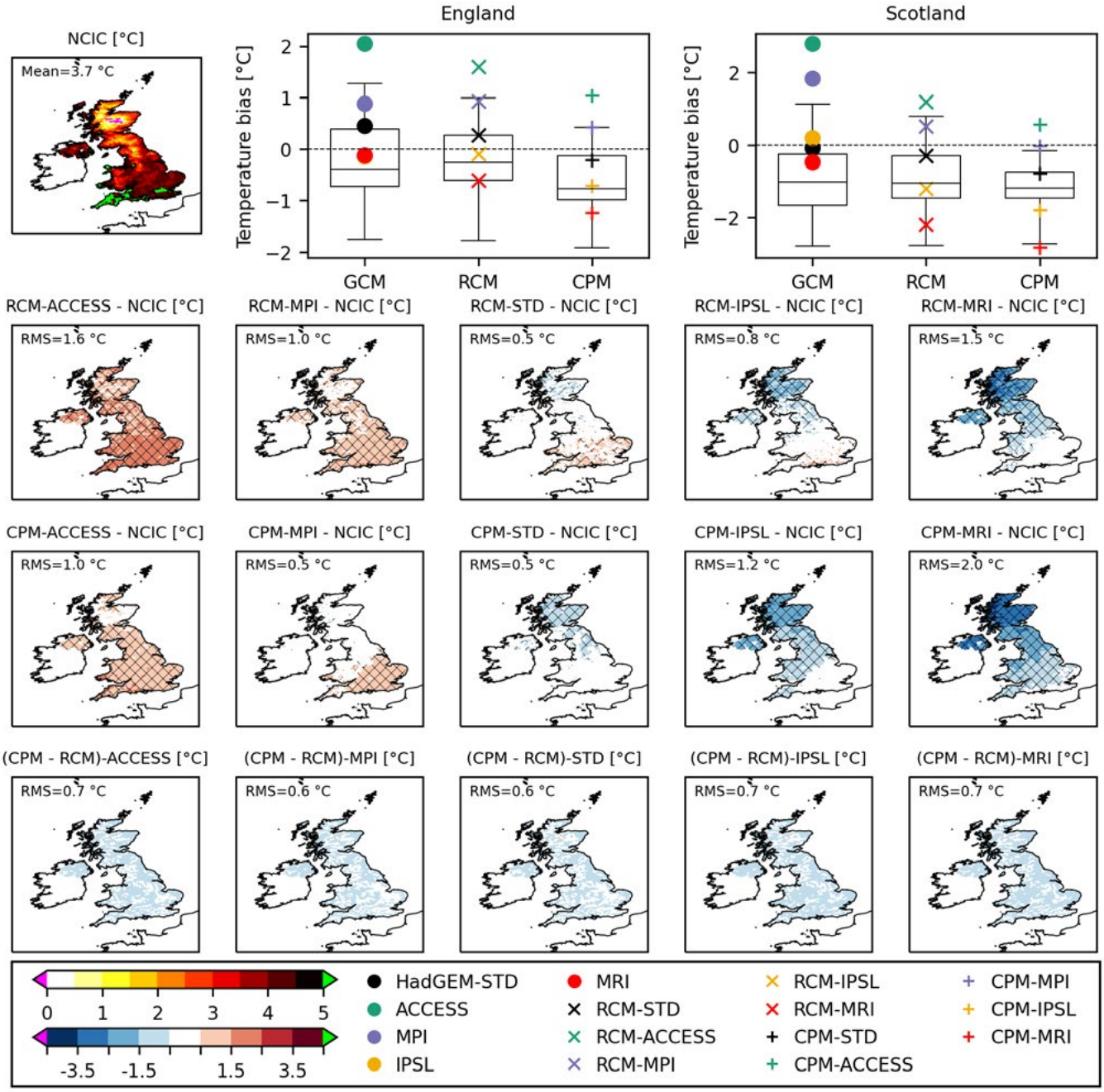

Figure 16. Biases in seasonal mean air temperature at 1.5m in winter for the baseline period (1980 – 2000). The top left panel shows the NCIC observations (Perry et al. 2009) on the 12 km RCM grid. The other panels on the top row show biases in regionally averaged winter mean temperature in the various CMIP5 GCMs and their nested regional models, for England and Scotland respectively. The box-and-whiskers indicate the distribution of biases in HadGEM-PPE, RCM-PPE and CPM-PPE: the box extends from the lower to the upper quartiles of the data, with the median shown by the solid horizontal line, and the whiskers show the full range of the data. Plots on the second row show spatial maps of winter mean temperature biases in the CMIP5-driven RCMs and RCM-STD, with equivalent plots for the CMIP5-driven CPMs and CPM-STD on the third row (the CPM data has been regridded onto the 12 km RCM grid). Hatched areas indicate where biases are significant compared to interannual variability at the 95% level, estimated using bootstrap resampling. Differences between CPMs and RCMs are shown on the bottom row. Note that models are ordered according to the seasonal mean SST bias in their driving GCM (Figure 6), from most positive (left) to most negative (right). The UK-wide mean or root-mean-square (RMS) bias is indicated in each panel as appropriate.

In winter, the sign of temperature biases in the CMIP5-driven RCMs are inherited from their driving global models (recall Figure 7), which are linked to SST biases in the Atlantic (Figure 6). Over Scotland, all CMIP5-driven RCMs produce lower temperatures than their driving GCMs; more snow over high ground in the RCMs (see Section 3.2.4.4 below) is consistent with this signal. This can lead to reduced biases (for RCM-MPI and RCM-ACCESS) or increased biases (for RCM-IPSL and RCM-MRI). In particular, RCM-MRI has a large

(and significant) cold bias in the far north, although there is one member of RCM-PPE that has a lower winter-mean temperature averaged over Scotland (and thus a worse cold bias). RCM-ACCESS has a larger warm bias across southern England than any other CMIP5-driven RCM (which is significant), stemming from the ACCESS GCM itself.

When the CMIP5-driven RCMs are down-scaled with the CPM, temperatures are further reduced across the UK. This leads to improved biases in CPM-MPI and CPM-ACCESS (less of a warm bias), but worsened biases in CPM-IPSL and CPM-MRI (more of a cold bias), particularly in the north. The bias in CPM-MRI is larger in magnitude than any in CPM-PPE. From the difference plots in the bottom row of Figure 16 it is apparent that the cooling signal is similar in all CPMs, regardless of the driving model, suggesting it is generated internally by the CPM. A contributing factor will be that the CPM has systematically less cloud cover than the RCM, with a corresponding reduction in downwelling longwave radiation (not shown).

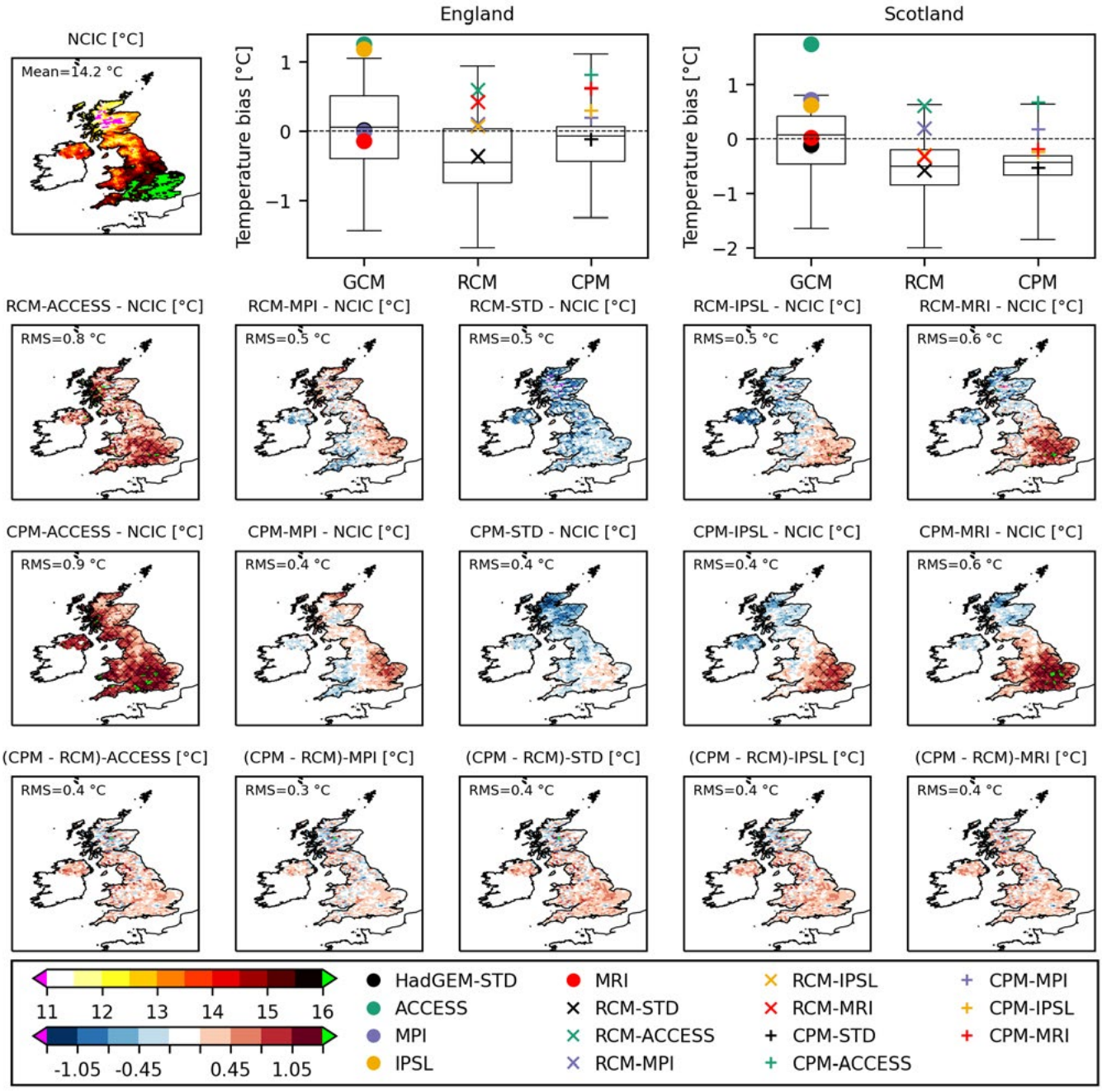

Figure 17. Biases in seasonal mean air temperature at 1.5m in summer for the baseline period (1980 – 2000). The layout of the plots is the same as in Figure 16.

As in winter, summer temperatures over Scotland are lower in the RCMs than their driving global models, which leads to reduced biases in all models except RCM-MRI. Over England, the RCMs driven by ACCESS and IPSL both have lower temperatures than their parent models, on average, whereas the converse is true for RCM-MRI. As a result, biases over England are smaller in RCM-ACCESS and RCM-IPSL than their driving models, but larger in RCM-MRI. Generally, biases in the RCMs are not significant compared to natural variability, apart from in RCM-MRI and RCM-ACCESS in southeastern England.

Over Scotland, summer temperatures are very similar in the CMIP5-driven CPMs and their parent RCMs, on average, but over England temperatures are higher in the CPMs, resulting in slightly larger biases, which can be significant. A factor here will be that the CPMs have drier soils in summer than their driving RCMs (see Section 3.2.4.3 below).

Seasonal mean precipitation biases in winter and summer are presented in Figures 18 and 19, respectively.

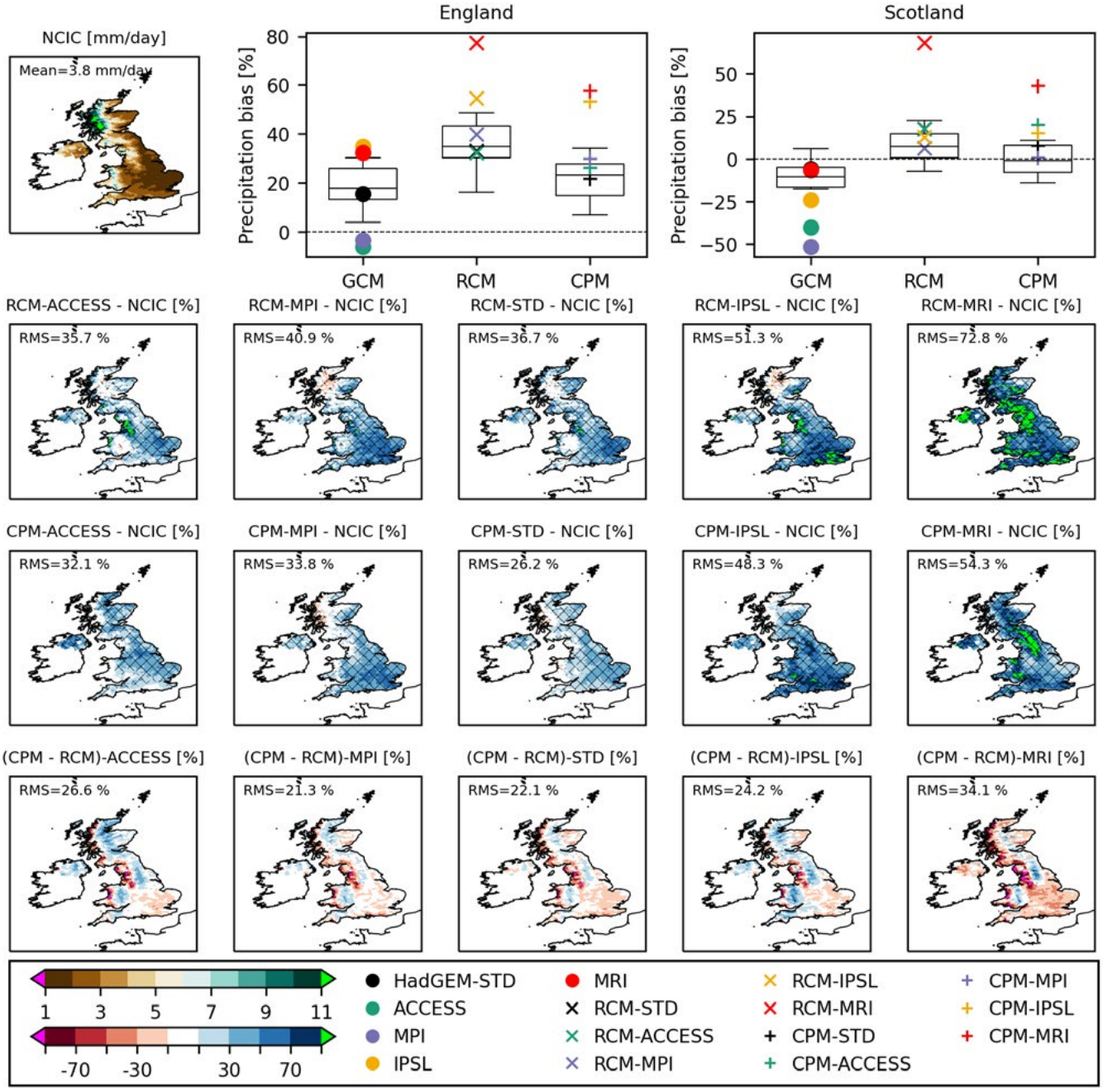

Figure 18. Biases in seasonal mean precipitation in winter for the baseline period (1980 – 2000). The layout of the plots is the same as in Figure 16.

All the CMIP5-driven RCMs produce much more winter precipitation across the UK than their driving global models. This is typical of RCMs, because their higher horizontal resolution enables them to better capture fine-scale motions (e.g. Jones et al. 1995). This increase in precipitation reduces the pre-existing dry bias in the north present in ACCESS, MPI and IPSL but enhances the wet bias over southeastern England seen in all CMIP5-4 GCMs (Figure 8). As for winter mean temperature (Figure 16), RCM-MRI again stands out, having a large (and significant) positive precipitation bias across the UK. Recall from Figure 5 that, in winter, the MRI model has an overly strong low-level south-westerly flow over the UK. Since the Scottish mountains are substantially higher in the RCM than the MRI GCM, this will lead to a strong orographic enhancement of precipitation in the RCM. Note that the bias in precipitation in RCM-MRI lies considerably outside the range of RCM-PPE across the UK.

Overall, winter precipitation biases in the CMIP5-driven CPMs are smaller than, or similar to, those in their driving RCMs, although a general wet bias persists. Biases are significant across much of the UK, and CPM-MRI and CPM-IPSL have larger biases than any member of CPM-PPE. Note that the CPMs tend to produce less precipitation along the western coast of the UK than their driving RCMs, with more precipitation further inland. This is potentially a consequence of the convection scheme in the RCM failing to advect winter showers across coastlines (Kendon et al. 2020). The CPMs also tend to be drier in southeast England, potentially a rain shadow effect caused by higher mountains to the west in the 2.2 km model.

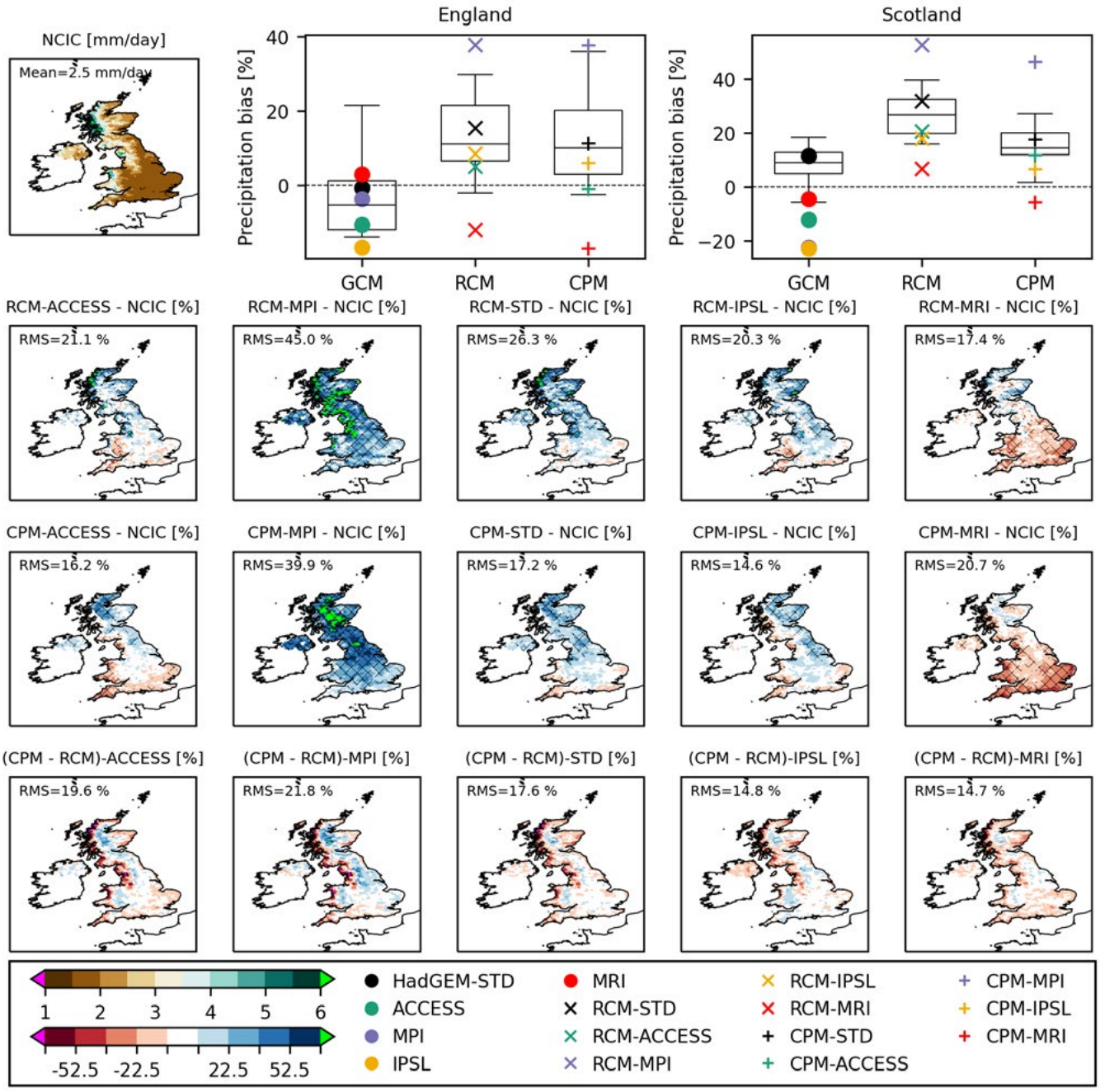

Figure 19. Biases in seasonal mean precipitation in summer for the baseline period (1980 – 2000). The layout of the plots is the same as in Figure 16.

In summer, the RCMs again produce more precipitation across the UK compared to their driving global models, on average. The exception is RCM-MRI which is drier than its parent model over England. The increase in precipitation leads to a reduced bias in RCM-IPSL compared to its driving model since IPSL has a dry bias across the UK (Figure 8), but an increased bias in RCM-MPI which is too wet, especially in the north. Averaged over the UK, the CMIP5-driven CPMs are all drier than their driving RCMs, with reduced biases except for CPM-MRI that has an increased dry bias over England. This is consistent with drier soils in summer in the CPMs compared to the RCMs (Section 3.2.4.3).

For all regional models except those driven by MPI, precipitation biases in summer are smaller than in winter. The MPI-driven models have larger positive biases than any member of the UKCP18 regional PPEs across the UK, particularly over Scotland, with biases that are significant compared to natural variability.

3.2.2 **Daily variability**

We now examine how well the CMIP5-driven regional models can simulate temperature and precipitation on daily timescales.

Figure 20 shows biases in the 1st percentile of the distribution of daily mean temperatures in winter, i.e. cold winter days. Note that the daily mean temperature is computed as an average of the daily minimum and maximum temperatures to match what is available from the NCIC observational dataset.

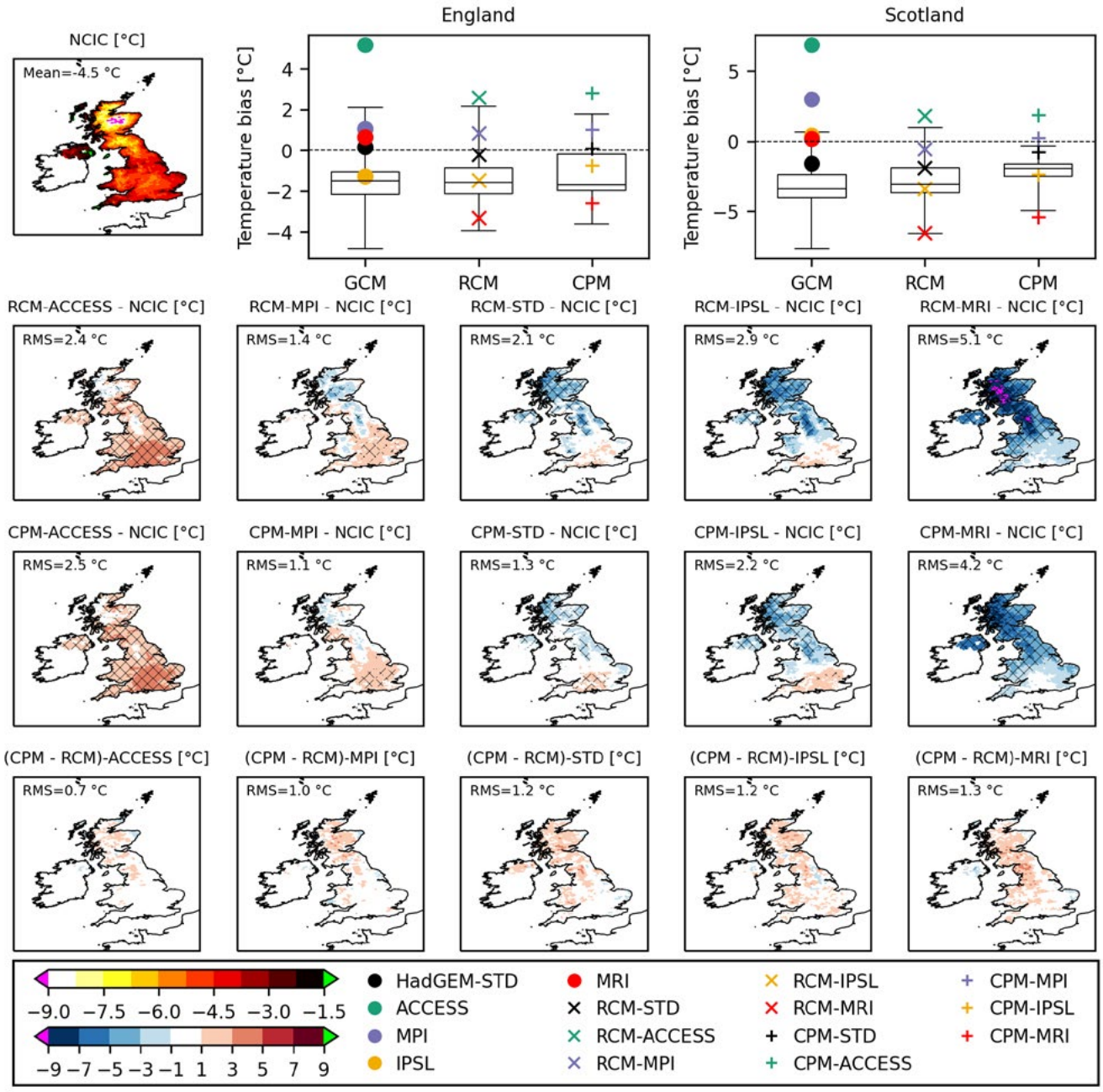

Figure 20. Biases in the temperature on cold winter days (defined as the 1st percentile of the distribution of daily mean air temperature at 1.5m in winter, where the daily mean temperature is computed as the average of the daily maximum and minimum temperatures) for the baseline period (1980 – 2000). The top left panel shows NCIC observations (Perry et al. 2009) on the 12 km RCM grid. The other panels on the top row show biases in the regionally averaged temperature on cold winter days in the various CMIP5 GCMs and their nested regional models, for England and Scotland respectively. The box-and-whiskers indicate the distribution of biases in HadGEM-PPE, RCM-PPE and CPM-PPE: the box extends from the lower to the upper quartiles of the data, with the median shown by the solid horizontal line, and the whiskers show the full range of the data. Plots on the second row show spatial maps of biases in the temperature on cold winter days in the CMIP5-driven RCMs and RCM-STD, with equivalent plots for the CMIP5-driven CPMs and CPM-STD on the third row (the CPM data has been regridded onto the 12 km RCM grid). Hatched areas indicate where biases are significant compared to interannual variability at the 95% level, estimated using bootstrap resampling. Differences between CPMs and RCMs are shown on the bottom row. Note that models are ordered according to the seasonal mean SST bias in their driving GCM (Figure 6), from most positive (left) to most negative (right). The UK-wide mean or root-mean-square (RMS) bias is indicated in each panel as appropriate.

The temperature on cold winter days is too low everywhere in the UK in RCM-MRI, particularly in the north where there is a large and significant cold bias (the seasonal mean performance of this model in Scotland was flagged previously; Figure 16), consistent with this model producing significant amounts of lying snow (see Section 3.2.4.4). Note there is one member of RCM-PPE with a similar negative bias. By contrast, cold winter days are significantly too warm in RCM-ACCESS, except over high ground, as in the ACCESS GCM itself. RCM-MPI has the smallest overall bias of the RCMs.

The CPMs predict slightly higher temperatures on cold winter days than their driving RCMs, particularly in the north. This is opposite to the behaviour for average winter temperatures where the CPMs were consistently cooler (Figure 16). This warming leads to reduced biases in CPM-MRI and CPM-IPSL on cold winter days compared to their parent RCMs, although note that biases in CPM-MRI are still large (and significant), lying outside the range of CPM-PPE in Scotland.

Biases in the temperature on hot summer days (defined as the 99th percentile of the distribution of daily mean summer temperatures) are shown in Figure 21. RCM-MPI is similar to RCM-STD (with a slightly smaller overall bias), with hot summer days being significantly too cold in Scotland. The other three CMIP5-driven RCMs have small biases in the north, but hot summer days are too hot in England, especially in RCM-ACCESS and RCM-MRI, which lie towards the upper end of the RCM-PPE distribution. Recall that summer mean temperatures over England were too high in these models too (Figure 17). This is consistent with these models having substantially drier soils in summer than the other two CMIP5-driven RCMs (see Section 3.2.4.3 below).

The nested CPMs all predict an increase in the temperature of hot summer days compared to their driving RCMs, across the UK. Drier soils in the CPMs are likely to be a contributing factor. CPM-MRI, CPM-ACCESS and, to a lesser extent, CPM-IPSL display a significant warm bias in southeastern England, with CPM-MRI and CPM-ACCESS having a large bias over England more generally (~3ºC), lying outside the range of CPM-PPE.

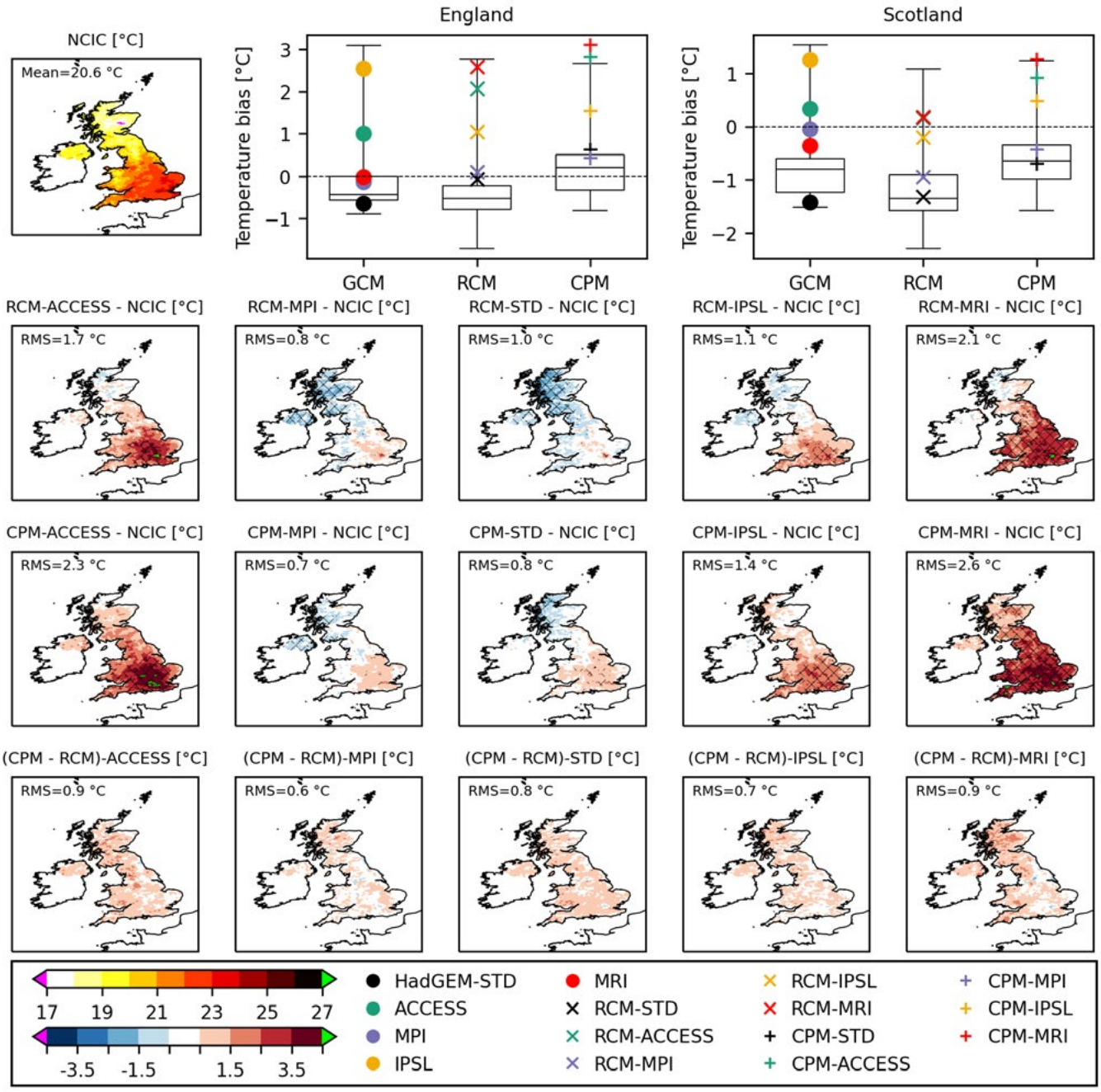

Figure 21. Biases in the temperature on hot summer days (defined as the 99th percentile of the distribution of daily mean air temperature at 1.5m in summer, where the daily mean temperature is computed as the average of the daily maximum and minimum temperatures) for the baseline period (1980 – 2000). The layout of the plots is the same as in Figure 20.

Biases in the fraction of wet days (defined as days where the accumulated precipitation exceeds 1 mm), the average wet-day intensity, and heavy daily precipitation (defined as the 99th percentile of all daily values) are shown in Figures 22, 23 and 24 for winter and Figures 25, 26 and 27 for summer.

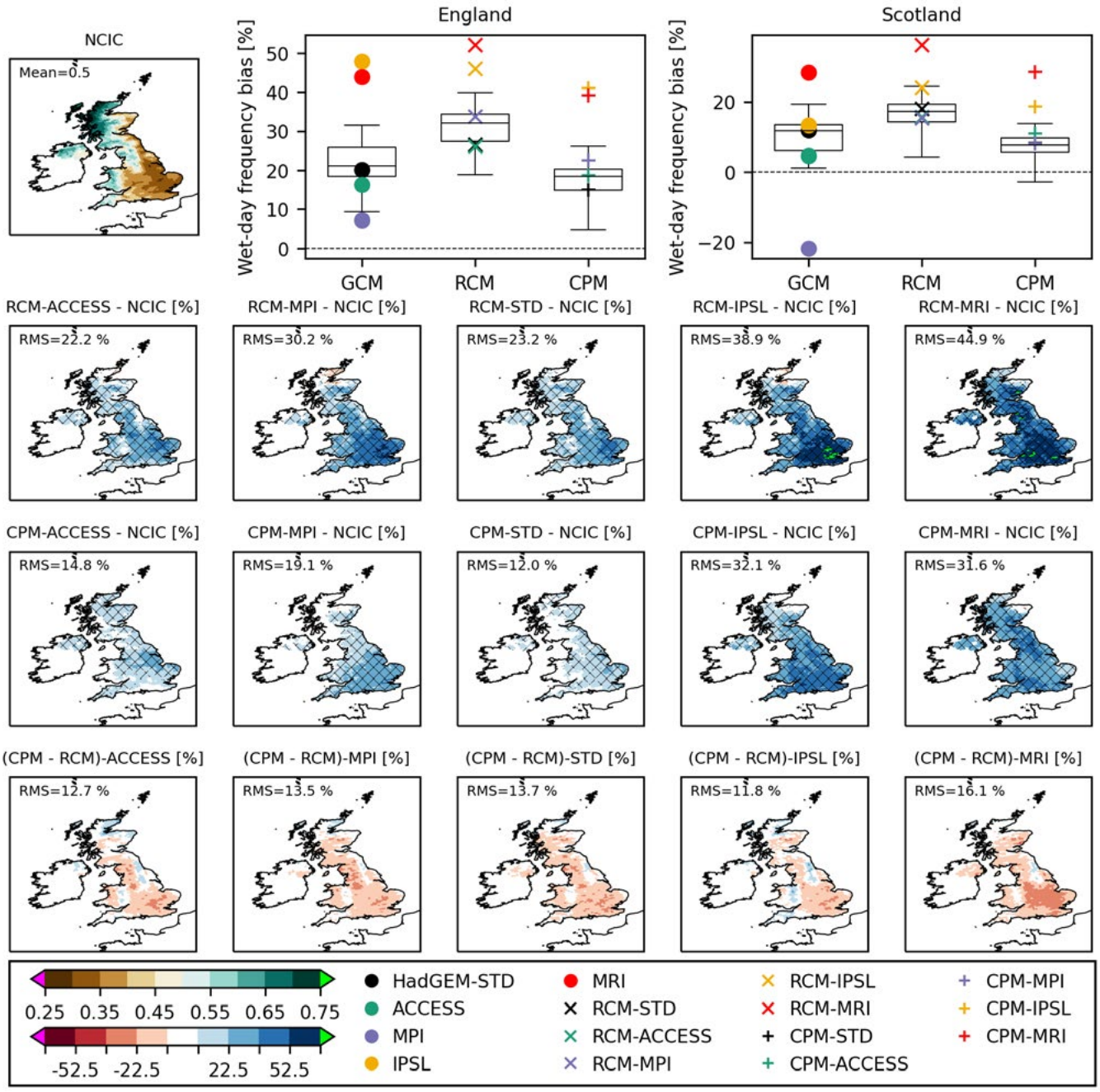

Figure 22. Biases in wet day fraction (defined as days where the precipitation accumulation exceeds 1 mm) in winter for the baseline period (1980 – 2000). The layout of the plots is the same as in Figure 20.

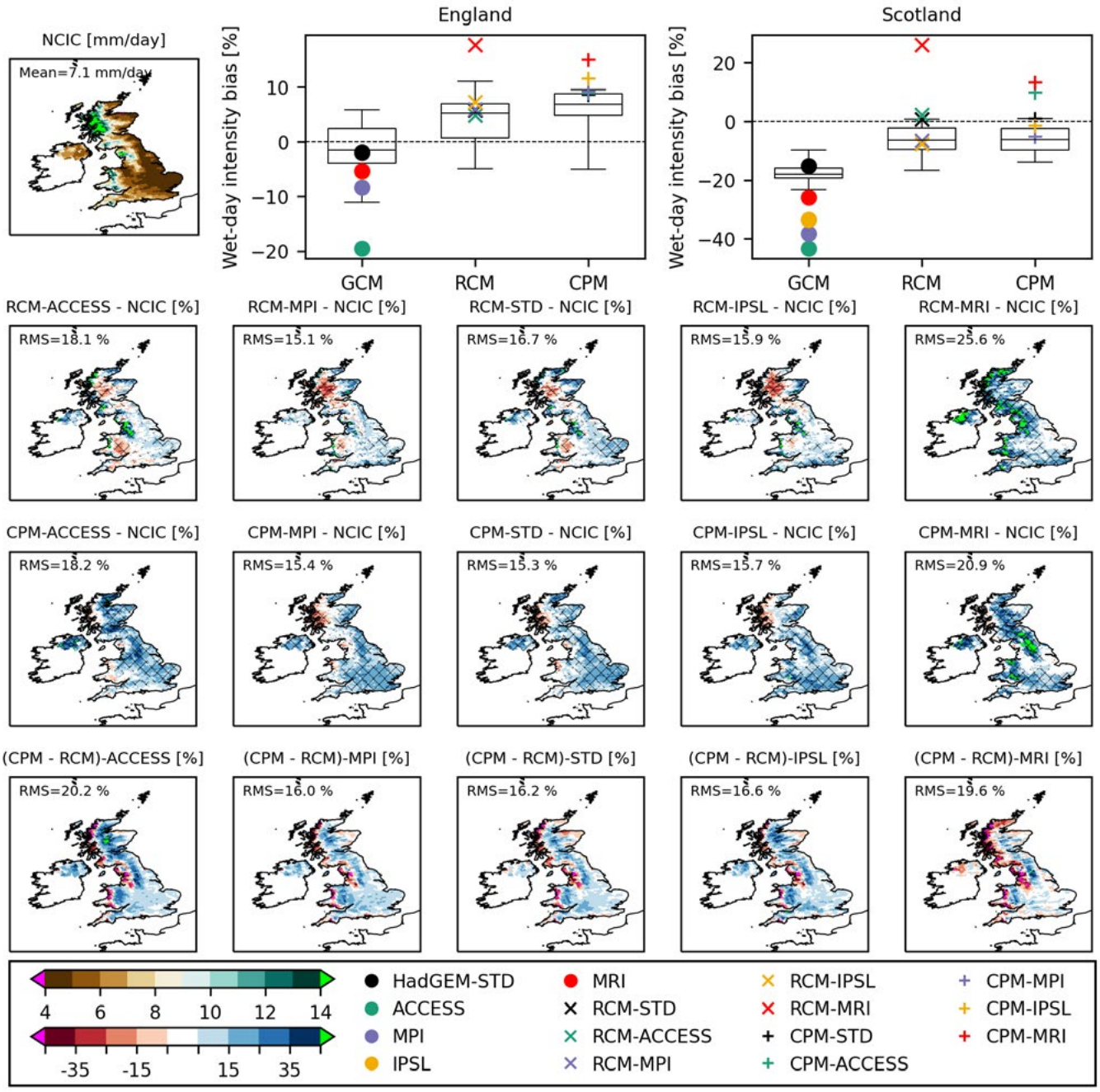

Figure 23. Biases in wet day intensity in winter for the baseline period (1980 – 2000). The layout of the plots is the same as in Figure 20.

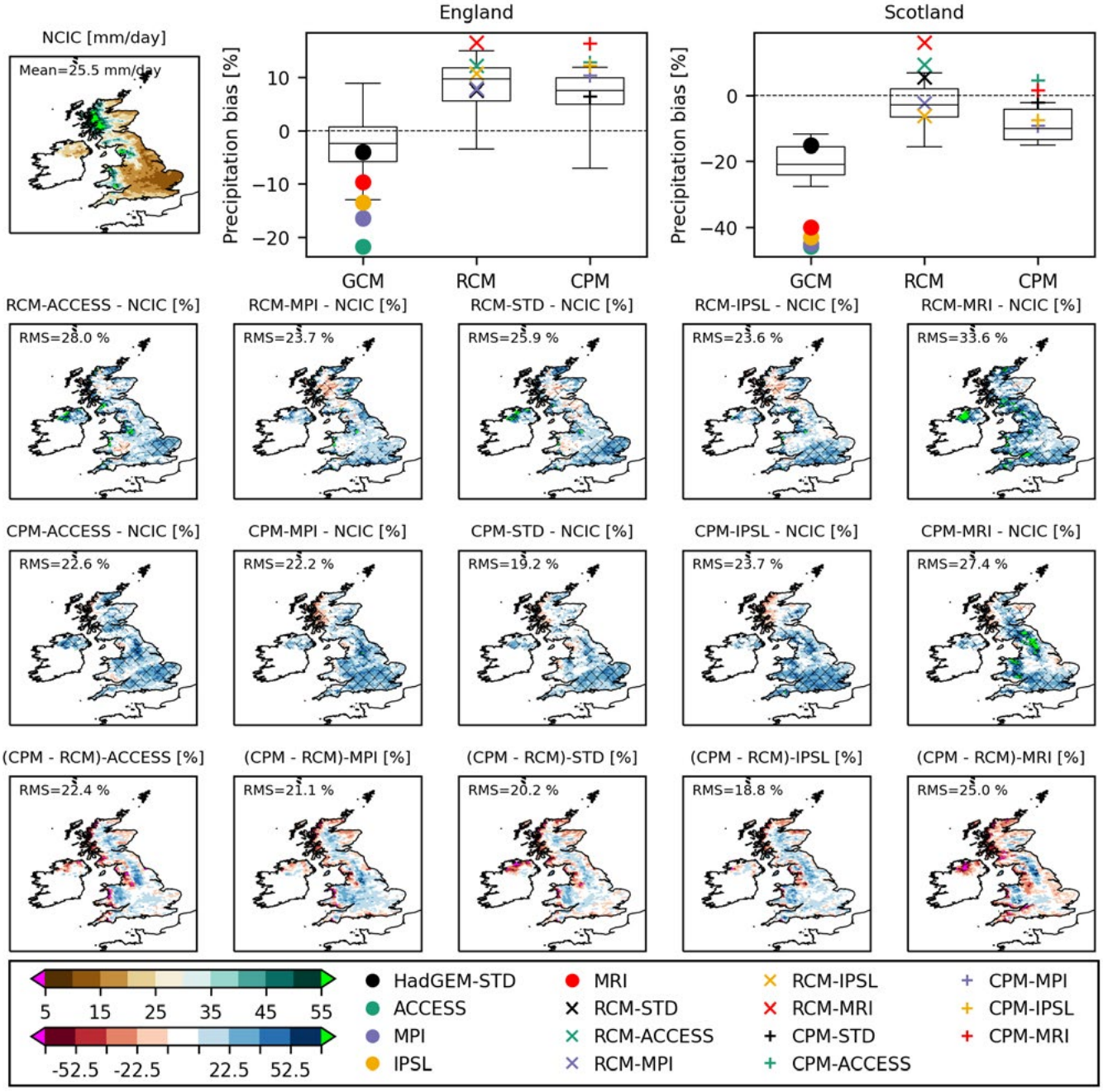

Figure 24. Biases in heavy daily precipitation amounts (defined as the 99th percentile of the distribution of daily precipitation, including all values) in winter for the baseline period (1980 – 2000). The layout of the plots is the same as in Figure 20.

In winter, all RCMs have significant positive biases in wet-day fraction across the UK (except the very far north in some of the models), with the ordering of the CMIP5-driven models by UK-wide RMS bias being the same as for winter mean precipitation (Figure 18). Note that RCM-IPSL and RCM-MRI have a larger bias in wet-day fraction than any member of RCM-PPE across England, largely inherited from their driving GCMs. This is also true over Scotland for RCM-MRI.

The RCMs tend to under-estimate wet-day intensity and heavy daily precipitation over mountainous regions, except for RCM-MRI which has a positive bias in both metrics over much of the UK, particularly in the west and south where biases can be significant. Again, biases in RCM-MRI lie above the upper end of the RCM-PPE distribution. The performance of the other CMIP5-driven RCMs is similar and comparable to RCM-PPE. Too many wet days with too much rainfall on those days in RCM-MRI is consistent with the pronounced wet bias in winter mean precipitation in this model (Figure 18).

In all nested CPMs, wet-day fractions in winter tend to be lower and thus closer to observed values, although a general positive bias remains, especially in the models driven by IPSL and MRI. These models have larger biases than any member of CPM-PPE across much of the UK, which are significant. There is a general reduction in wet-day intensity and heavy precipitation in the vicinity of coastlines in the CMIP-5 driven CPMs, with an enhancement further inland, most notably over high ground. This leads to a systematic reduction of biases in CPM-MRI compared to RCM-MRI, but signals are mixed for the other model pairs.

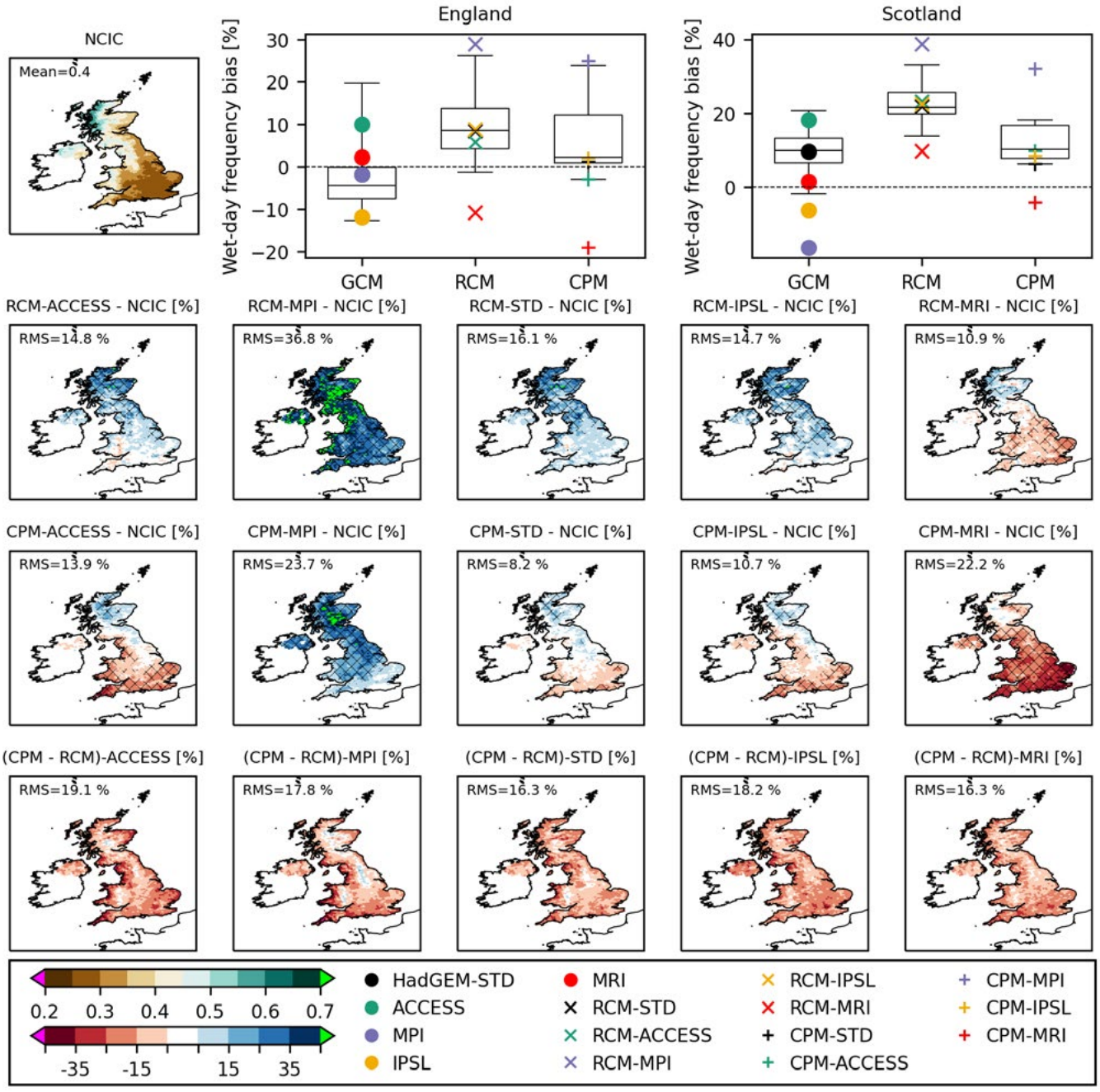

Figure 25. Biases in wet day fraction (defined as days where the precipitation accumulation exceeds 1 mm) in summer for the baseline period (1980 – 2000). The layout of the plots is the same as in Figure 20.

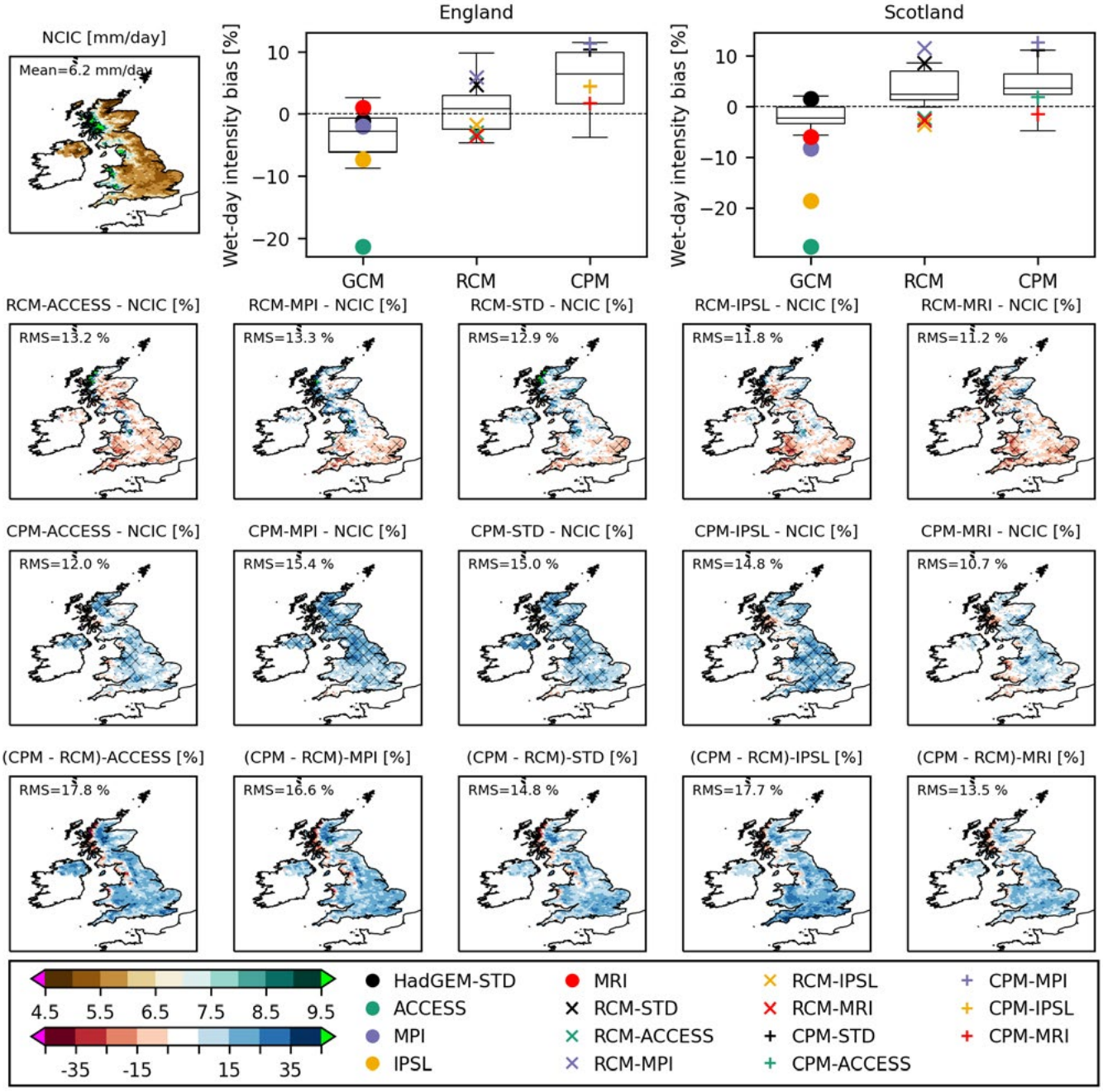

Figure 26. Biases in wet day intensity in summer for the baseline period (1980 – 2000). The layout of the plots is the same as in Figure 20.

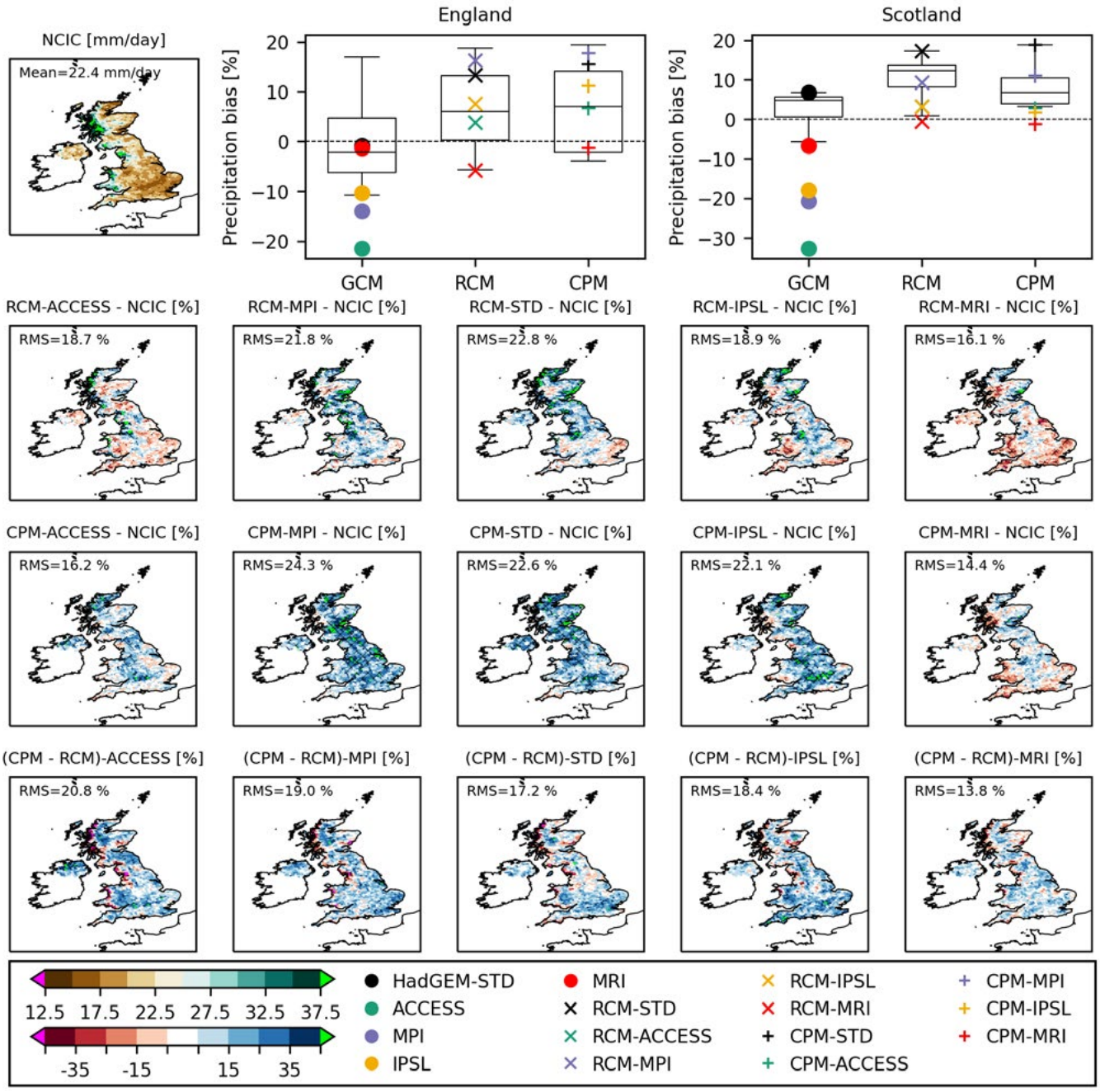

Figure 27. Biases in heavy daily precipitation amounts (defined as the 99th percentile of the distribution of daily precipitation, including all values) in summer for the baseline period (1980 – 2000). The layout of the plots is the same as in Figure 20.

Biases in wet-day fraction in the CMIP5-driven RCMs are more mixed in summer than in winter. For example, RCM-MPI exhibits a significant positive bias in the number of wet days across the UK, lying outside the range of RCM-PPE, whereas RCM-MRI has a negative bias over England (significant in places). The RCMs tend to under-estimate the intensity of wet summer days over high ground (as in winter; Figure 23), but also over low-lying regions such as southeast England. Similar patterns are evident in biases in heavy daily precipitation in summer although signals are less clear. Biases in both metrics are comparable in size to those in RCM-PPE and largely insignificant. For RCM-MRI, too few wet days with too little rainfall on those days matches with the dry bias in summer mean precipitation over England in this model (Figure 19). Overall, the RCMs have smaller biases in summer than in winter for the three daily precipitation metrics considered, except for wet-day fraction in RCM-MPI.

Down-scaling the RCMs with the CPM leads to a reduction in the number of wet summer days across the UK, generally leading to better overall agreement with observations (as measured by the UK-wide RMS bias). The exception is CPM-MRI in the south because the negative bias in wet-day fraction in the parent RCM is exacerbated, becoming significant over England and Wales. CPM-MPI still has a significant wet bias across much of the UK, lying outside the range of CPM-PPE. Wet-day intensity and heavy daily precipitation in summer tend to increase over England in the CPMs, which can either reduce or increase biases, depending on the model pair. Biases in both metrics are similar to those in CPM-PPE.

To summarise how well the CMIP5-driven regional models are able to reproduce the observed shape of the full distribution of daily mean temperatures and precipitation amounts, we use the Perkins skill score (PSS; Perkins et al. 2007). This is a simple measure of the degree of overlap between two distributions, ranging from 0 for no overlap to 1 for a perfect match. Figure 28 displays PSS values for daily temperature and precipitation from the CMIP5-driven regional models, with the distribution of scores from RCM-PPE and CPM-PPE shown for comparison.

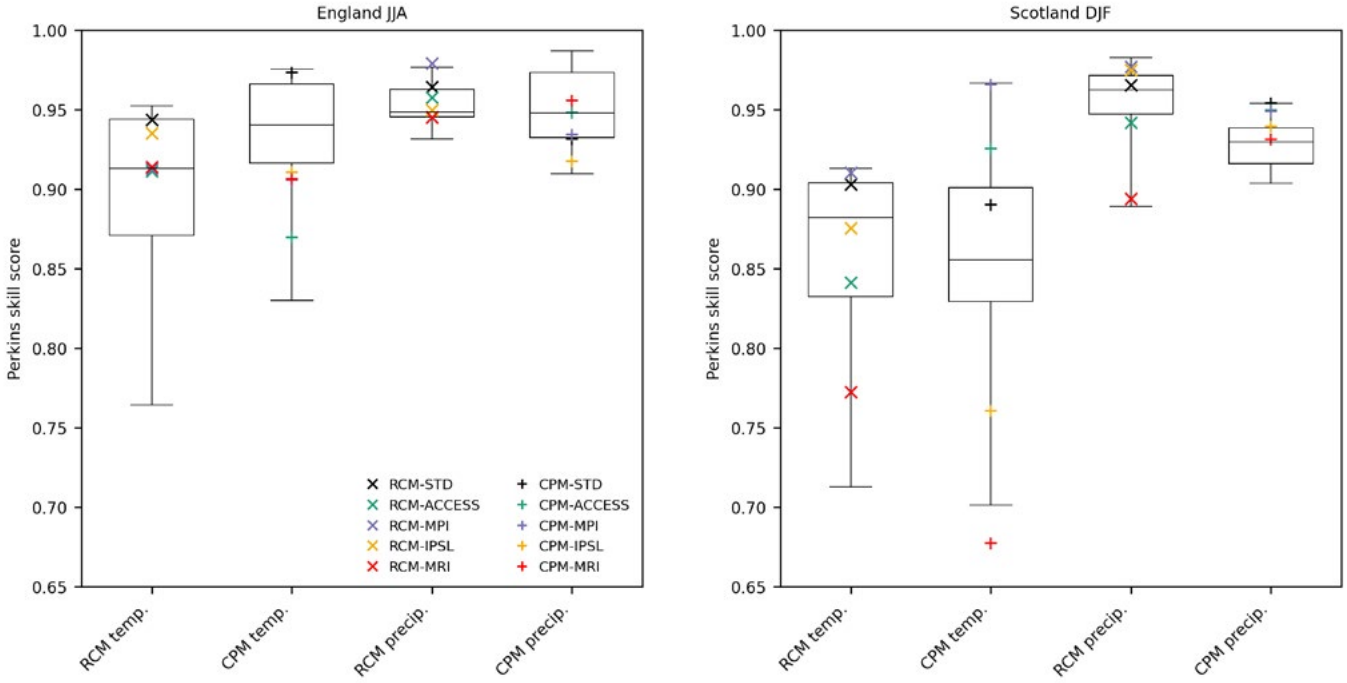

Figure 28. Perkins skill score (PSS) values measuring how well the CMIP5-driven RCMs and CPMs can reproduce the observed distributions of daily mean air temperature at 1.5m and precipitation over the baseline period (1980 – 2000). Before constructing distributions, NCIC observations (Perry et al. 2009) and CPM data were regridded onto the 12 km RCM grid. Daily mean temperature values were computed as the average of the daily maximum and minimum temperatures, then assigned to a set of equally spaced bins of width 0.5ºC spanning the range of the data. For precipitation, the bins used were 0.0, 0.05, 0.16, 0.18, 0.27, 0.41, 0.62, 0.95, 1.45, 2.2, 3.4, 5.1, 7.8, 11.9, 18.1, 27.5, 42.0, 63.9, 97.4, 148.4, 500.0 mm/day, and the counts in each bin were multiplied by the average rain-rate for that bin to give the contribution of each bin to the total rainfall. PSS values for the CMIP5-driven regional models are shown for England in summer (left panel) and Scotland in winter (right panel). The distributions of PSS values from RCM-PPE and CPM-PPE are shown by the box-and-whiskers: the box extends from the lower to the upper quartiles of the data, with the median shown by the solid horizontal line, and the whiskers show the full range of the data.

The various CMIP5-driven regional models generally show good skill in capturing the shape of the observed distributions, with PSS values above 0.8 in all but 3 cases. Note that the PSS values always lie within the ranges of RCM-PPE and CPM-PPE, except for winter temperatures over Scotland in CPM-MRI. In other words, the CMIP5-driven regional models produce distributions of daily temperature and precipitation comparable to those obtained from existing UKCP18 regional simulations.

Over Scotland in winter, RCM-MRI produces distributions of daily temperatures and precipitation that are skewed towards lower temperatures and higher accumulations than observed, respectively, leading to low PSS values (note there is one member of RCM-PPE that gives lower PSS values though). This is consistent with the large (and significant) cold and wet biases seen in the north of the UK in this model in this season (Figures 16 and 18). The nested CPM-MRI reduces the contribution to the total rainfall from days with high rainfall accumulations, shifting the precipitation distribution back towards observations (consistent with reduced biases in Figures 18 and 24 and higher PSS compared to RCM-MRI), but winter days are generally colder than in the driving RCM (consistent with Figure 16), further skewing the distribution towards lower temperatures and leading to the lowest PSS value of any model. The distribution of temperatures in CPM-IPSL is skewed in a similar way, but to a lesser extent, which is why this model also has a low PSS value for winter temperatures in Scotland (although there is one member of CPM-PPE with a lower value).

3.2.3 **Hourly precipitation variability**

We now examine how well models can represent precipitation variability on hourly timescales. Given that CPMs have repeatedly been shown to offer added value over RCMs for short-duration precipitation (e.g. Chan et al. 2014, Kendon et al. 2017, Vanden Broucke et al. 2019, Ban et al. 2021, Caillaud et al. 2021), only the 2.2 km models are considered in this section. As discussed previously (Section 2.4), we only use CPM data that has been regridded onto a 5km OSGB grid to reduce the impact of any unphysical precipitation extremes generated by the model dynamics.

Figures 29 and 30 show biases in heavy hourly precipitation (defined as the 99.95th percentile of all hourly values, corresponding to approximately one event per season) in winter and summer, respectively.

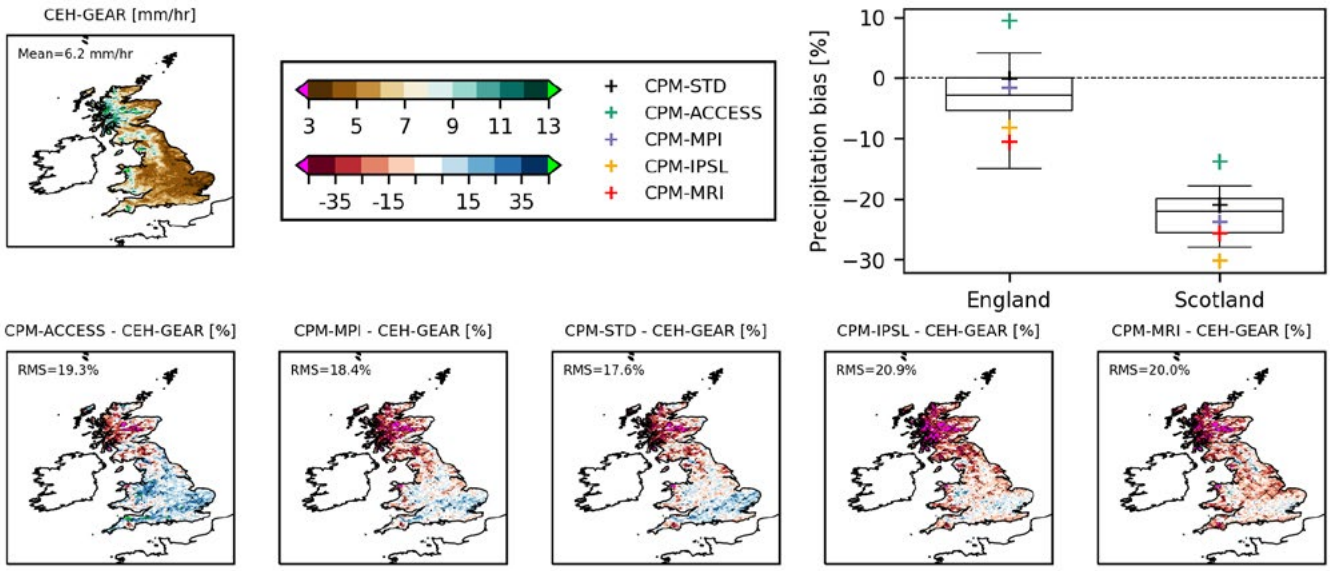

Figure 29. Biases in heavy hourly precipitation amounts (defined as the 99.95th percentile of hourly precipitation, including all values) in winter for the baseline period (1980 – 2000). The top left panel shows CEH-GEAR observations (Lewis et al. 2018) for the period 1990 – 2014, regridded onto the 5km OSGB grid. Note that Northern Ireland is not included in the CEH-GEAR dataset. The top right panel shows biases in regionally averaged heavy hourly precipitation in the various CMIP5-driven CPMs and CPM-STD. The box-and-whiskers indicate the distribution of biases in CPM-PPE: the box extends from the lower to the upper quartiles of the data, with the median shown by the solid horizontal line, and the whiskers show the full range of the data. Plots on the second row show spatial maps of biases in heavy hourly precipitation in the CMIP5-driven CPMs and CPM-STD (the CPM data has been regridded onto the 5km OSGB grid). Hatched areas indicate where biases are significant compared to interannual variability at the 95% level, estimated using bootstrap resampling. Note that models are ordered according to the seasonal mean SST bias in their driving GCM (Figure 6), from most positive (left) to most negative (right). The mean or root-mean-square (RMS) bias across Great Britain is indicated in each panel as appropriate.

In winter, the CPMs tend to under-estimate the intensity of heavy hourly precipitation events over high ground, particularly in Scotland where all CMIP5-driven CPMs and CPM-STD have a significant bias compared to interannual variability. Biases in CPM-ACCESS and CPM-IPSL are smaller and larger than in any member of CPM-PPE, respectively. Over England, the majority of CPMs also under-estimate heavy hourly precipitation on average, but biases are smaller and generally not significant. CPM-ACCESS is an exception, as this model over-estimates the intensity of these events over England, again lying above the upper end of the CPM-PPE distribution.

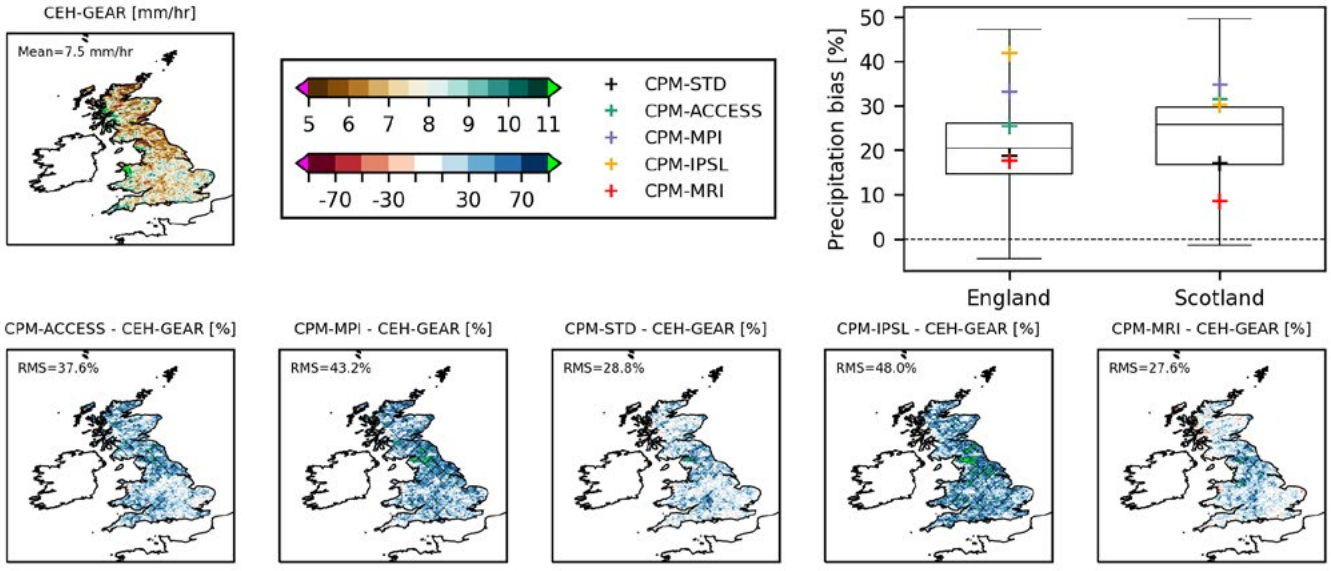

Figure 30. Biases in heavy hourly precipitation amounts (defined as the 99.95th percentile of hourly precipitation, including all values) in summer for the baseline period (1980 – 2000). The layout of the plots is the same as in Figure 29.

In summer, CPMs generally over-estimate the intensity of heavy hourly precipitation events across the UK. There is a large spread in biases across CPM-PPE, and all the CMIP5-driven CPMs lie within the ensemble range. Of the CMIP5-driven CPMs, CPM-MRI has the smallest overall bias (largely insignificant), and CPM-IPSL the largest (significant across much of England and Wales).

As a final comment, note that the spatial patterns of biases in heavy hourly precipitation amounts for each season are similar across the various CMIP5-driven CPMs. This possibly suggests that the biases are inherent to the CPM itself, with the driving GCM having less of an influence on intense hourly events.

The diurnal cycle of precipitation in the CMIP5-driven CPMs is shown in Figure 31, along with radar observations. We focus on England in summer months since this is when we expect the signal of the diurnal cycle to be clearest. The observations suggest an afternoon peak around 15 UTC, whereas rainfall in the CPMs peaks earlier, around 13 UTC in all models except CPM-MRI which has a later peak closer to the observations. However, the amplitude of the diurnal cycle is clearly too low in this model, lying below the observations (and all other models) at all hours of the day, consistent with the dry bias in summer mean precipitation over England (Figure 19). The other CMIP5-driven CPMs produce diurnal cycles that lie within the range of CPM-PPE, except for the secondary rainfall peak in the early hours of the morning in CPM-MPI.

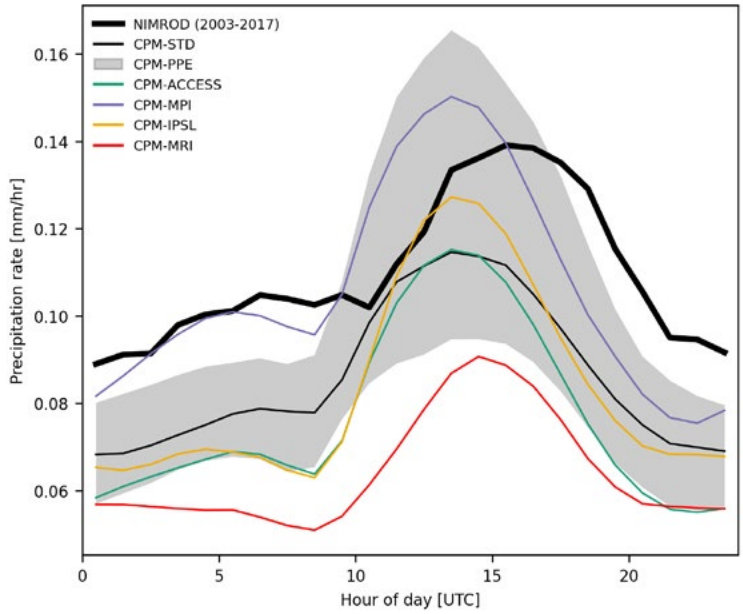

Figure 31. Diurnal cycle of precipitation, averaged over England in summer, for the baseline period (1980 – 2000). Results are shown for the CMIP5-driven CPMs and CPM-STD, along with the CPM-PPE range. NIMROD radar observations (Harrison et al. 2000) for the period 2003 – 2017 are shown for comparison. All data has been regridded onto the 5km OSGB grid.

Figure 32 evaluates the statistical distribution of hourly precipitation rates in the various CPMs for each season, considering all land points in Great Britain (because the CEH-GEAR dataset does not include Northern Ireland). Overall, the CMIP5-driven CPMs mostly generate distributions that lie within the range spanned by CPM-PPE. There are some exceptions, such as CPM-ACCESS in spring which produces a greater contribution to the total rainfall from high rain-rates, with less coming from low rain-rates. Nonetheless, the key point is that the ability of the CPM to better reproduce the observed distribution of hourly rainfall compared to the RCM is preserved when boundary conditions are supplied by alternative GCMs.

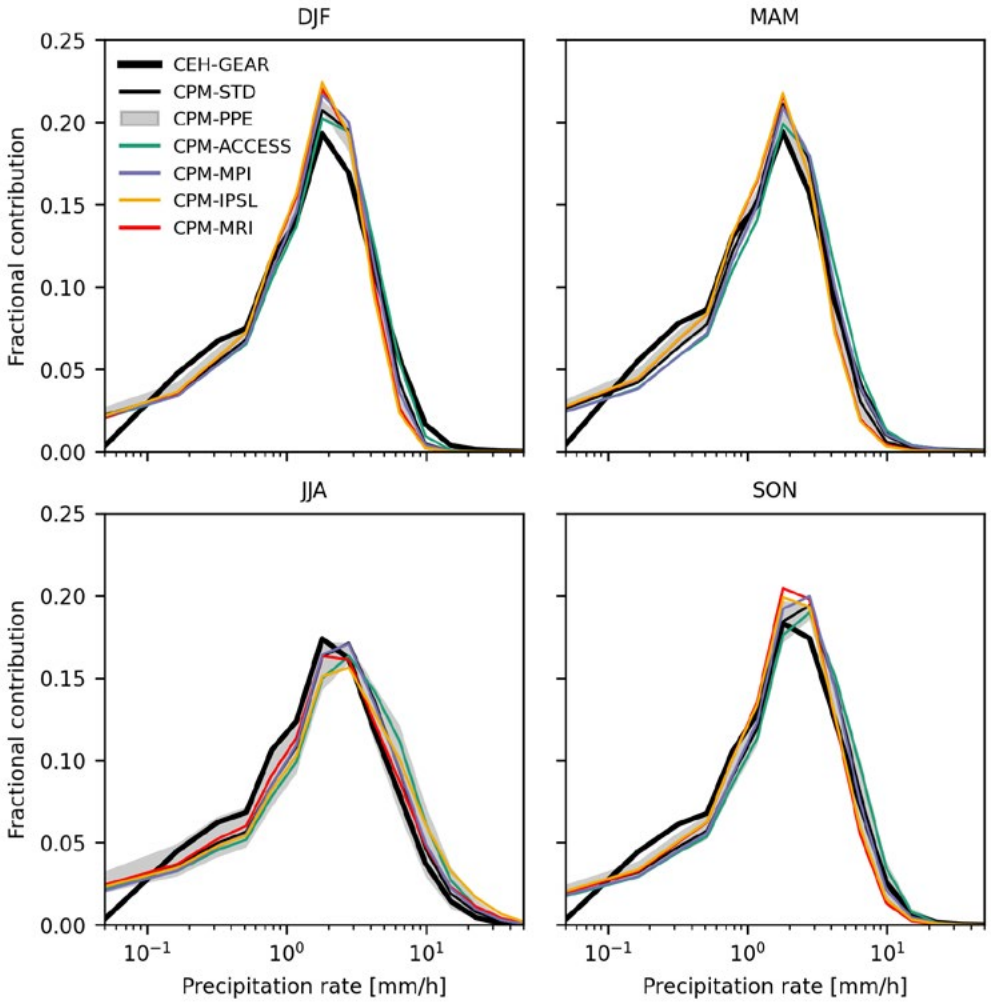

Figure 32. Fractional contribution of different hourly precipitation rates to the total precipitation over Great Britain, for each season. Precipitation rates for all hours (wet and dry) were placed in bins of 0.0, 0.1, 0.23, 0.41, 0.62, 0.95, 1.4, 2.2, 3.4, 5.1, 7.8, 11.9, 18.1, 27.5, 42.0, 63.9, 97.4, 148.0, 500.0 mm/hr, and the counts in each bin were multiplied by the average rain-rate for that bin to give the contribution of each bin to the total rainfall. Results are shown for the CMIP5-driven CPMs and CPM-STD, along with the CPM-PPE range. CEH-GEAR observations (Lewis et al. 2018) for the period 1990 – 2014 are also shown for comparison. All data has been regridded onto the 5km OSGB grid.

3.2.4 **High impact events**

3.2.4.1 **Extreme hourly precipitation**

To characterise the extreme tail of the hourly precipitation distribution, we use the method described in Shooter and Brown (2024) to calculate 30-year return levels. This is an evolution of the approach used in the previous UKCP Local science report (Kendon et al. 2021). In short, generalized Pareto distributions are fitted spatially to the upper tail of hourly rainfall using the 98th percentile for wet hours as a threshold level. Stationary distributions are fitted to the 20-year baseline and future periods separately, for all grid-points simultaneously, using the Generalised Additive Modelling (GAM) framework developed by Youngman (2018). The mean rainfall for each grid-box is used as a spatial covariate for each period.

Estimates of 30-year return levels derived from hourly precipitation data from the CPMs are shown in Figures 33 and 34, for winter and summer respectively. Note that we have not yet computed 30-year return levels from observational datasets using the method of Shooter and Brown (2024), so we cannot assess model biases. Instead, we focus on how the CMIP5-driven CPMs compare to CPM-PPE.

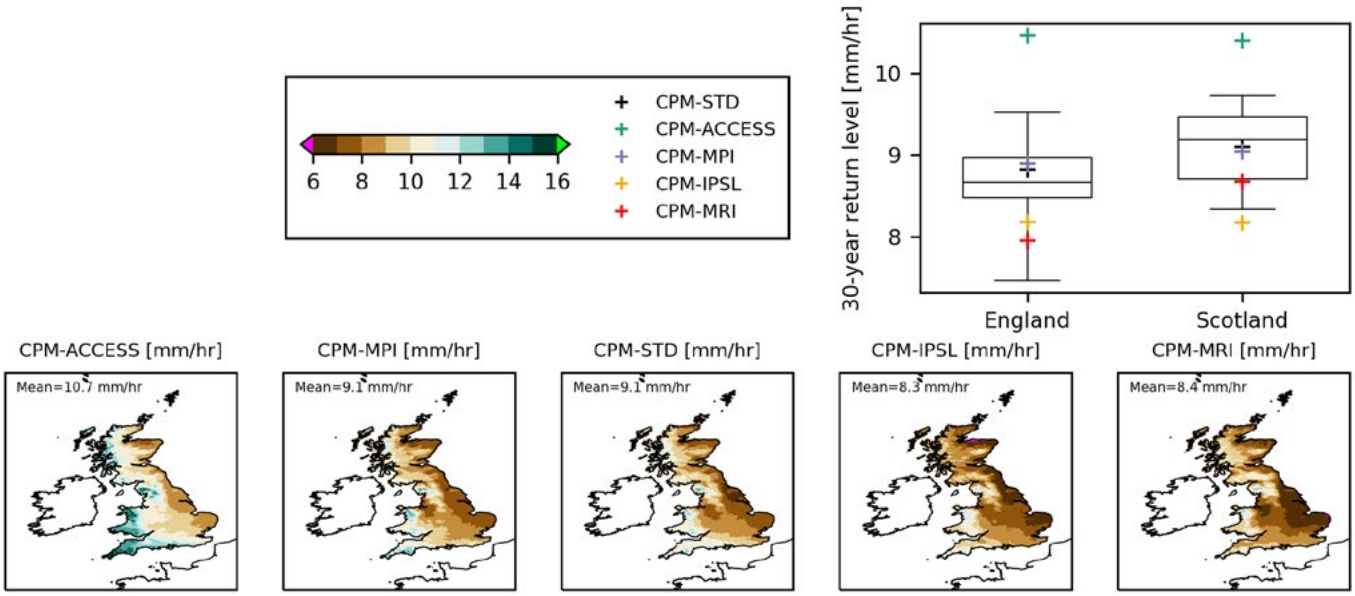

Figure 33. 30-year return level of hourly precipitation in winter for the baseline period (1980 – 2000). The top right panel shows regionally averaged return levels in the various CMIP5-driven CPMs and CPM-STD. The box-and-whiskers indicate the distribution of return levels in CPM-PPE: the box extends from the lower to the upper quartiles of the data, with the median shown by the solid horizontal line, and the whiskers show the full range of the data. All data has been regridded onto the 5km OSGB grid before computing return levels. Plots on the second row show spatial maps of 30-year return levels in the CMIP5-driven CPMs and CPM-STD (on the 5km OSGB grid). Note that models are ordered according to the seasonal mean SST bias in their driving GCM (Figure 6), from most positive (left) to most negative (right). The average 30-year return level over Great Britain is indicated in each panel.

In winter, the intensity of rare rainfall extremes is greater in CPM-ACCESS than any other CPM (recall that this model produces the largest heavy hourly precipitation amounts too; Figure 29), with particularly high 30-year return levels found in the west of the UK. Previous work suggests that CPM-PPE under-estimates the 30-year return level, especially in the north (see Figures 3.5.3 and 3.5.4 in Kendon et al. 2021), hence CPM-ACCESS may have smaller biases. The other CMIP5-driven CPMs tend to lie within the CPM-PPE range, apart from CPM-IPSL for Scotland which favours less severe rainfall extremes. Note that the ordering of the CMIP5-driven CPMs by their regional-average 30-year return levels is the same as for heavy hourly precipitation (Figure 29).

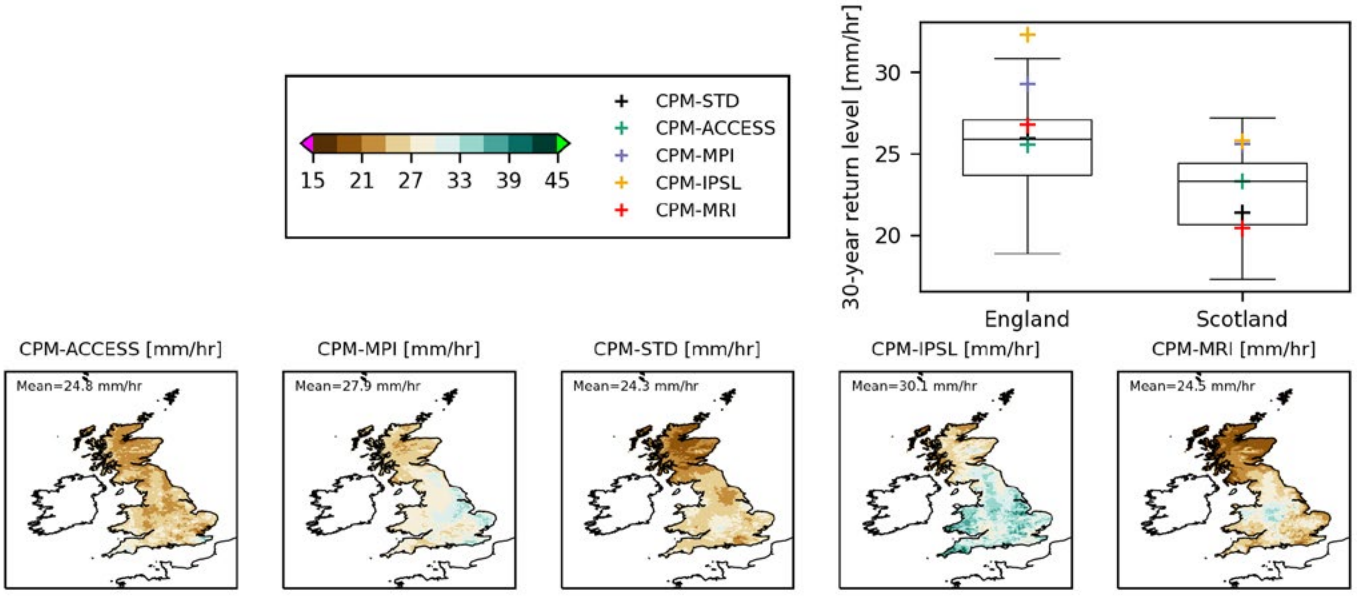

Figure 34. 30-year return level of hourly precipitation in summer for the baseline period (1980 – 2000). The layout of the plots is the same as in Figure 33.

In summer, 30-year return levels are considerably higher than in winter, with a larger spread across CPM-PPE. Generally, the CMIP5-driven CPMs lie within the range of CPM-PPE; the only exception is CPM-IPSL which produces more intense rare extremes over England than any other CPM (this model had the largest positive bias in heavy hourly precipitation of all the CMIP5-driven CPMs for this region; Figure 30). Note that upper-end values for the 30-year return level in the CPM-PPE distribution in Figure 34 are higher than those presented in Kendon et al. (2021; see their Figures 3.5.2-3.5.4), because hourly precipitation data was regridded onto the 12 km RCM grid in Kendon et al. (2021), whereas we are using CPM data on a 5 km grid.

3.2.4.2 **Hot and cold spells**

The Met Office issues high temperature warnings based on multi-day temperatures; the threshold for public health is typically around 30°C for daily maximum temperature. We thus define a hot spell to be when the daily maximum temperature is above 30°C for two or more consecutive days. Similarly for low temperatures, a cold spell is said to occur when the daily mean temperature is below +2°C for two or more consecutive days. We also define intense cold spells using a more severe threshold of -2°C.

Figure 35 shows the number of hot spells, averaged over England. We focus on this region as hot spells only really occur in the southeast of the UK (and are still relatively rare). The CPM driven by MRI systematically predicts the highest number of hot spells of all the models, with a large positive bias compared to NCIC observations. This is consistent with summer mean temperatures and hot summer day temperatures being too high in this model in southern England (Figures 17 and 21). The CPMs driven by ACCESS and IPSL also over-estimate the number of hot spells but to a lesser extent. Note that all the CMIP5-driven CPMs except CPM-MRI lie within the range of CPM-PPE, which encompasses the observations.

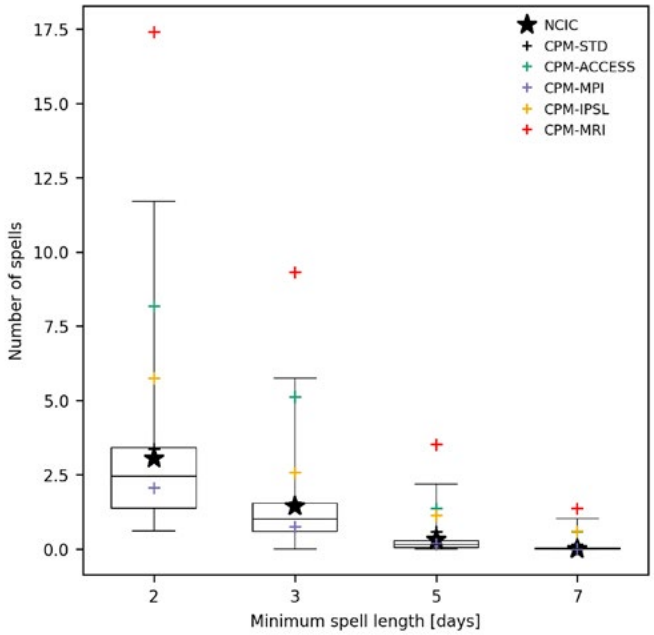

Figure 35. Frequency of hot spells over England in the baseline period (1980 – 2000), for a range of different minimum spell lengths. Results from the CMIP5-driven CPMs and CPM-STD are shown, along with observed values from NCIC. The distribution of hot spell frequencies in CPM-PPE is shown by the box-and-whiskers: the box extends from the lower to the upper quartiles of the data, with the median shown by the solid horizontal line, and the whiskers show the full range of the data. All data has been regridded onto the 5km OSGB grid.

Cold spells in the UK occur mostly over high ground in Scotland, with intense cold spells being less frequent than cold spells. The number of cold and intense cold spells, averaged over Scotland, is shown in Figure 36. The CPM driven by MRI again stands out as having the largest numbers of both types of event, substantially over-estimating the observed numbers. This is consistent with CPM-MRI having a large cold bias in winter mean temperature (Figure 16) and the temperature of cold winter days (Figure 20) in the north of the UK. This model produces large amounts of lying snow over Scotland (see Section 3.2.4.4) which will be a contributing factor. CPM-IPSL also has a positive bias in the number of cold and intense cold spells, performing comparably to CPM-STD. The CPMs driven by ACCESS and MPI give similar results to each other, slightly under-predicting the number of cold and intense cold spells for shorter spell lengths but converging towards observations as the minimum spell length increases. Note that these models lie outside the range of CPM-PPE, as do the observed values.

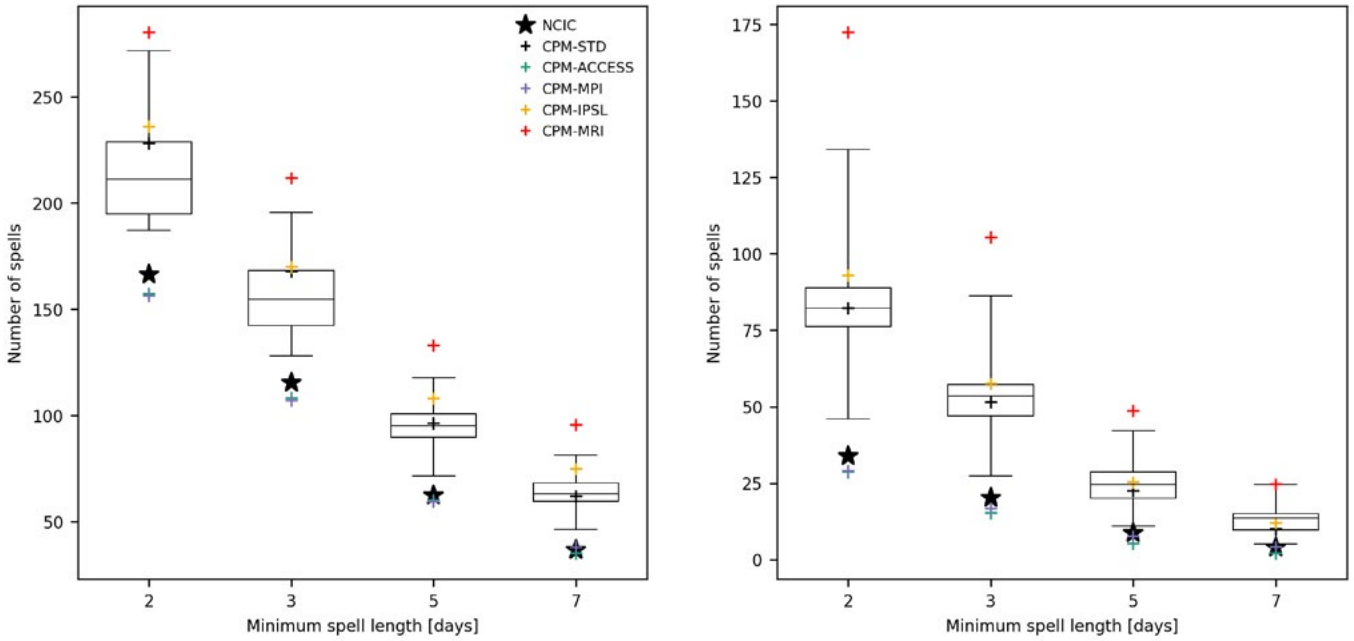

Figure 36. Frequency of cold (left panel) and intense cold (right panel) spells over Scotland in the baseline period (1980 – 2000), for a range of different minimum spell lengths. The layout of the plots is the same as in Figure 35.

As a final comment, there is not always a simple correspondence between biases in the number of hot or cold spells and seasonal mean temperature biases. For example, CPM-ACCESS has a larger warm bias in average summer temperatures than CPM-MRI over England (Figure 17), consistent with drier soils, but fewer hot spells (Figure 35). Similarly, winter mean temperatures over Scotland are higher in CPM-ACCESS than CPM-MPI (Figure 16) yet they predict very similar numbers of cold and intense cold spells (Figure 36). This is because other factors also contribute to differences in the number of hot or cold spells between models, such as differences in the day-to-day variability of temperature and large-scale variability (i.e. the sequence of weather patterns and their persistence) inherited from the driving global model.

3.2.4.3 **Soil moisture**

Soil moisture provides an important control on near-surface air temperatures, especially for England in the summer months when evapotranspiration becomes limited by the available soil moisture, hence we focus on this region here. Figure 37 shows the annual cycle of soil moisture, averaged over England, for the top 1 m of soil. The top 1 m of soil (referred to as the root zone) is most relevant for transpiration because land cover in the UK is mainly classified as grass and, for this surface type, 86% of the modelled root distribution lies within this layer (Best et al. 2011). This diagnostic is not available from the CMIP5-4 GCMs so only results from the RCMs and CPMs are presented in Figure 37 (even if root-zone soil moisture was available from the various GCMs, a comparison would be difficult as they all use very different land surface schemes, whereas the RCMs and CPMs both use JULES).

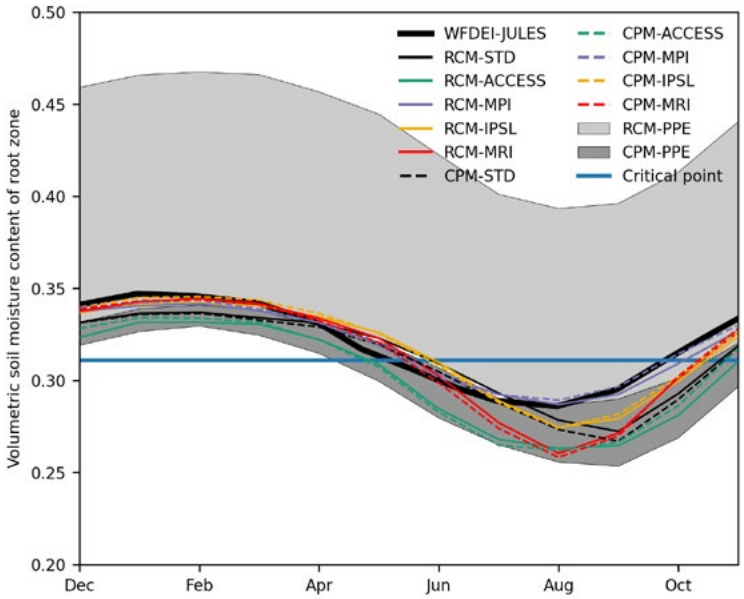

Figure 37. Annual cycle of soil moisture in the top 1 m of soil, averaged over England, for the baseline period (1980 - 2000). Results from the RCMs and CPMs are shown, along with the annual cycle constructed from WFDEI-JULES data (Weedon et al. 2014), which is a proxy for the observed soil moisture. All CPM data has been regridded onto the 12 km RCM grid before spatial averaging. The horizontal blue line indicates the critical level below which transpiration from vegetation becomes limited by the available soil moisture.

In RCM-PPE parameters in the land surface scheme are perturbed, leading to wide variations in soil moisture across the ensemble (Murphy et al. 2018), with RCM-STD having the driest soils. Soil moisture is similar in CPM-PPE members as no land surface parameter perturbations are applied. The CMIP5-driven RCMs and CPMs use the same land surface configuration as RCM-STD and CPM-STD, respectively.

Soils are drier in summer in RCM-ACCESS and RCM-MRI than in the other CMIP5-driven RCMs, consistent with these models having higher summer mean temperatures over England (Figure 17) and larger positive biases in the temperature of hot summer days (Figure 21). Note that, except for RCM-MPI, soil moisture in summer months is lower in the CMIP5-driven RCMs than in RCM-STD (and thus any member of RCM-PPE) and soils are too dry compared to WFDEI-JULES.

When the CMIP5-driven RCMs are down-scaled further with the CPM, the amplitude of the annual cycle of soil moisture is increased, with the CPMs having wetter soils in winter and drier soils in summer. Drier soils in summer are likely due to the more intense but intermittent nature of rainfall in explicit-convection models (e.g. Berthou et al. 2020, Halladay et al. 2024), and are a likely driver of higher summer mean temperatures and higher temperatures on hot summer days over England in the CPMs compared to their driving RCMs (Figures 17 and 21).

3.2.4.4 **Snow**

Lying snow in the UK is mostly found on high ground in Scotland in winter, hence we examine snow in the models for this region only. Observations of lying snow are available from NCIC, but these are subjective in nature, based on whether an observer judges the ground to be more than half covered by snow. Therefore, we do not assess the performance of the CMIP5-driven regional models using these observations, but instead compare their behaviour with the existing UKCP18 RCM and CPM ensembles which have already been deemed plausible (these models were compared with NCIC snow observations in Kendon et al. 2021).

Figure 38 shows the annual cycle of snowfall amount and lying snow, averaged over Scotland, as well as the fraction of Scotland land area covered by snow. To compute this latter quantity, a threshold must first be applied to decide whether a grid box qualifies as being covered by snow or not. In Kendon et al. (2021) a threshold of 0.02 mm was used to define a day of lying snow; we adopt the same threshold here (noting that our results are qualitatively unchanged when using different thresholds ranging from 0.01 to 1 mm).

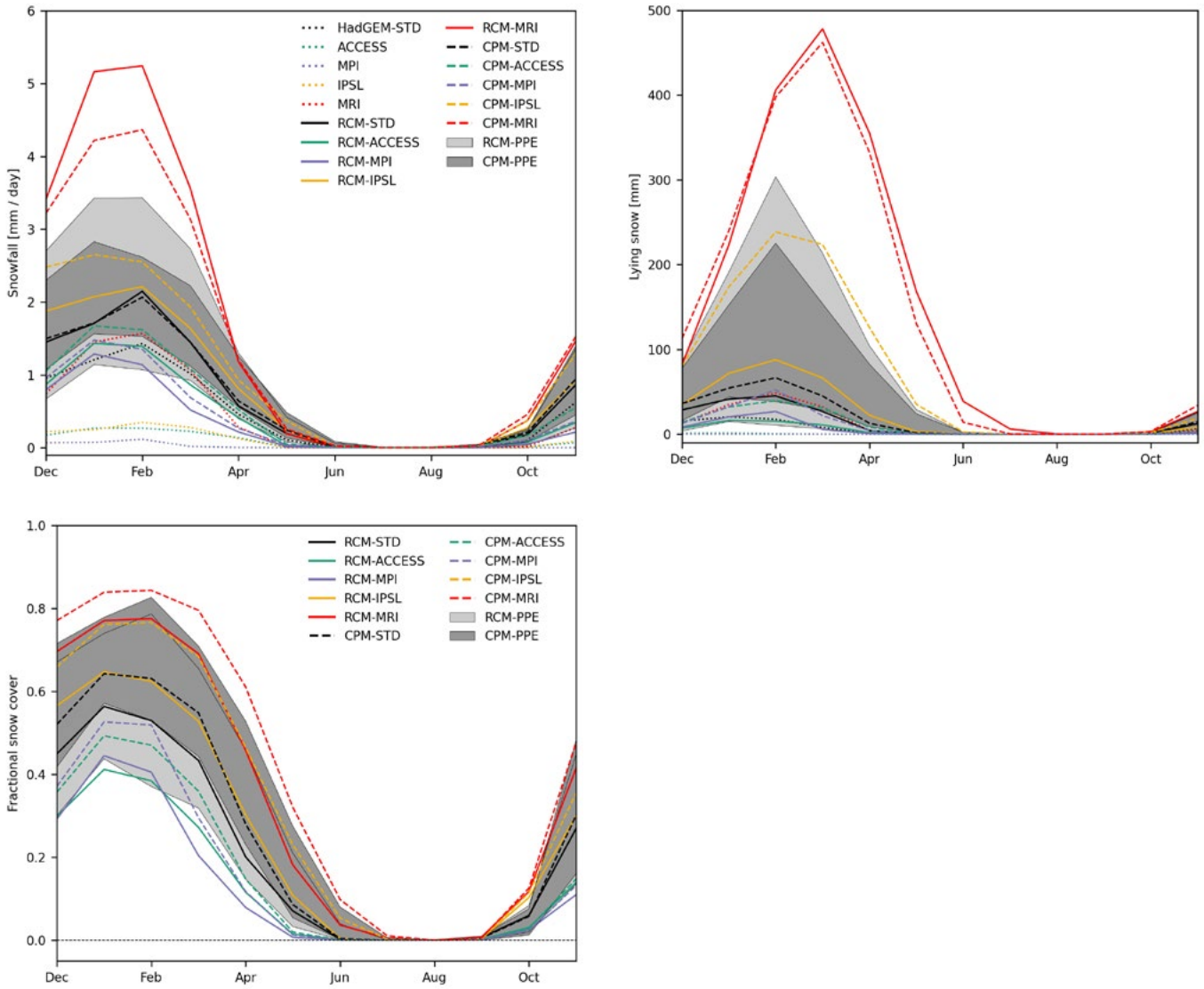

Figure 38. Annual cycle of snowfall (top left) and lying snow (top right), averaged over Scotland, for the baseline period (1980 – 2000). Results from GCMs, RCMs and CPMs are shown (although note that the lying snow diagnostic is not available from IPSL) and all data has been regridded onto a common n96 grid (with spacings of 1.875º and 1.25º in the longitudinal and latitudinal directions, respectively) before spatial averaging. Note that a snow density of 250 kg/m^3 has been assumed to convert the units of lying snow to mm. The bottom left panel shows the annual cycle of the fraction of Scotland covered by snow in the RCMs and CPMs only (since this is computed using daily data that is not available from the CMIP5-4 GCMs). This has been calculated by applying a threshold of 0.02 mm to decide whether grid boxes are snow covered or not on each day, where all CPM data was first regridded onto the 12 km RCM grid.

All the CMIP5-driven RCMs produce more snowfall in winter than their driving global models, commensurate with the general increase in precipitation upon down-scaling. Higher mountains, and thus lower air temperatures, in the RCMs will also be conducive to more snowfall and snow on the ground. Snowfall amounts in RCM-MRI are significantly greater than in any other model, in part because this model produces more winter precipitation over Scotland (recall the large wet bias in the north of the UK in Figure 18), but also because the fraction of precipitation falling as snow is higher, consistent with this model having lower air temperatures than the other RCMs in the lower troposphere (below 500 hPa), on average (not shown). Winter snowfall in the other CMIP5-driven RCMs lies within the range of RCM-PPE.

Apart from the MRI model, further down-scaling of the CMIP5-driven RCMs with the CPM leads to an additional increase in snowfall over Scotland, despite winter precipitation in these CPMs being similar to that in their driving RCMs, on average (Figure 18). This is because a greater fraction of precipitation falls as snow in the CPMs compared to the RCMs (not shown). Again, lower air temperatures associated with increased elevation will be a contributing factor. The annual cycle of snowfall in all CMIP5-driven CPMs except CPM-MRI is comparable to CPM-PPE, whereas CPM-MRI produces substantially more snowfall than any member of this ensemble in winter and early spring.

The increased snowfall amounts in the CMIP5-driven regional models lead to more snow on the ground than in their driving global models (noting that a lying snow diagnostic is not available from IPSL). This is consistent with lower winter temperatures in the north of the UK (Figure 16) because the presence of snow will raise the surface albedo, reflecting more incident shortwave radiation and enabling lower temperatures and lying snow to persist for longer (the so-called snow albedo feedback). Lying snow amounts in the CMIP5-driven RCMs and CPMs are comparable to RCM-PPE and CPM-PPE, respectively, apart from those driven by MRI which produce much more snow on the ground than any other model. This is consistent with these models having the largest cold biases in winter mean temperature (Figure 16) and the temperature of cold winter days (Figure 20), and the CPM producing too many cold spells (Figure 36) over Scotland.

In both regional models driven by MRI, snow cover persists throughout spring and into early summer, which is not seen in any other model. This has the potential to induce persistent temperature biases via snow albedo feedback effects, which could lead us to question the plausibility of temperature projections derived from these models. However, the magnitude of the snow albedo feedback is likely to depend more on the area of land covered by snow, rather than the snow depth itself. Figure 38 suggests that the fraction of Scotland covered by snow in RCM-MRI and CPM-MRI is comparable to some of the members of RCM-PPE and CPM-PPE, albeit the more extreme ones. This is further reinforced by Figure 39 which compares snow cover in Scotland in May and June in CPM-MRI with the member of CPM-PPE that produces the most snow: although snow amounts are clearly much larger in CPM-MRI, the spatial coverage is similar. Therefore, despite the presence of lying snow late in the year in the MRI-driven models, it is possible that snow albedo effects will not be implausibly strong compared to (some of) the existing UKCP18 regional models.

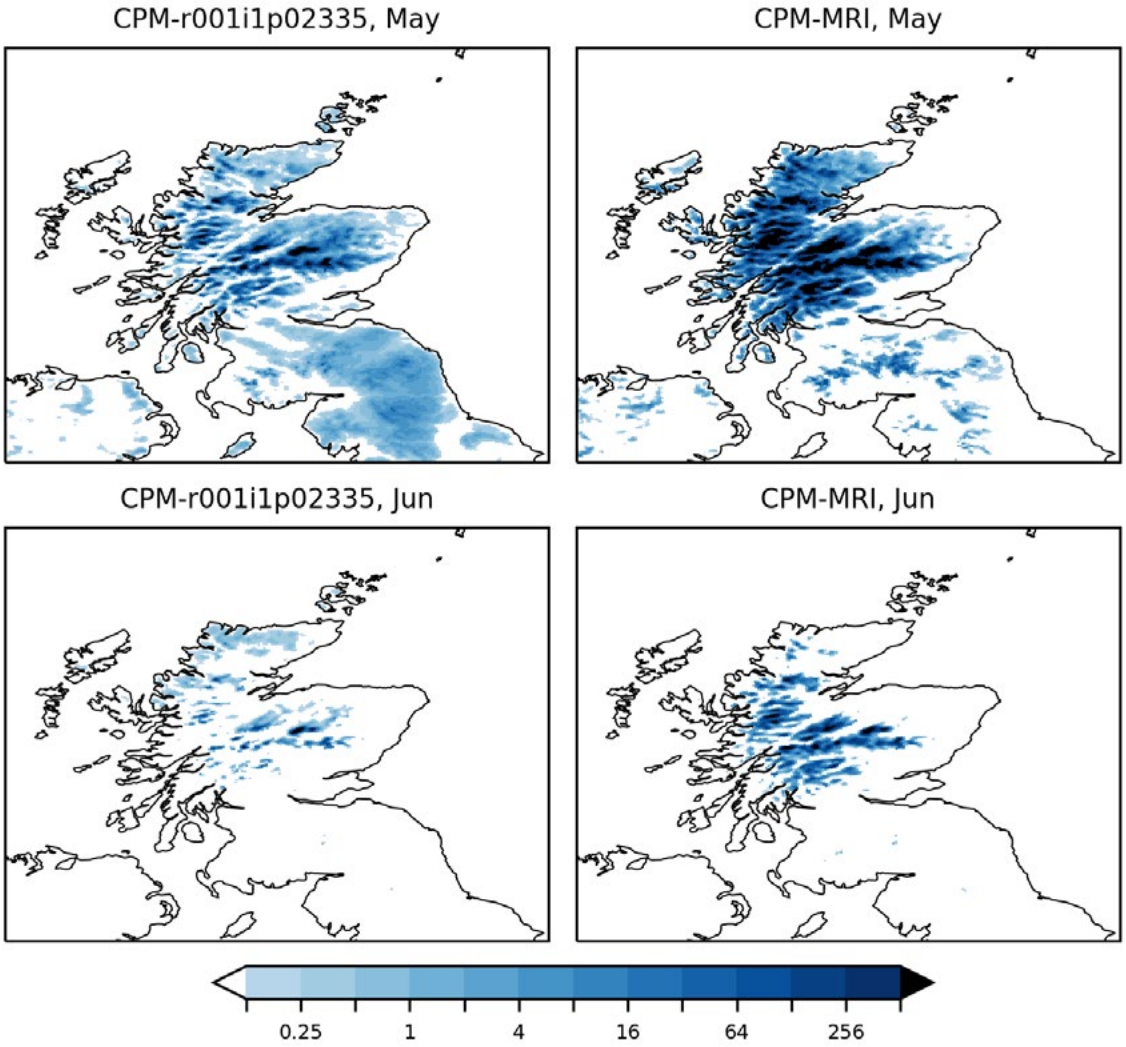

Figure 39. Monthly mean lying snow [mm] in Scotland in May (top row) and June (bottom row), comparing the CPM-PPE member that produces the most snow on the ground (left column) with CPM-MRI (right column). All data is on the native 2.2 km CPM grid.

4 Summary of present-day performance

In preceding sections, biases in the CMIP5-driven regional models have been assessed for a broad selection of metrics relating to temperature and precipitation, across a range of timescales. Before moving on to examine future projections from these models, it is useful to summarise this information to enable us to easily identify any issues with model performance that may lead us to question their reliability.

To judge whether the bias of a CMIP5-driven regional model for a particular metric is acceptable, we use the maximum absolute bias found in CPM-PPE, B_{ref}, as a benchmark. This is appropriate since CPM-PPE members have already been deemed plausible and released as part of UKCP18. Note that the maximum absolute bias from RCM-PPE could equally have been used as a benchmark, but this would have been less of a stringent test since RCM-PPE typically has larger biases than CPM-PPE for the set of metrics considered here. The key point is that the same benchmark is used for assessing the performance of both CMIP5-driven RCMs and CPMs, ensuring a fair comparison.

We have devised the following colour-coding system to characterise the bias, B, for a particular model and metric:

- Grey. The bias is not significant (at the 95% level) compared to interannual variability, as estimated using bootstrap resampling (recall Section 2.6). Based on present-day performance, there is no reason not to use projections from this model for this metric.
- Green. The bias is significant, but no larger than any found in CPM-PPE: $|B| <= B_{ref}$. Projections from this model for this metric are thus considered equally as plausible as those from existing regional PPE members.
- Yellow. The bias is significant and outside the range of CPM-PPE: $B_{ref} < |B| <= 1.5 \times B_{ref}$. Exercise caution when using projections from this model for this metric.
- Orange. The bias is significant and large, $|B| > 1.5 \times B_{ref}$, but largely inherited from the driving GCM already included in UKCP Global as part of the CMIP5-13. Exercise caution when using projections from this model for this metric.
- Red. The bias is significant and large, $|B| > 1.5 \times B_{ref}$, and generated by the down-scaling step. Projections from this model for this metric are considered unreliable.

In the case where the bias is large ($|B| > 1.5 \times B_{ref}$), we need to decide whether a CMIP5-driven regional model bias is inherited from its driving model or not (to differentiate between orange and red flags). To do this, we compare the absolute difference in bias between a CMIP5-driven regional model and its driving model with the typical difference between pairs of ensemble members in the corresponding PPE:

$$J = \frac{|B_{cmip5,child} - B_{cmip5,drv}|}{\sigma_{PPE}} \quad \text{(Eq 1)}$$

where

$$\sigma^2_{PPE} = \frac{1}{N}\sum_{i=1}^{N}(B_{i,child} - B_{i,drv})^2 \quad \text{(Eq 2)}$$

and N=12 is the number of PPE members. We consider a regional model to be following its driving model if $J <= 2$ (an orange flag), and if $J > 2$ this is interpreted as a large departure of a regional model from its driving model (a red flag). In the case where a CPM has a large bias ($|B| > 1.5 \times B_{ref}$) and a small deviation from its driving RCM ($J <= 2$), and its driving RCM has a red flag, then the CPM will also be assigned a red flag (instead of orange) because this means the large bias has been generated by the GCM to RCM step, not inherited from the GCM.

The choice of the threshold values $1.5 \times B_{ref}$ and $J = 2$ are subjective, but we emphasise that the purpose of the scorecard is not to rigorously rank models, but simply to collate all the information from Section 3 and highlight any cases where there are issues with model performance that may lead to less confidence in model projections.

Figure 40 shows scorecards for biases in the CMIP5-driven RCMs and CPMs, for all the seasonal mean and daily metrics presented in Section 3. We focus on daily timescales and longer so that information is available from all GCMs, RCMs and CPMs. The main points to take from Figure 40 are as follows.

Figure 40. Summary of the present-day performance of the CMIP5-driven regional models in winter (left panels) and summer (right panels), for a selection of regionally averaged temperature and precipitation metrics (on daily timescales and longer). All data has been regridded onto a common n96 grid with spacings of 1.875° and 1.25° in the longitudinal and latitudinal directions, respectively, and spatial averaging of metrics was performed before computing biases. The meaning of the various colours is briefly described in the legend; see the text for full details.

Winter

- Winter temperature biases in all CMIP5-driven regional models are either insignificant (grey flags) or comparable in size to those in CPM-PPE (green flags), apart from CPM-MRI which has (marginal) yellow flags for winter mean temperature and the temperature of cold winter days in Scotland because of slightly larger negative biases than found in CPM-PPE (see Figures 16 and 20, respectively). Although these biases are only just outside the CPM-PPE range, they are large (the average temperature on cold winter days is more than 5ºC too low). CPM-MRI also over-estimates the number of cold and intense cold spells over Scotland, lying outside the CPM-PPE range (Figure 36). RCM-MRI has a larger negative bias than CPM-MRI for the temperature of cold winter days in Scotland (Figure 20) and also receives a yellow flag (note that it lies within the RCM-PPE range though). These biases are consistent with the MRI-driven regional models producing much more snow on the ground in Scotland during winter than any of the other models (Figure 38). On balance, we advise caution if using winter temperature projections from the MRI-driven regional models for Scotland as we have lower confidence in them.
- Significant biases in winter precipitation metrics in CPM-ACCESS and CPM-MPI are similar to those in CPM-PPE, all with green flags except for the positive bias in winter mean precipitation in Scotland in CPM-ACCESS that is given a yellow flag as it lies outside the CPM-PPE range (Figure 18). RCM-ACCESS

and RCM-MPI have more yellow flags than their nested CPMs for winter precipitation metrics, most notably for wet day fraction where the RCMs have larger positive biases (Figure 22). Note that significant biases in winter precipitation metrics in RCM-ACCESS and RCM-MPI all lie within the range of RCM-PPE though. Based on present-day performance, we consider winter precipitation projections from the regional models driven by MPI and ACCESS to be as plausible as those from the existing regional PPEs.

- RCM-MRI and CPM-MRI have red and orange flags for metrics related to winter precipitation for Scotland and England. This is because both models significantly over-estimate winter mean precipitation (Figure 18), wet-day fraction (Figure 22; bias inherited from MRI itself) and wet-day intensity (Figure 23). Given these performance issues, we consider projections for all winter precipitation metrics from these models unreliable.
- RCM-IPSL and CPM-IPSL have an orange flag for wet-day frequency in England, due to a large positive bias inherited from the IPSL GCM (Figure 22), which translates into large positive biases in winter mean precipitation too (Figure 18). Biases in wet-day fraction are smaller for Scotland, but RCM-IPSL still receives an orange flag and CPM-IPSL has a yellow flag. On the other hand, biases in wet-day intensity in the IPSL-driven models are small and comparable to biases in the PPEs (CPM-IPSL has a yellow flag for wet-day intensity in England, but this is marginal), see Figure 23. Similarly for biases in heavy daily precipitation amounts (Figure 24). It is possible that the IPSL-driven regional models could give reliable projections for the intensity of winter precipitation, even if wet-day frequency is not well represented in the driving GCM, but an assessment of the underlying physical processes would be required first. Nonetheless, we suggest caution in using winter precipitation projections from RCM-IPSL and CPM-IPSL.

Summer

- Biases are generally less significant in summer than in winter, presumably because there is more year-to-year variability.
- Summer temperature biases in all CMIP5-driven regional models are either insignificant (grey flags) or comparable in size to those in CPM-PPE (green flags), apart from CPM-MRI and CPM-ACCESS which have a yellow flag for the temperature of hot summer days in England because of a slightly larger positive bias than found in CPM-PPE (see Figure 21). We therefore consider summer temperature projections from CMIP5-driven models as plausible as those from the existing UKCP18 PPEs. However, users should be aware that both CPM-MRI and CPM-ACCESS considerably over-estimate the temperature of hot summer days (by ~3ºC) and the number of hot spells (Figure 35) for England.
- Biases in all summer precipitation metrics are either insignificant (grey flags) or within the range of CPM-PPE (green flags) for CPM-ACCESS, CPM-IPSL and CPM-MRI. This is also the case for RCM-ACCESS, RCM-IPSL and RCM-MRI, except for two yellow flags for wet day fraction in Scotland in RCM-ACCESS and RCM-IPSL due to larger positive biases than found in CPM-PPE (Figure 25; note that these biases are within the range of RCM-PPE though). Based on the present-day performance of the regional models driven by ACCESS, IPSL and MRI we consider their projections for future changes in metrics related to summer precipitation equally as plausible as those from the existing regional PPEs.
- RCM-MPI and CPM-MPI have large positive biases in wet-day fraction (Figure 25), resulting in large positive biases in summer mean precipitation (Figure 19). The regional model biases are much larger than in the MPI GCM too. Red flags are thus assigned to both metrics over Scotland. Over England, yellow

flags are assigned, but this is only because there are some poorly performing members of CPM-PPE. Biases in wet-day intensity are smaller (~10% level; Figure 26) and comparable to those in the PPEs (yellow flags for Scotland are marginal), as are biases in heavy daily precipitation amounts (Figure 27). However, the large biases in summer wet-day frequency and mean precipitation, which are generated by the down-scaling step, means we have low confidence in projections from the MPI-driven regional models for all summer precipitation metrics.

In summary, biases in the regional models driven by the CMIP5-4 GCMs are mostly comparable to those in the existing UKCP18 regional PPEs, at least for the metrics considered here. We therefore have no reason to consider projections from these models any less plausible than those from RCM-PPE and CPM-PPE. Two important exceptions are winter and summer precipitation in the regional models driven by MRI and MPI, respectively, where issues with model performance in the present-day lead us to consider projections for future changes in precipitation in these seasons to be unreliable. In addition, caution should be applied if using projections for (i) winter temperatures over Scotland from the MRI-driven regional models, and (ii) winter precipitation from the IPSL-driven regional models.

5 Future changes

In this section we examine climate change projections for the UK (under the RCP8.5 emissions scenario) from the regional models driven by the CMIP5-4 set of GCMs, focussing on temperature and precipitation.

5.1 Seasonal mean changes

Future changes in near-surface air temperature in winter and summer are shown in Figures 41 and 42, respectively. In all models, mean temperature increases everywhere in both seasons, with larger absolute increases in summer. In these figures, and equivalent ones in the following sections, regional models are ordered by the future SST increases (averaged over an area around the UK; recall Figure 10) in their driving GCMs, because this is a key driver of temperature changes over UK land. Note this results in a different ordering of models compared to similar plots in Section 3.

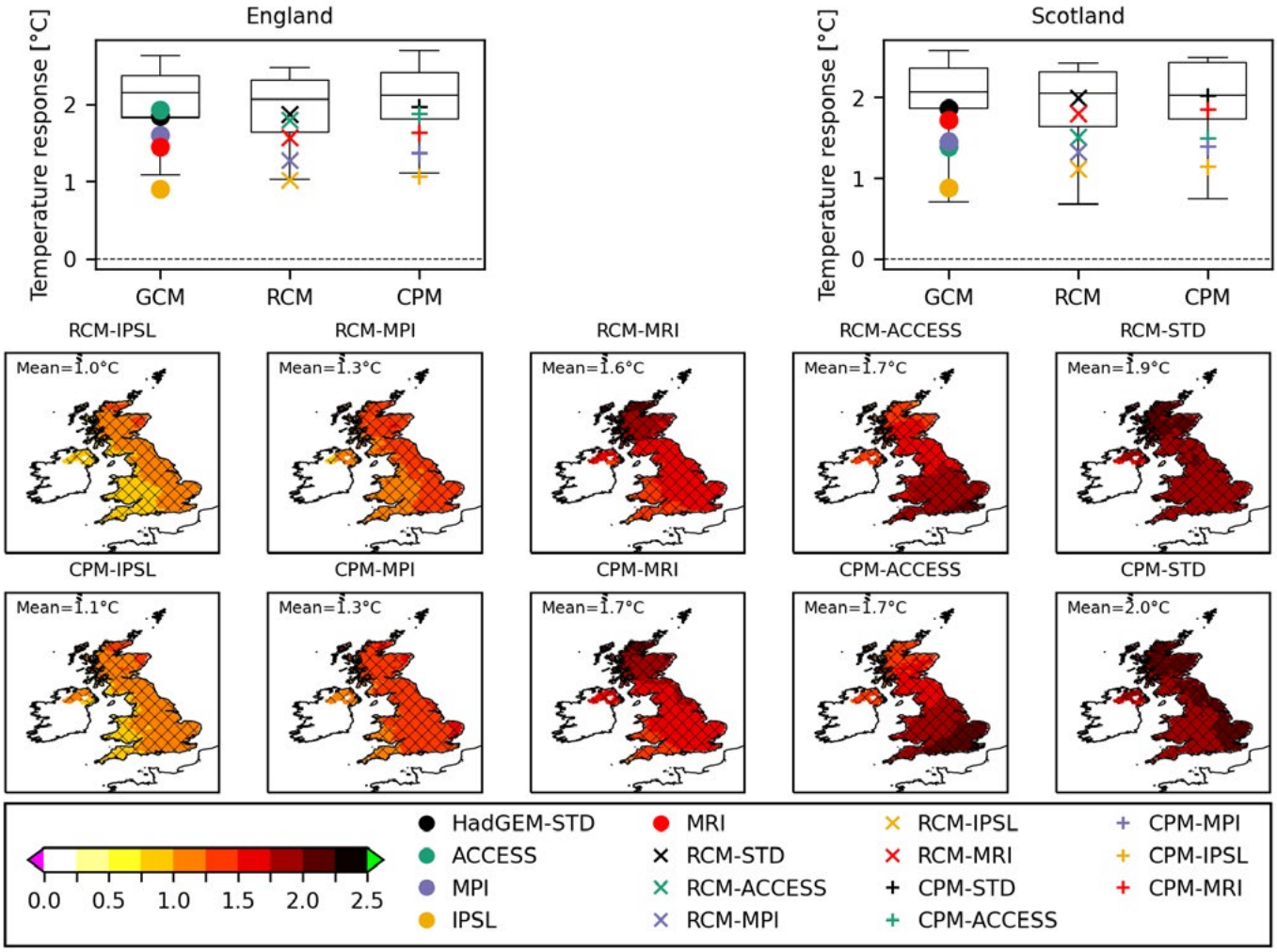

Figure 41. Future changes in seasonal mean air temperature at 1.5m in winter, defined as differences between a 21-year future period, centred on the year when the global mean surface temperature reaches 3ºC above pre-industrial (see Table 5), and baseline period (1980 – 2000). The panels on the top row show changes in regionally averaged winter mean temperature in the various CMIP5 GCMs and their nested regional models, for England and Scotland respectively. The box-and-whiskers indicate the distribution of responses in HadGEM-PPE, RCM-PPE and CPM-PPE: the box extends from the lower to the upper quartiles of the data, with the median shown by the solid horizontal line, and the whiskers show the full range of the data. Plots on the second row show spatial maps of winter mean temperature changes in the CMIP5-driven RCMs and RCM-STD, with equivalent plots for the CMIP5-driven CPMs and CPM-STD on the third row (the CPM data has been regridded onto the 12 km RCM grid). Hatched areas indicate where future changes are significantly different from zero (at the 95% level), estimated using bootstrap resampling. Note that models are ordered from left to right by increasing seasonal mean SST change averaged over a region around the UK (see Figure 10). The UK-mean response is indicated in each panel.

Future temperature increases in winter in the CMIP5-driven regional models are significant across the UK, and typically lie towards the lower end of the distribution of responses from RCM-PPE and CPM-PPE (i.e. less future warming). In particular, RCM-IPSL and CPM-IPSL project less winter warming over England than any member of RCM-PPE and CPM-PPE, respectively. The regional model responses largely follow those of the CMIP5-4 GCMs which, in the UK-average sense, are positively correlated with future increases in SSTs around the UK (computed as the average over the green box in Figure 10).

Recall that RCM-MRI and CPM-MRI produce much more snowfall and lying snow over Scotland in the present-day than MRI itself (Figure 38), consistent with the significant cold bias in winter mean temperature flagged in Figure 16. As this snow melts in the future, temperature increases could be amplified by snow-albedo feedback effects. However, the responses of MRI and its nested regional models are similar, suggesting this is not having a large effect, likely because there is still a significant amount of snow remaining in these regional models when the global warming level reaches 3ºC above pre-industrial; see Section 5.4.4 below. Although we see no evidence from the projections themselves that the MRI-driven models should not be used, we recommend that caution is exercised because of the large present-day biases in winter temperature in the north of the UK. Winter temperature projections from the other CMIP5-driven regional models are considered equally as plausible as those from the UKCP18 regional PPEs since there are no notable performance concerns in the present-day.

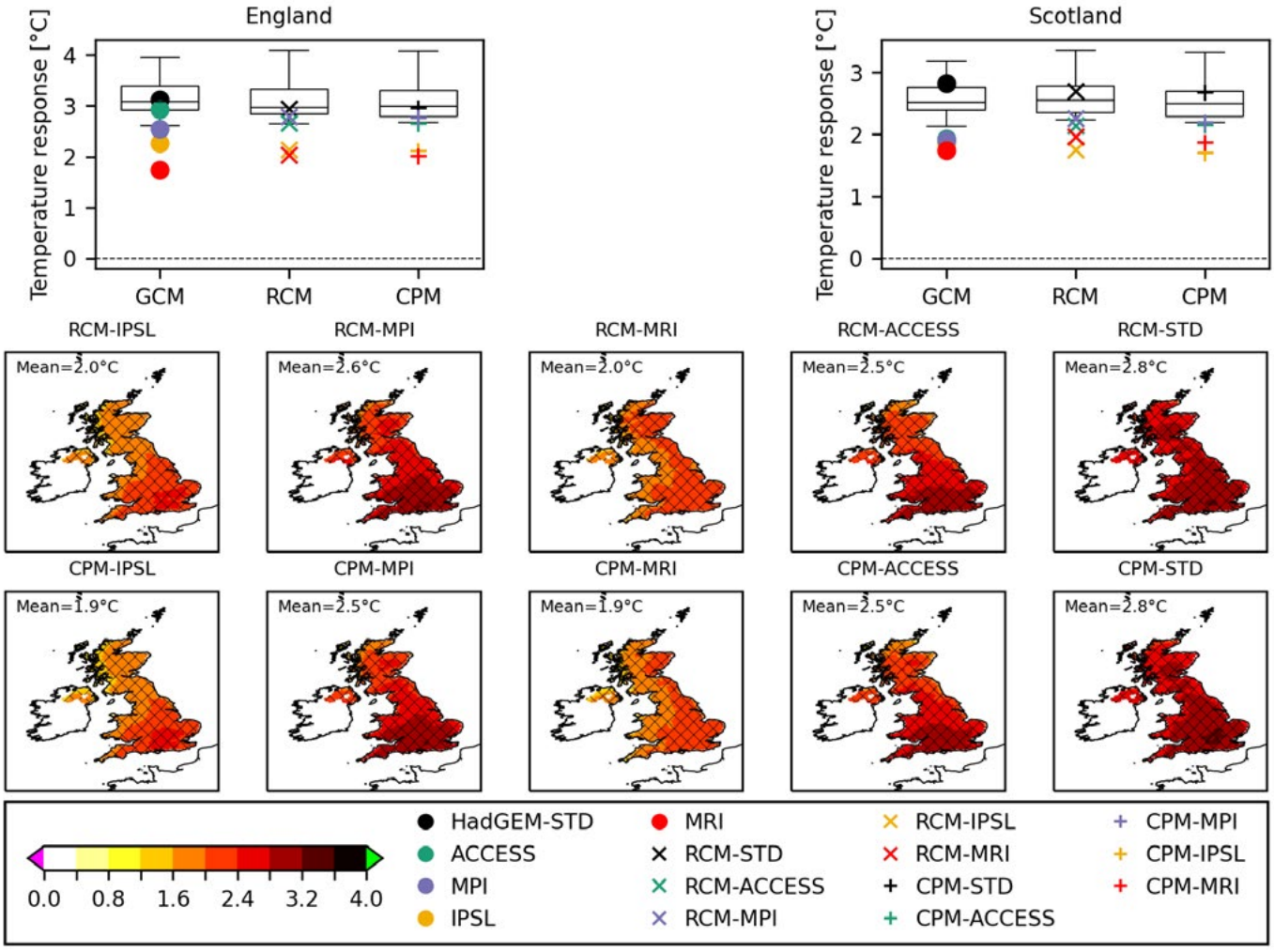

Figure 42. Future changes in seasonal mean air temperature at 1.5m in summer. The layout of the plots is the same as in Figure 41.

In summer, the CMIP5-4 GCMs project smaller future temperature increases than HadGEM-PPE, apart from ACCESS over England. When the CMIP5-4 GCMs are down-scaled, summer temperature responses in the nested regional models (which are significant across the UK) are similar to those of their driving global models. As a result, the regional models driven by IPSL and MRI project notably less future warming than any member of RCM-PPE and CPM-PPE, while the responses of the regional models driven by ACCESS and MPI lie close to the lower bound of the PPEs. Based on present-day performance, we have no reason to consider these projections any less plausible than those from the existing UKCP18 regional PPEs. Therefore, we have successfully extended the range of plausible future summer outcomes now available from UKCP18, one of the main aims of down-scaling alternative global models from CMIP5.

In Figure 38 it was noted that snow remains on the ground too long in Scotland in the regional models driven by MRI, lasting into early summer, which is not the case in MRI itself. This snow is no longer present when the global warming level reaches 3ºC above pre-industrial (see Section 5.4.4 below), but any additional warming related to the melting of snow and associated snow-albedo feedback effects must be small since summer temperature responses in RCM-MRI and CPM-MRI are comparable to those of the MRI GCM over Scotland. Therefore, the persistence of lying snow in the MRI-driven regional models does not appear to negatively affect their summer temperature projections.

Projected changes in precipitation in winter and summer are presented in Figures 43 and 44, respectively.

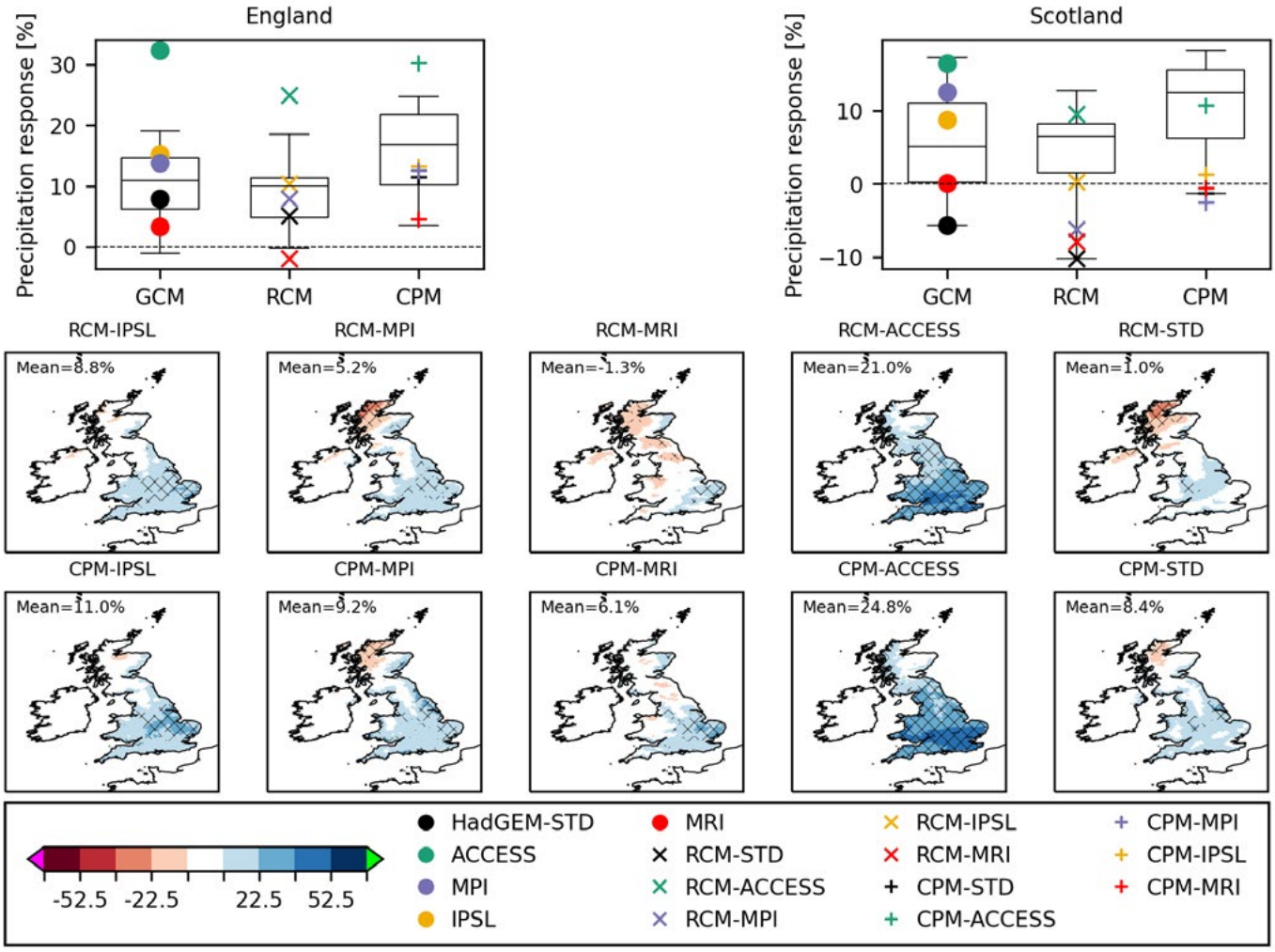

Figure 43. Future changes in seasonal mean precipitation in winter. The layout of the plots is the same as in Figure 41.

Model projections for winter precipitation mostly suggest an increase in the future, particularly over England. As noted in Kendon et al. (2021), CPM-PPE consistently shows larger increases (or smaller decreases) than RCM-PPE (and HadGEM-PPE) over land, linked to more convective showers in the CPM, likely advected inland from over the sea (Kendon et al. 2020). Over England, ACCESS projects the largest future increase, lying above the upper bound of HadGEM-PPE. This is also the case in the regional models driven by ACCESS, where increases are significant compared to natural variability and can exceed 50% locally in the CPM. Such an outcome would have impactful consequences in terms of river flows and flood risk. Given that there were no notable issues with regional model performance in the present-day, these projections are considered plausible.

The other CMIP5-driven regional models mostly project a future increase in winter precipitation over England, with little change or a decrease over Scotland. The responses are generally not significantly different from zero (the IPSL-driven models over southeastern England are an exception) and lie within, or just outside, the ranges of RCM-PPE and CPM-PPE. However, recall that projections from the MRI-driven regional models are considered unreliable because of large (and significant) present-day biases in winter precipitation that were generated by the down-scaling step (e.g. Figure 18). The projections from the IPSL-driven models should also be used with caution, because of large biases inherited from the IPSL GCM itself. The MPI model is an interesting case because the GCM projects a future increase in winter precipitation over Scotland, lying in the upper quartile of the HadGEM-PPE distribution, but the sign of the projected change is reversed upon down-scaling, with the nested RCM lying towards the lower end of the RCM-PPE distribution. This is explored further below. Note that CPM-MPI predicts a larger future decrease in winter precipitation over Scotland than any member of CPM-PPE.

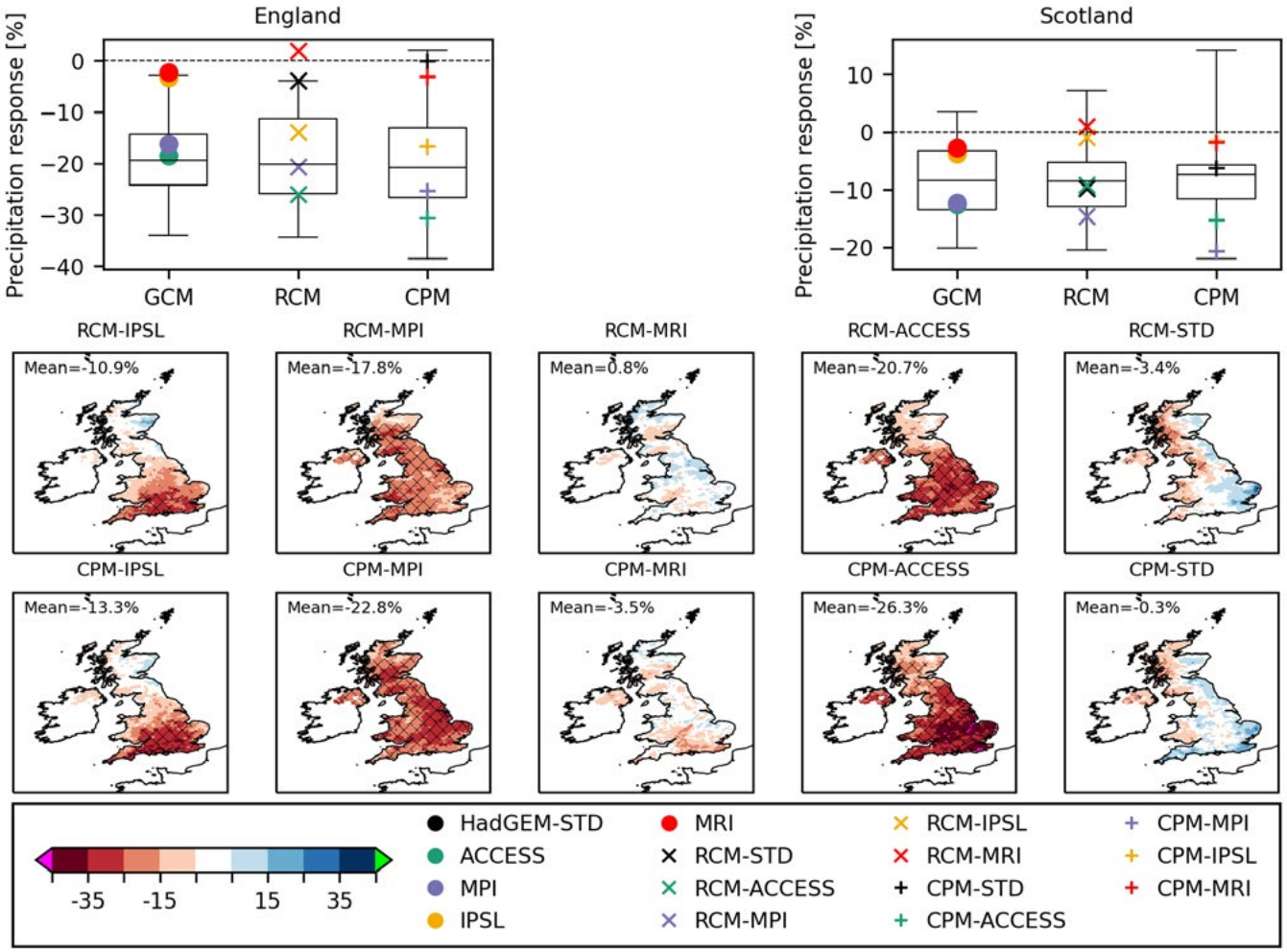

Figure 44. Future changes in seasonal mean precipitation in summer. The layout of the plots is the same as in Figure 41.

In summer, most members of the various PPEs project a substantial decrease in precipitation, particularly over England, although responses span a broad range. Note that future decreases are not as large as reported in Kendon et al. (2021; see their Figure 5.1) because they computed them using a later future period (2060 – 2080), when the global mean warming level is above 3ºC in these models.

The regional models driven by MPI and ACCESS also project future decreases in summer precipitation across the UK, typically lying towards the lower end of the PPE distributions. These signals are significant across England and parts of Scotland. Based on our assessment of present-day performance, projections from the ACCESS-driven models are considered plausible, but those from the MPI-driven models are deemed unreliable because of large (and significant) wet biases in summer mean precipitation generated during the down-scaling step (e.g. Figure 19).

The regional models driven by MRI display little future change in summer precipitation, across the UK, with responses typically lying in the upper quartile of the distribution of responses from RCM-PPE and CPM-PPE. The same is true for the IPSL-driven models over Scotland (over England these models project a future decrease, significant in the south). There are no reasons to consider projections from these models any less plausible than those from the existing UKCP18 regional PPEs. Sampling future summer outcomes with less of a reduction in precipitation was another key motivation for this work.

5.2 **Future changes at the daily time scale**

Projected changes in the temperature of cold winter days are presented in Figure 45. All models project an increase in temperature in the future, but increases are generally smaller in the IPSL, ACCESS and MPI GCMs and their nested regional models than most members of the corresponding PPEs. Indeed, the models driven by IPSL and ACCESS offer outcomes previously unsampled by the UKCP18 regional ensembles, following their driving global models. There are no performance issues in the present-day that would lead us to doubt the plausibility of these projections. By contrast, the MRI-driven models project larger future increases in the temperature of cold winter days than most members of RCM-PPE and CPM-PPE, but we have less confidence in these projections since there are large cold biases in the present-day, especially over Scotland (where biases can be ~ -5ºC; Figure 20), consistent with excessive snow on the ground (Figure 38).

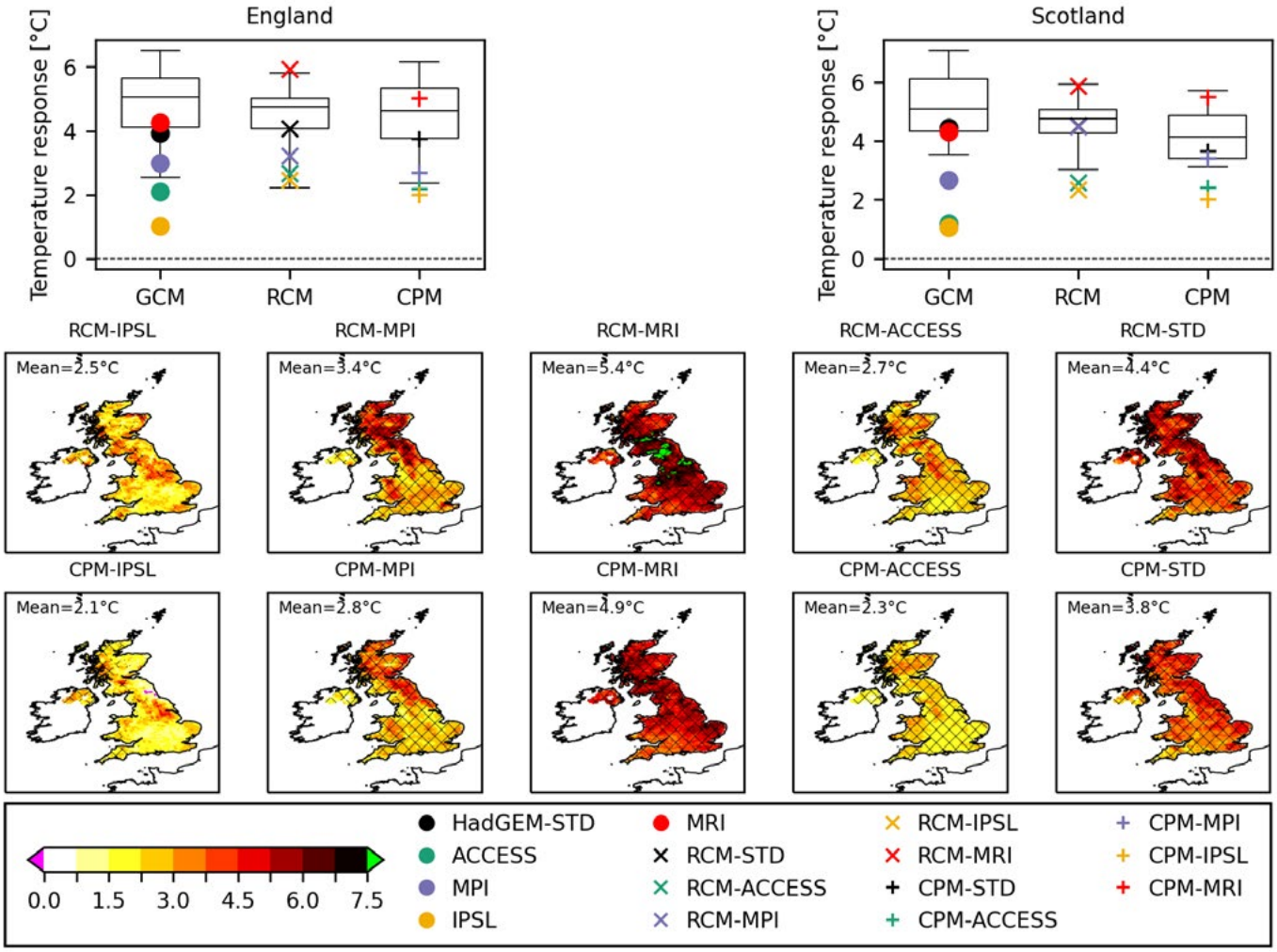

Figure 45. Future changes in the temperature of cold winter days (the 1st percentile of the distribution of daily mean air temperatures at 1.5m in winter, where the daily mean temperature is computed as the average of the daily maximum and minimum temperatures), defined as differences between a 21-year future period, centred on the year when the global mean surface temperature reaches 3ºC above pre-industrial (see Table 5), and baseline period (1980 – 2000). The panels on the top row show changes in the regionally averaged temperature on cold winter days in the various CMIP5 GCMs and their nested regional models, for England and Scotland respectively. The box-and-whiskers indicate the distribution of responses in HadGEM-PPE, RCM-PPE and CPM-PPE: the box extends from the lower to the upper quartiles of the data, with the median shown by the solid horizontal line, and the whiskers show the full range of the data. Plots on the second row show spatial maps of changes in the temperature of cold winter days in the CMIP5-driven RCMs and RCM-STD, with equivalent plots for the CMIP5-driven CPMs and CPM-STD on the third row (the CPM data has been regridded onto the 12 km RCM grid). Hatched areas indicate where future changes are significantly different from zero (at the 95% level), estimated using bootstrap resampling. Note that models are ordered from left to right by increasing seasonal mean SST change averaged over a region around the UK (see Figure 10). The UK-mean response is indicated in each panel.

Figure 46 shows future changes in the temperature of hot summer days. The IPSL and MRI GCMs project smaller future increases than most members of HadGEM-PPE, lying in the lower quartile of the distribution. By contrast, the responses of the ACCESS and MPI models lie closer to the centre of the distribution. When the CMIP5-4 GCMs are down-scaled, their future changes are largely preserved by the nested RCMs and CPMs, with the exception of ACCESS over England where RCM-ACCESS displays considerably less warming than its driving model. The responses of the ACCESS-driven regional models lie below the lower bound of the regional PPEs over England, as do those of the regional models driven by IPSL and MRI across the UK, representing new future outcomes. However, it should be remembered that the regional models driven by MRI and ACCESS have large positive biases in the temperature of hot summer days in England (~3ºC; Figure 21), so we have lower confidence in their future changes. Nonetheless, some members of the PPEs display comparable biases, so we consider projections from the MRI-driven and ACCESS-driven models at least as plausible as those from the UKCP18 regional ensembles.

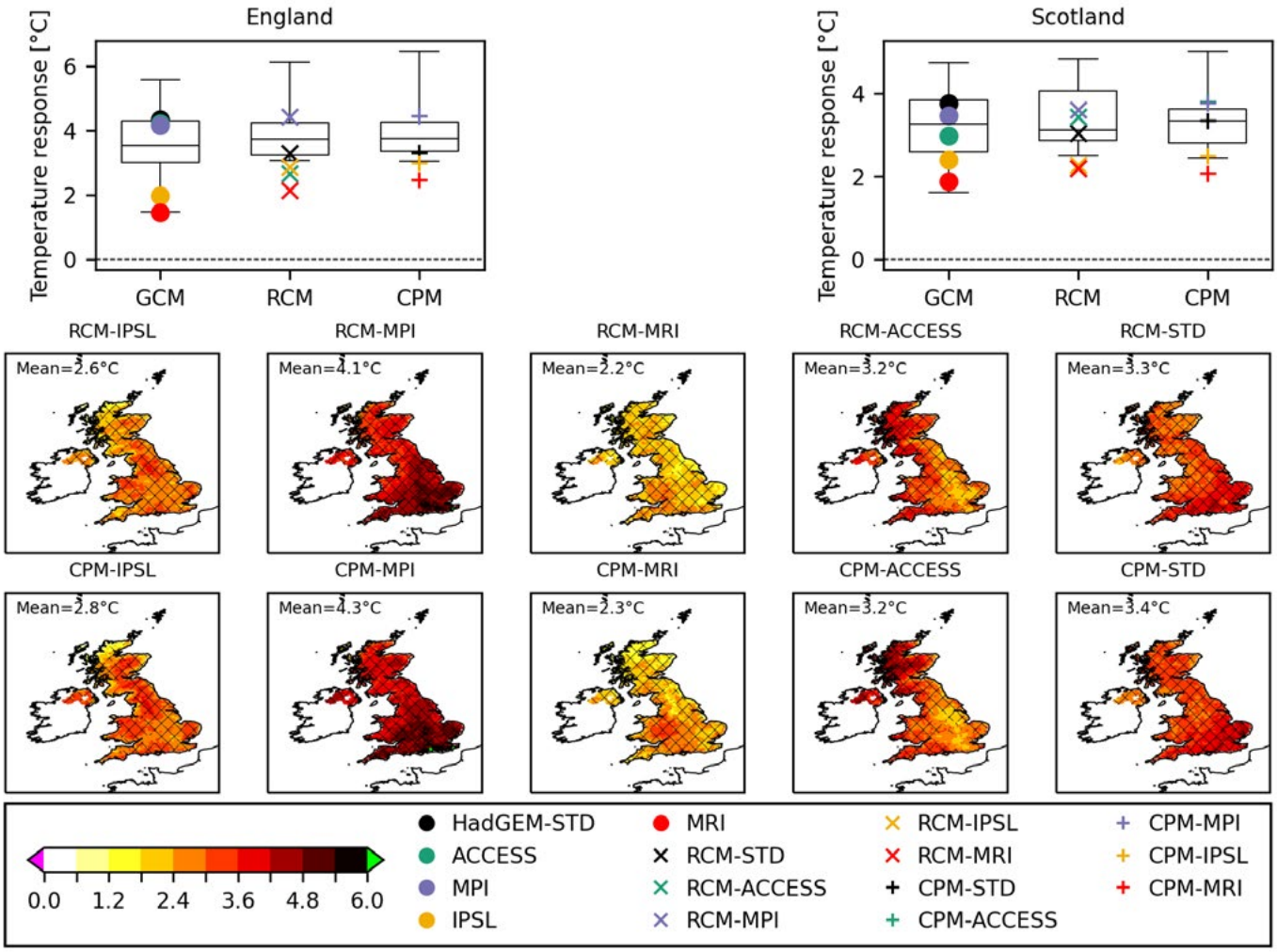

Figure 46. Future changes in the temperature of hot summer days (defined as the 99th percentile of the distribution of daily mean air temperatures at 1.5m in summer, where the daily mean temperature is computed as the average of the daily maximum and minimum temperatures). The layout of the plots is the same as in Figure 45.

Future changes in the fraction of wet days (defined as days where the accumulated precipitation exceeds 1 mm), the average wet-day intensity, and heavy precipitation (defined as the 99th percentile of all daily values) are shown in Figures 47, 48 and 49 for winter and Figures 50, 51 and 52 for summer.

As discussed in Kendon et al. (2021), members of CPM-PPE tend to show a greater future increase, or less of a decrease, in wet-day fraction in winter than members of RCM-PPE. This is also true for all the regional models driven by CMIP5-4 GCMs (Figure 47). The regional models driven by ACCESS project an increase in the frequency of wet days across the UK, lying towards the upper end of the distribution of responses from RCM-PPE and CPM-PPE, largely inherited from the ACCESS GCM itself. By contrast, the other CMIP5-driven models project future decreases in wet-day fraction over Scotland, lying towards the lower end of the regional PPE ranges. However, future changes in winter wet-day fraction in all CMIP5-driven models are not significantly different from zero across most of the UK.

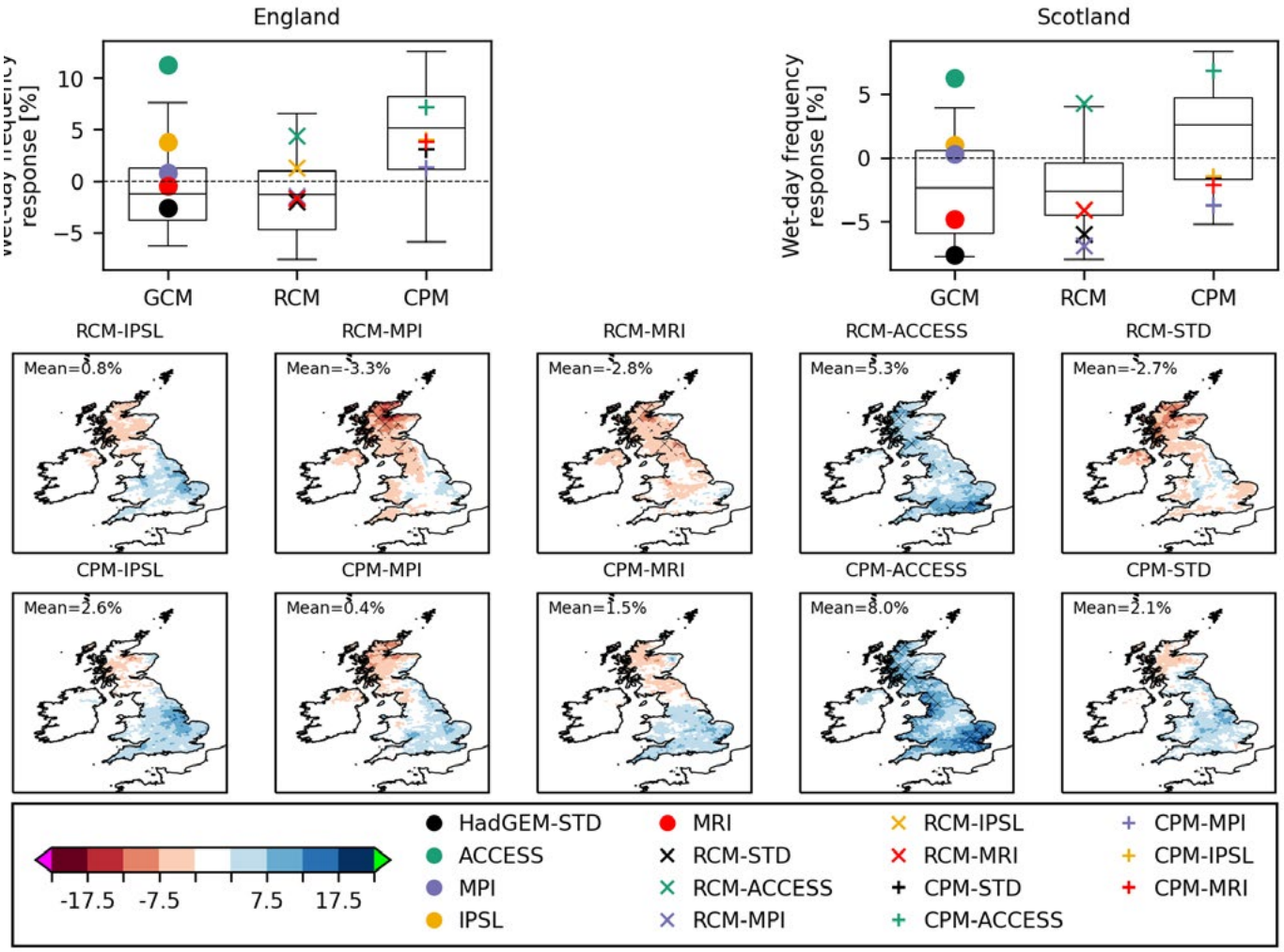

Figure 47. Future changes in wet-day fraction (defined as days where the precipitation accumulation exceeds 1 mm) in winter. The layout of the plots is the same as in Figure 45.

Over England, all the CMIP5-driven regional models except RCM-MRI and CPM-MRI project significant future increases in wet-day intensity, following their driving global models. Similar behaviour is seen in the various PPEs. Future increases in ACCESS lie at the upper end of the distribution of responses from HadGEM-PPE, and its nested regional models project larger increases than any members of RCM-PPE and CPM-PPE, respectively. This is also true for future changes in heavy daily precipitation amounts (Figure 49). Coupled with increases in wet-day frequency over England (Figure 47), this explains why future increases in winter precipitation over England are larger in the ACCESS-driven regional models than any of the others (Figure 43). Future increases in wet-day intensity over England in the regional models driven by MPI and IPSL lie close to the centre of the distribution of responses from the regional PPEs, whereas those driven by MRI lie below the lower bound of the PPEs, projecting little future change in wet-day intensity. However, issues with the present-day performance of the MRI-driven models for winter precipitation means we do not consider these projections reliable.

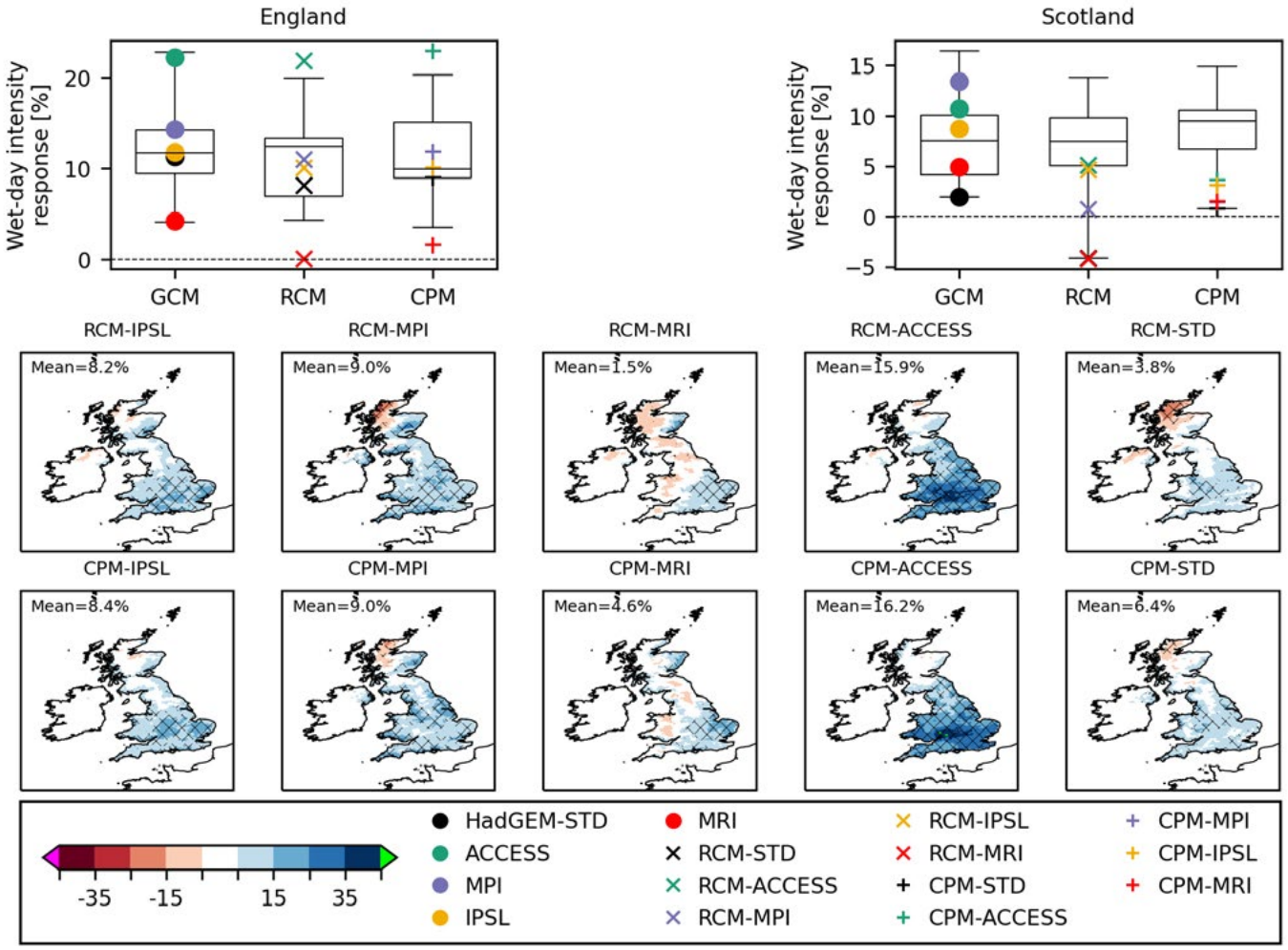

Figure 48. Future changes in wet-day intensity in winter. The layout of the plots is the same as in Figure 45.

The CMIP5-4 GCMs also project future increases in wet-day intensity for Scotland. However, when down-scaled with the RCM, future increases are systematically reduced (or even become decreases in the case of RCM-MRI) and are not significantly different from zero. Similar behaviour is seen in the future changes of heavy daily precipitation amounts (Figure 49). Differences between GCM and nested RCM are most pronounced for the MPI model. This was also the case for winter mean precipitation: recall from Figure 43 that the MPI GCM projects an upper-end increase in winter precipitation over Scotland in the future, whereas RCM-MPI suggests a lower-end decrease. From Figures 47 and 48 it is evident the GCM response is driven by an increase in wet-day intensity, whereas the RCM response is the result of a decrease in the frequency of wet days. Further analysis would be required to understand the underlying physical mechanism behind this interesting difference.

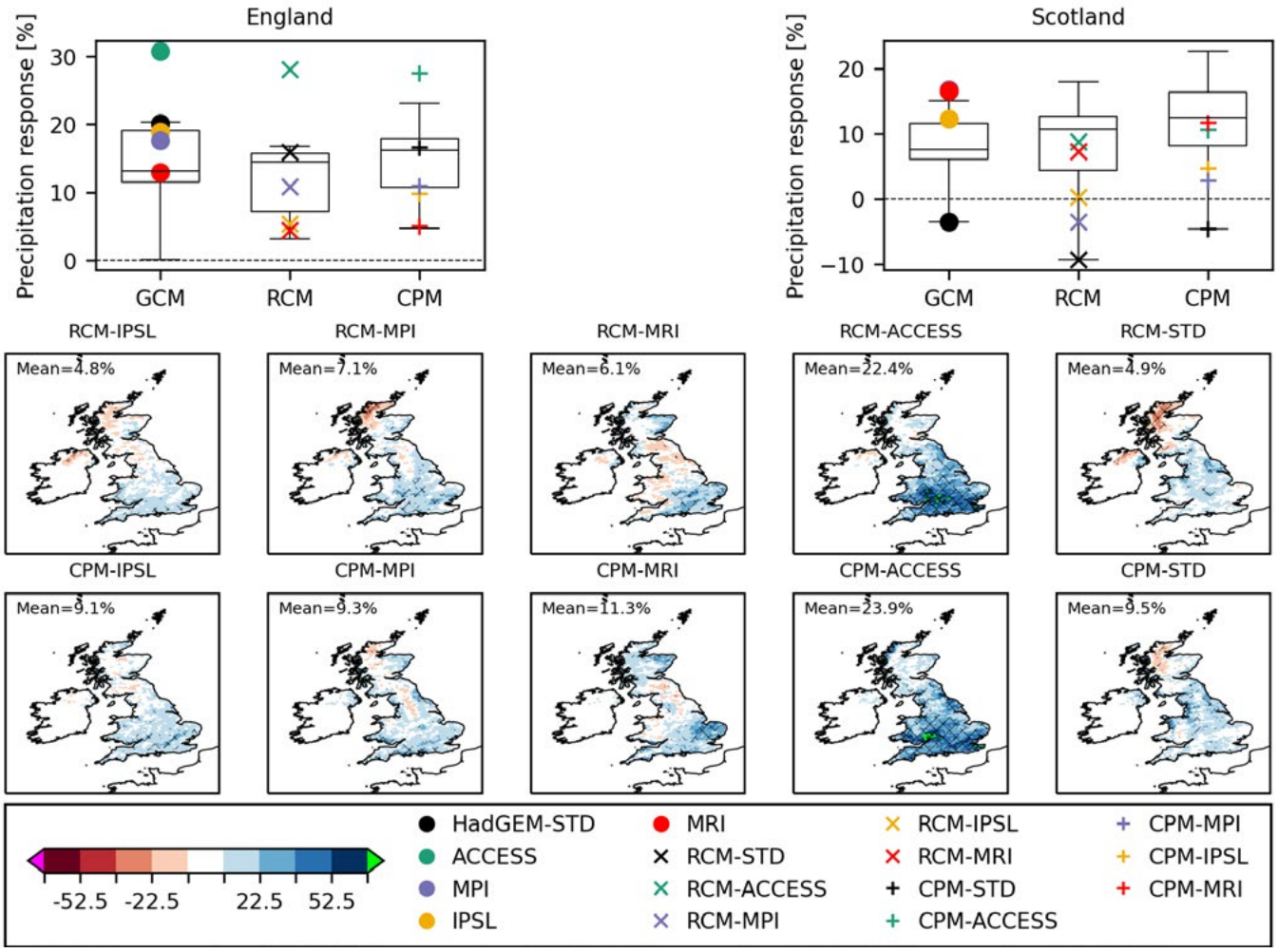

Figure 49. Future changes in heavy daily precipitation amounts (defined as the 99th percentile of the distribution of daily precipitation, including all values) in winter. The layout of the plots is the same as in Figure 45.

In summer there is a decrease in the frequency of wet days in nearly all models (Figure 50), with larger decreases in CPMs compared to RCMs, including in the models driven by CMIP5-4 GCMs. There are significant decreases across the UK in the regional models driven by MPI and ACCESS, and also RCM-IPSL and CPM-IPSL in southern England. By contrast, the models driven by MRI show little future change in summer wet-day fraction, with responses lying above (in the case of RCM-MRI) or close to (in the case of CPM-MRI) the upper bound of the corresponding regional PPEs. Future changes in the CMIP5-driven regional models largely follow those of their driving global models.

Future changes in the amount of rainfall on wet days in summer in the CMIP5-driven regional models are small and not significantly different from zero (Figure 51), as are changes in heavy daily precipitation amounts (Figure 52). In both cases, responses of the CMIP5-driven models lie within the envelope of the regional PPEs. Increases in wet-day intensity are larger (or decreases are smaller) in all CMIP5-driven CPMs compared to their driving RCMs, which balances the larger reduction in wet-day frequency in the CPMs (Figure 50), leading to similar projections for changes in summer mean precipitation (Figure 44).

In light of Figures 50 and 51, it is clear that the upper-end reductions in UK summer mean precipitation in the regional models driven by MPI and ACCESS (Figure 44) is driven by decreases in wet-day frequency in summer. Similarly for the IPSL-driven models over England. Over Scotland, a small future decrease in summer wet-day frequency in the IPSL-driven models is offset by a small future increase in the intensity of rainfall on those days, leading to little overall change in summer mean precipitation. In the MRI-driven models there is little future change in either wet-day frequency or intensity across the UK, and thus little change in summer mean precipitation.

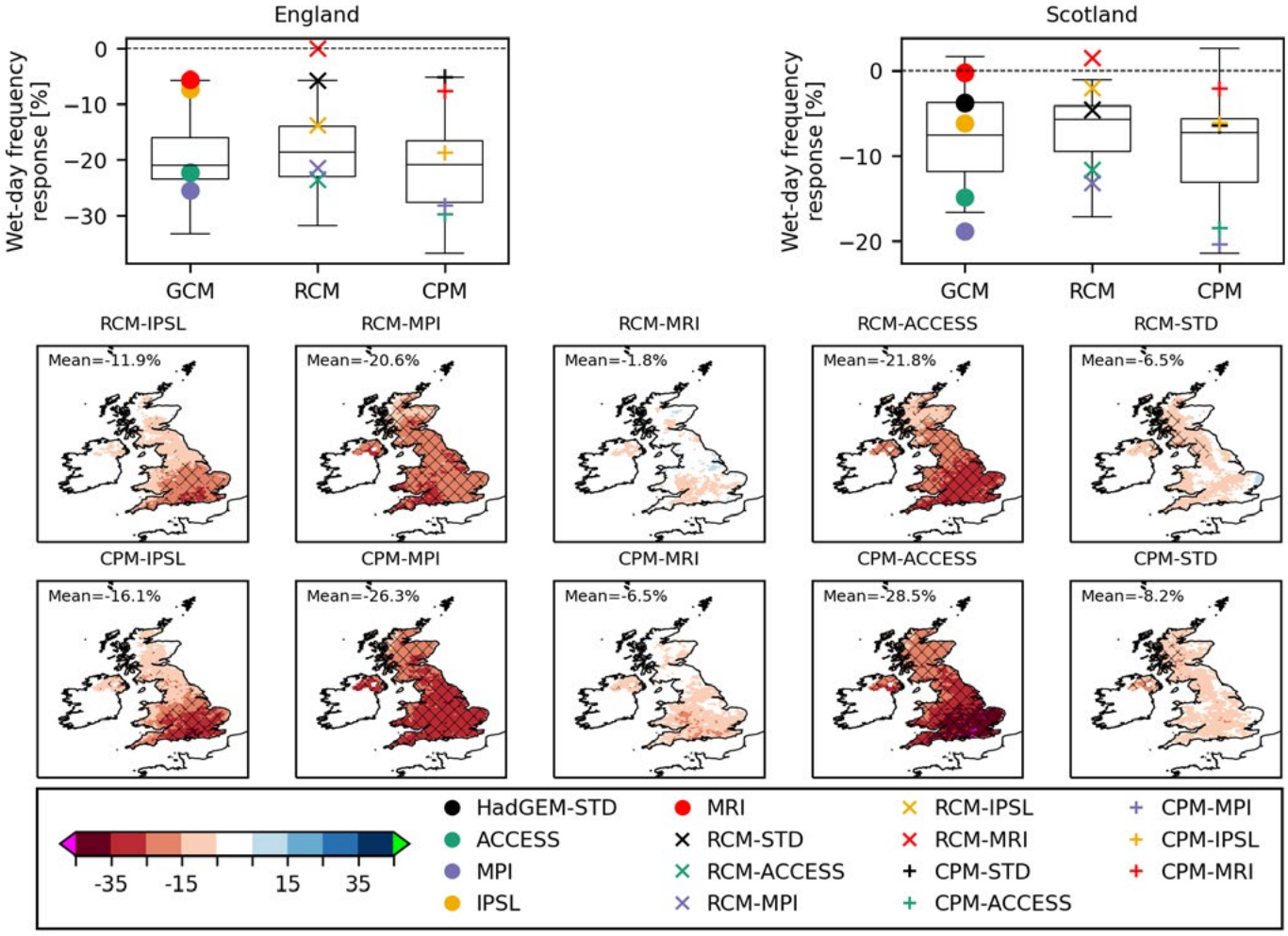

Figure 50. Future changes in wet-day fraction (defined as days where the precipitation accumulation exceeds 1 mm) in summer. The layout of the plots is the same as in Figure 45.

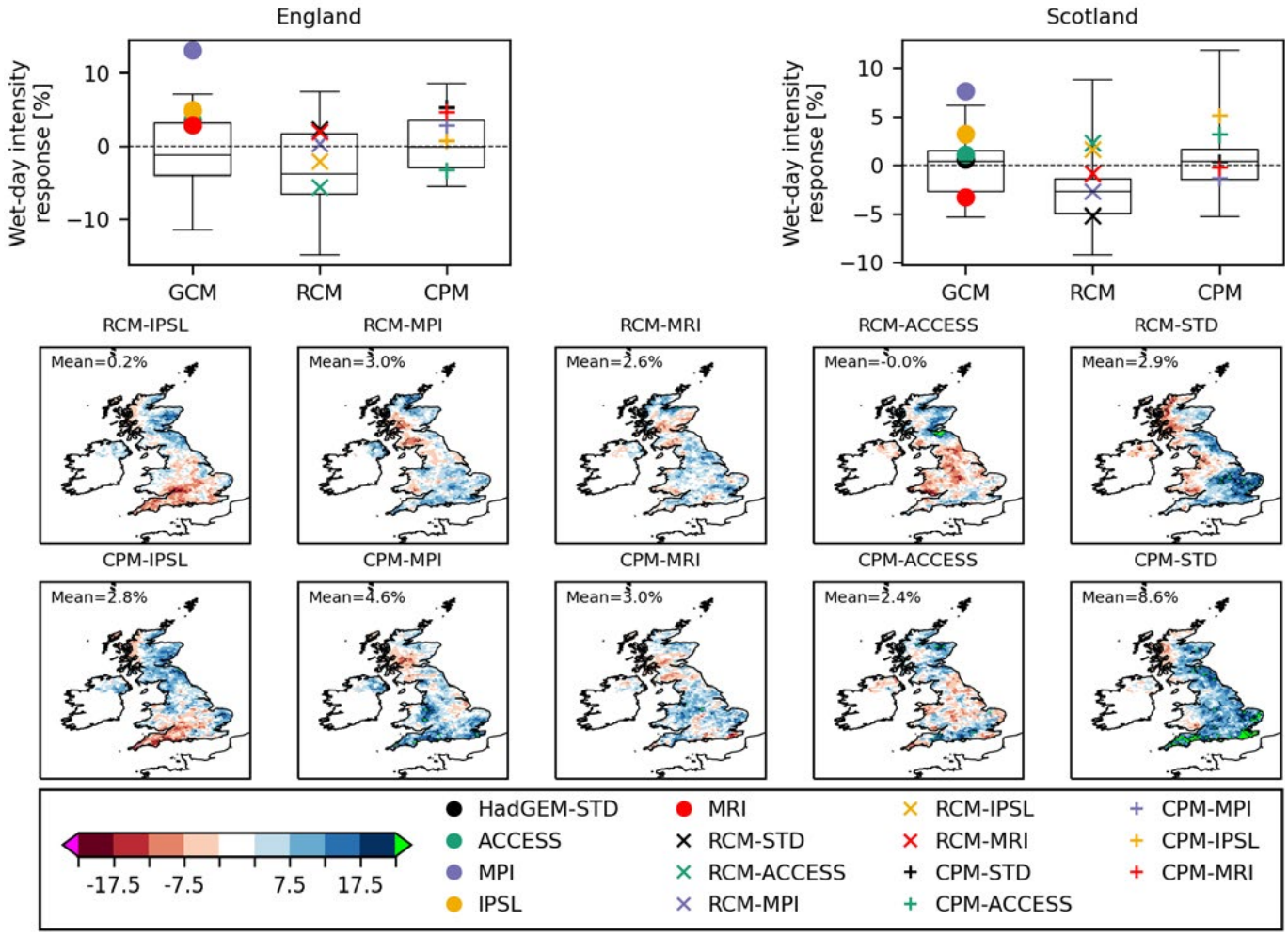

Figure 51. Future changes in wet-day intensity in summer. The layout of the plots is the same as in Figure 45.

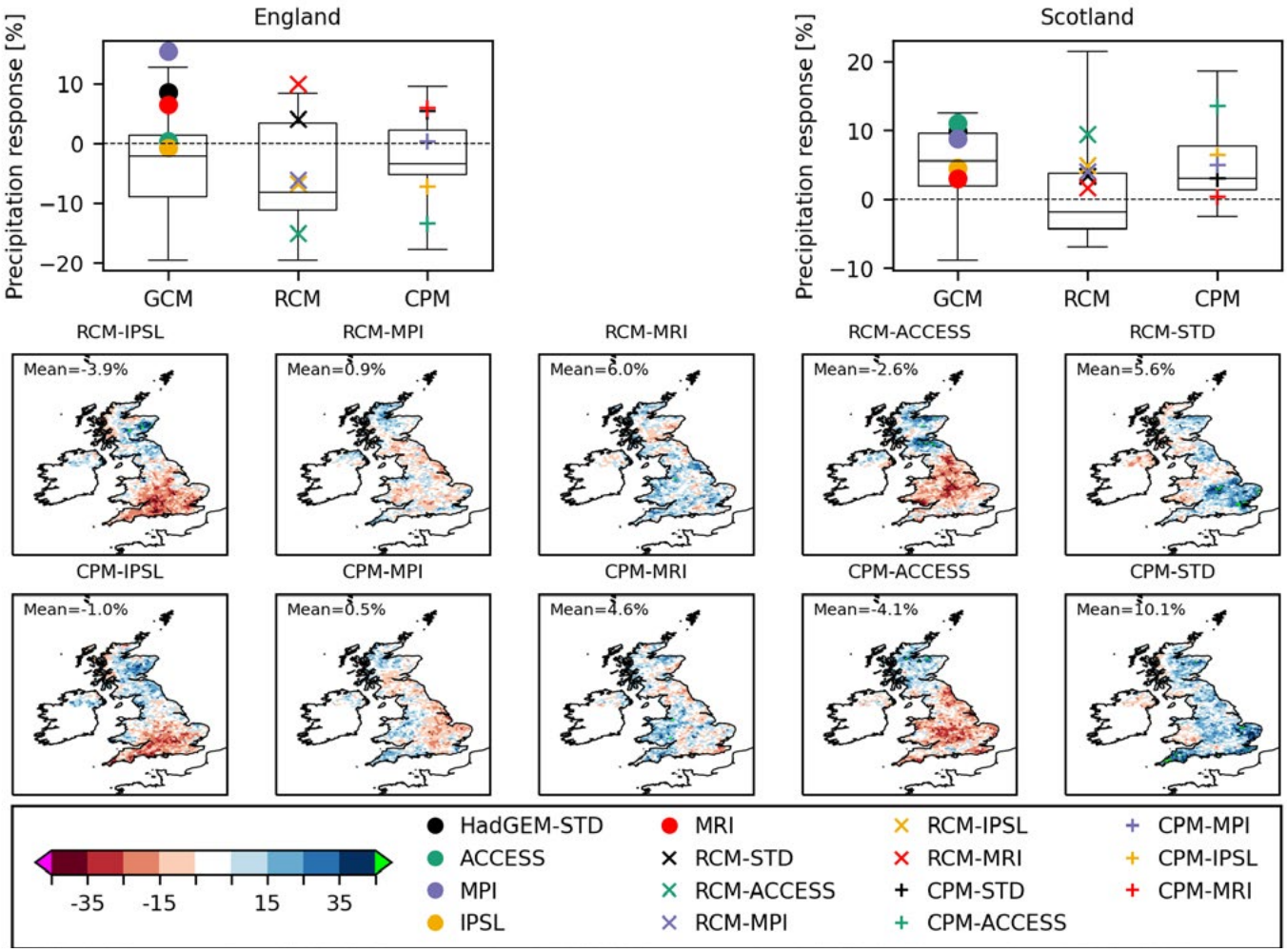

Figure 52. Future changes in heavy daily precipitation amounts (defined as the 99th percentile of the distribution of daily precipitation, including all values) in summer. The layout of the plots is the same as in Figure 45.

5.3 Future changes at the hourly time scale

Figures 53 and 54 show future changes in heavy hourly precipitation (defined as the 99.95th percentile of all hourly values, corresponding to approximately one event per season) in winter and summer, respectively. We only consider the CPMs since we have more confidence in their projections on sub-daily timescales compared to those from coarser resolution models. As before, all CPM data has been regridded onto the 5km OSGB grid.

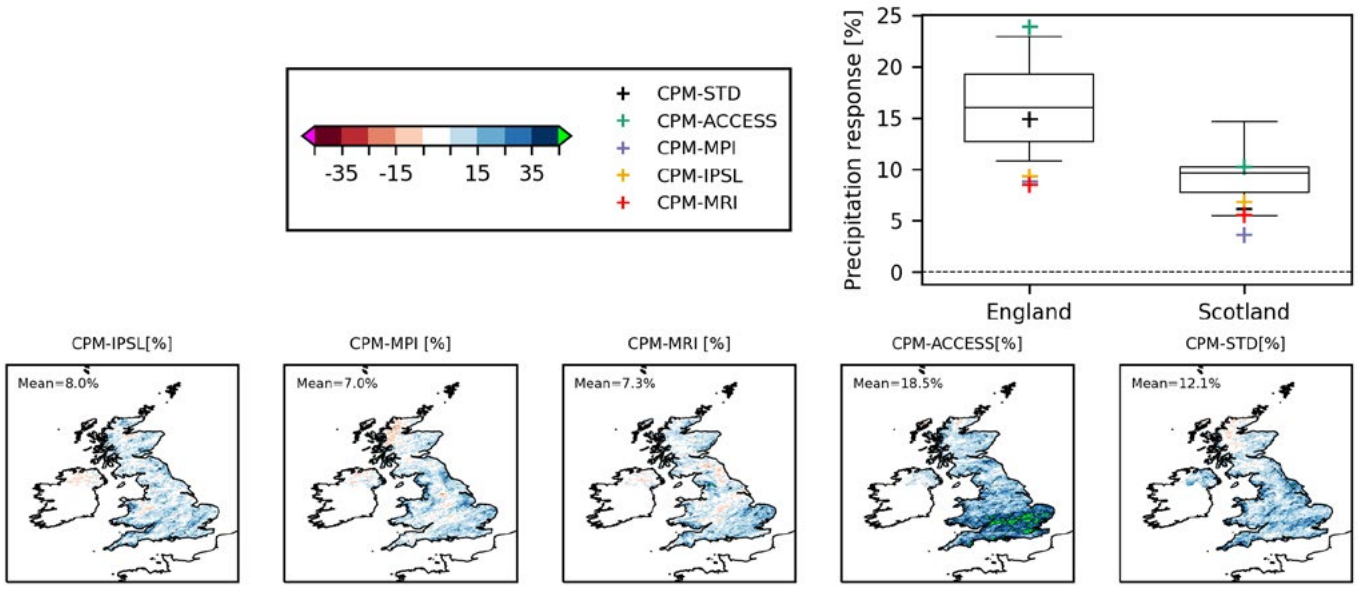

Figure 53. Future changes in heavy hourly precipitation amounts (the 99.95th percentile of hourly precipitation, including all values) in winter, defined as differences between a 21-year future period, centred on the year when the global mean surface temperature reaches 3ºC above pre-industrial (see Table 5), and baseline period (1980 – 2000). The top right panel shows changes in regionally averaged heavy hourly precipitation in the various CMIP5-driven CPMs and CPM-STD. The box-and-whiskers indicate the distribution of responses in CPM-PPE: the box extends from the lower to the upper quartiles of the data, with the median shown by the solid horizontal line, and the whiskers show the full range of the data. Plots on the second row show spatial maps of changes in heavy hourly precipitation in the CMIP5-driven CPMs and CPM-STD (the CPM data has been regridded onto the 5km OSGB grid). Hatched areas indicate where future changes are significantly different from zero (at the 95% level), estimated using bootstrap resampling. Note that models are ordered from left to right by increasing seasonal mean SST change averaged over a region around the UK (see Figure 10). The UK-mean response is indicated in each panel.

In winter, CPM-PPE projects a future increase in heavy hourly precipitation across the UK, with more of an increase over England than Scotland. This is also the case in the CMIP5-driven CPMs. CPM-ACCESS is notable since it projects the largest future increases of any model over England. Responses are significant in southern England where CPM-ACCESS also projects significant future increases in winter mean precipitation (Figure 43), wet day intensity (Figure 48) and heavy daily precipitation amounts (Figure 49). Future changes in the other CMIP5-driven CPMs are smaller (not significantly different from zero) and similar to each other, typically lying towards the lower end or below the lower bound of the CPM-PPE distribution.

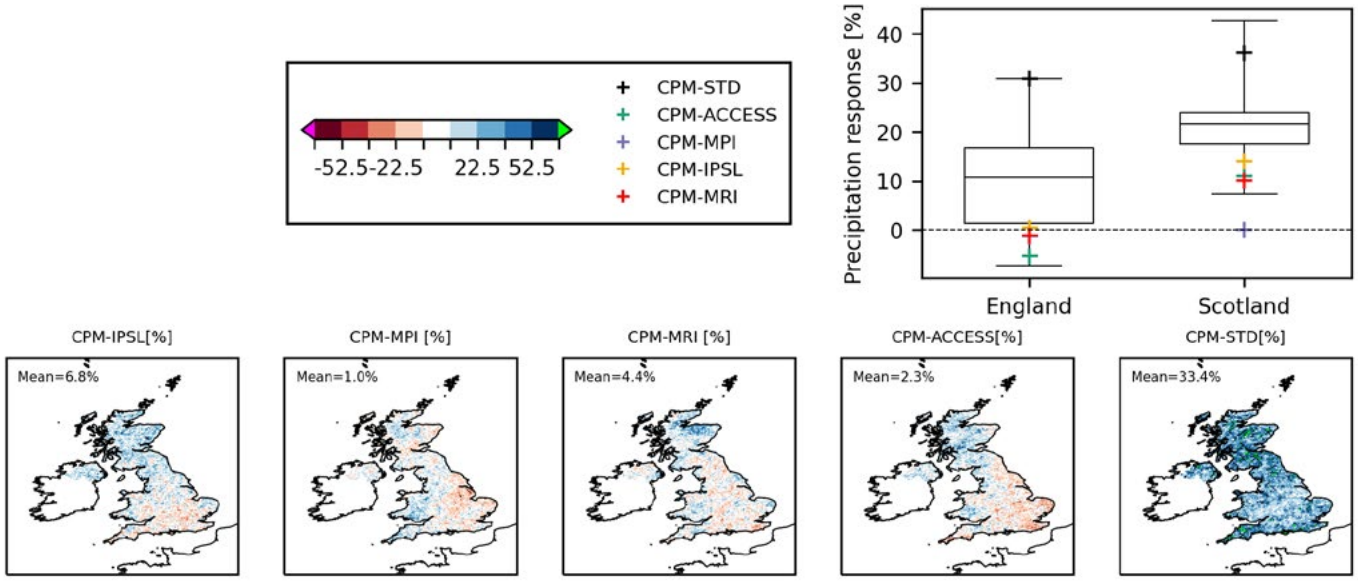

Figure 54. Future changes in heavy hourly precipitation amounts (defined as the 99.95th percentile of the distribution of hourly precipitation, including all values) in summer. The layout of the plots is the same as in Figure 53.

In CPM-PPE there is a larger spread in future changes in heavy hourly precipitation in summer compared to winter, with future decreases over England being possible. Responses tend to be larger over Scotland than England, and this is also the case for all the CMIP5-driven CPMs except CPM-MPI which projects no future change in heavy hourly precipitation across the UK (although it should be remembered that we consider projections for changes in summer precipitation from CPM-MPI to be unreliable due to large biases in the present-day, e.g. Figure 19). As in winter, future changes from the CMIP5-driven CPMs are similar to each other, lying at the lower end of the CPM-PPE distribution and not significantly different from zero. Note that CPM-STD displays an upper-end response, which is significant in the north, and thus is very different from the CMIP5-driven CPMs.

Figure 55 shows future changes in the statistical distribution of hourly precipitation rates in the various CPMs, for each season. In all seasons, there is a general shift in the CMIP5-driven CPM distributions so that moderate-to-heavy hourly rain-rates contribute more to the total rainfall, and low-to-moderate rain-rates less, than in the present-day. This is similar to the behaviour of CPM-PPE members. An exception is CPM-IPSL in spring where there is a decrease in the contribution from moderate rain-rates, an increase from low rain-rates and little change in the contribution from high rain-rates. Note that changes in the shape of the distribution in CPM-MPI and CPM-MRI in this season are small too. In winter, CPM-ACCESS stands out as having a more pronounced intensification of hourly rainfall than the other CMIP5-driven models, consistent with Figure 53. In summer, changes in the distribution of hourly rain-rates in the CMIP5-driven CPMs are notably smaller than in CPM-STD (which lies at the outer edge of the CPM-PPE envelope) consistent with Figure 54. To a lesser extent, this is the case in autumn too.

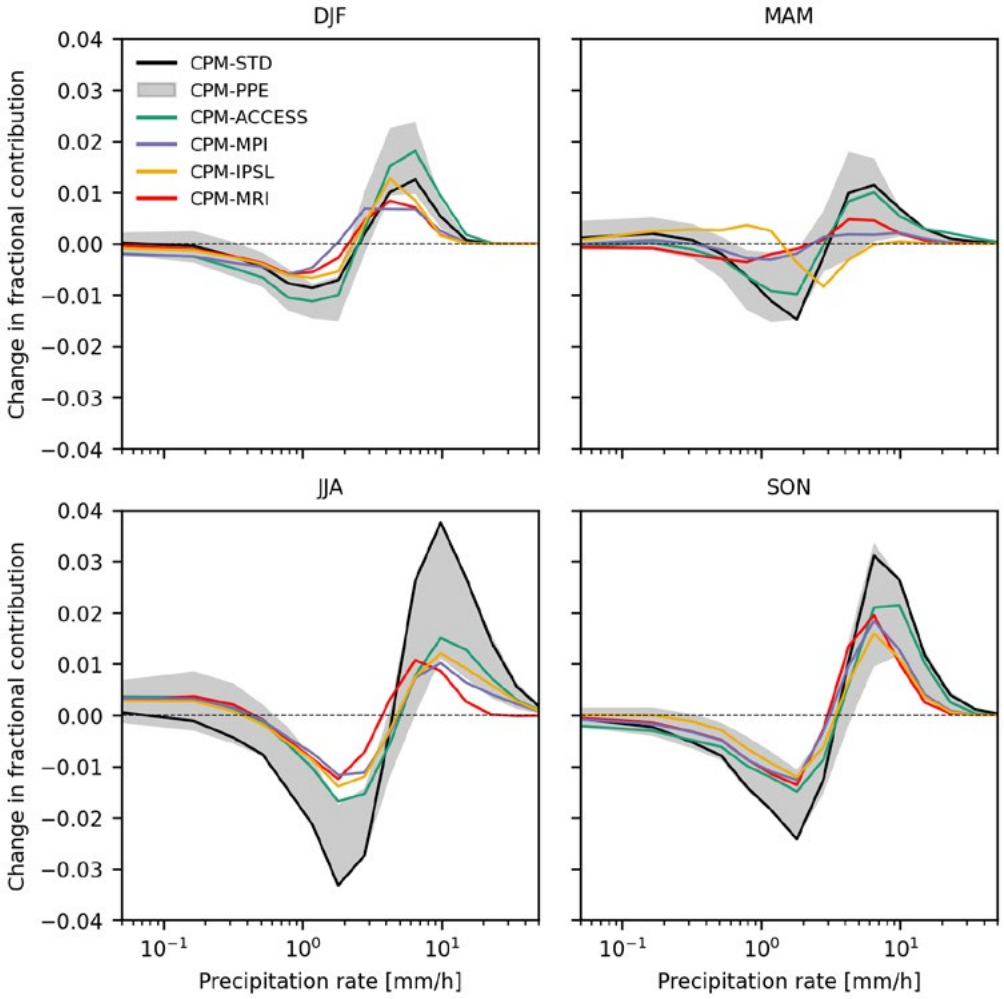

Figure 55. Future changes in the fractional contribution of different hourly precipitation rates to the total precipitation over the UK, defined as differences between a 21-year future period, centred on the year when the global mean surface temperature reaches 3ºC above pre-industrial (see Table 5), and baseline period (1980 – 2000). For each time period, fractional contributions were calculated by assigning precipitation rates for all hours (wet and dry) to bins of 0.0, 0.1, 0.23, 0.41, 0.62, 0.95, 1.4, 2.2, 3.4, 5.1, 7.8, 11.9, 18.1, 27.5, 42.0, 63.9, 97.4, 148.0, 500.0 mm/hr, then multiplying the counts in each bin by the average rain-rate for that bin to give the contribution of each bin to the total rainfall. Results are shown for the CMIP5-driven CPMs and CPM-STD, along with the CPM-PPE range, for each season. All data has been regridded onto the 5km OSGB grid.

5.4 Future changes in extreme events

5.4.1 Extreme hourly precipitation

Future changes in estimates of the 30-year return level of hourly precipitation in the CPMs are displayed in Figures 56 and 57, for winter and summer respectively.

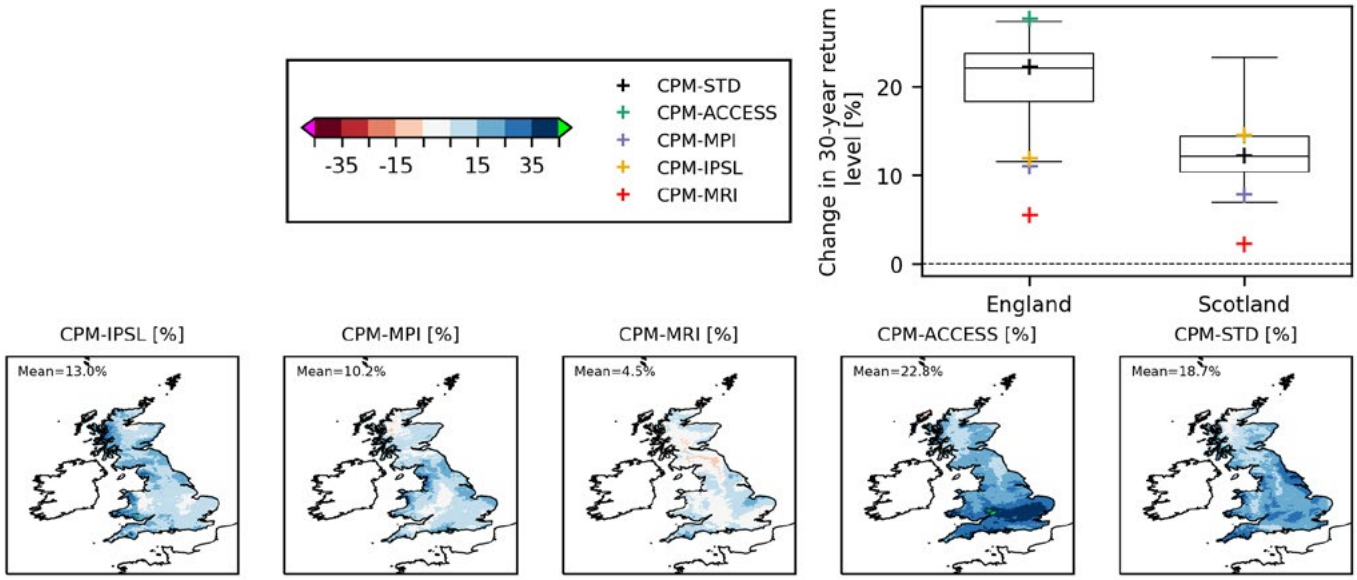

Figure 56. Future changes in 30-year return levels of hourly precipitation in winter, defined as differences between a 21-year future period, centred on the year when the global mean surface temperature reaches 3ºC above pre-industrial (see Table 5), and baseline period (1980 – 2000). The top right panel shows changes in regionally averaged return levels in the various CMIP5-driven CPMs and CPM-STD. The box-and-whiskers indicate the distribution of responses in CPM-PPE: the box extends from the lower to the upper quartiles of the data, with the median shown by the solid horizontal line, and the whiskers show the full range of the data. All data has been regridded onto the 5km OSGB grid before computing return levels. Plots on the second row show spatial maps of changes in 30-year return levels in the CMIP5-driven CPMs and CPM-STD (on the 5km OSGB grid). Whether future changes are significantly different from zero or not has not been assessed. Note that models are ordered from left to right by increasing seasonal mean SST change averaged over a region around the UK (see Figure 10). The UK-mean future change in 30-year return level is indicated in each panel.

In winter, the 30-year return level is projected to increase in the future in all models, with increases generally being larger for England than Scotland. As for heavy hourly precipitation amounts (Figure 53), CPM-ACCESS projects the largest future increases in hourly extremes for England, particularly in the south. By contrast, CPM-MPI and CPM-MRI provide low-end responses, with the latter lying below the lower bound of CPM-PPE and projecting little future change in the 30-year return level of hourly precipitation extremes. However, based on present-day performance, we have low confidence in projections for winter precipitation from the MRI-driven models (e.g. Figure 18).

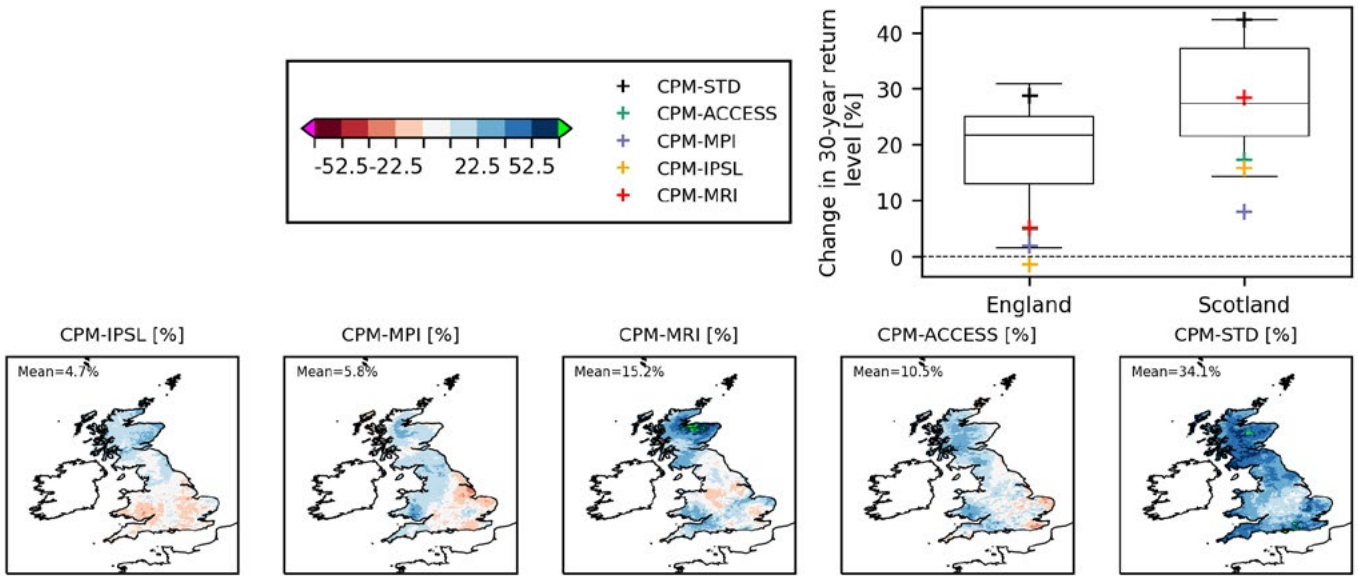

Figure 57. Future changes in 30-year return levels of hourly precipitation in summer. The layout of the plots is the same as in Figure 56.

Future increases in extreme hourly precipitation in summer tend to be larger for Scotland than England, opposite to winter. CPM-IPSL is different from all other models as it projects a small decrease for England, whereas the other CMIP5-driven CPMs project small increases, lying at the lower end of the CPM-PPE distribution. It is likely these responses are not significantly different from zero though. For Scotland, future increases in CPM-MPI are smaller than in any other model, although we have low confidence in projections for summer precipitation from the MPI-driven models because of large biases in the present-day (e.g. Figure 19). The other CMIP5-driven models lie within the CPM-PPE range. Note how CPM-STD is very different to the CMIP5-driven CPMs, projecting much larger increases in the 30-year return level. This is consistent with the behaviour seen for heavy hourly precipitation amounts in summer (Figure 54).

5.4.2 **Future changes in hot and cold spells**

We now examine future changes in hot spells over England and cold/intense cold spells over Scotland (see Section 3.2.4.2 for details of how spells are defined), corresponding to the regions most strongly affected by each type of event in the present-day.

Figure 58 shows CPM projections for how the number of hot spells, averaged over England, could change in the future. All models predict more hot spells (for a range of minimum spell lengths) which is consistent with large-scale warming, although other effects (e.g. land-atmosphere interactions) will exert an additional influence. Responses from the CMIP5-driven CPMs typically lie within the CPM-PPE range, with CPM-MRI and CPM-ACCESS consistently predicting the smallest and largest increases in the number of hot spells, respectively (note that CPM-ACCESS produces more hot spells in the future period than any other CMIP5-driven model). CPM-ACCESS has drier soils than CPM-MRI in present-day summer (Figure 37), with more of a decrease in the future (see Figure 60 below), consistent with the larger decrease of summer mean precipitation in this model (Figure 44). This could explain, at least in part, why there is more of a future increase in summer mean temperature (Figure 42) and in the number of hot spells in CPM-ACCESS compared to CPM-MRI. However, recall that both CPM-MRI and CPM-ACCESS considerably over-estimate the temperature of hot summer days (Figure 21) and the number of hot spells (Figure 35) in the present-day (as do some members of CPM-PPE), so we have lower confidence in projected changes in the number of hot spells from these models.

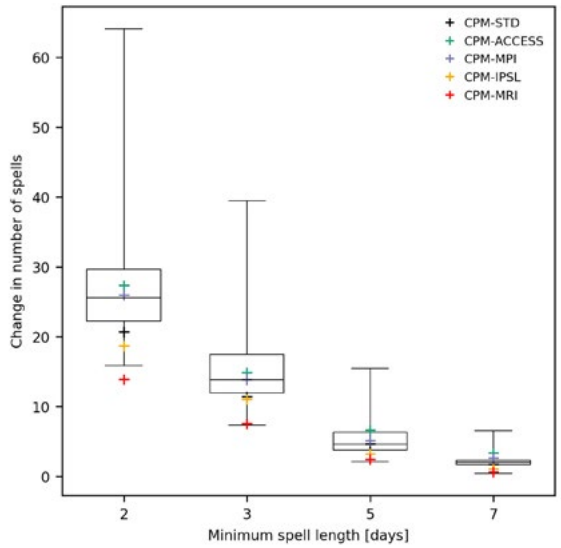

Figure 58. Future changes in the frequency of hot spells over England, defined as differences between a 21-year future period, centred on the year when the global mean surface temperature reaches 3ºC above pre-industrial (see Table 5), and baseline period (1980 – 2000). Results from the CMIP5-driven CPMs and CPM-STD are shown, for a range of different minimum spell lengths. The distribution of responses in CPM-PPE is shown by the box-and-whiskers: the box extends from the lower to the upper quartiles of the data, with the median shown by the solid horizontal line, and the whiskers show the full range of the data. All data has been regridded onto the 5km OSGB grid.

Future changes in the number of cold and intense cold spells over Scotland are shown in Figure 59. As one might expect in a warming climate, both types of event become less frequent in the future in all models. Considering cold spells, the responses of the CMIP5-driven CPMs lie within the range of CPM-PPE. However, for intense cold spells, new outcomes are possible, with CPM-MRI suggesting a greater decrease, and the CPMs driven by ACCESS and MPI a smaller decrease, than any member of CPM-PPE. More of a future decrease in the number of cold and intense cold spells in CPM-MRI than CPM-ACCESS and CPM-MPI is consistent with a greater increase in winter mean temperature (Figure 41) and the temperature of cold winter days (Figure 45) in this model. However, recall that we have lower confidence in projections from CPM-MRI because of large biases in winter mean temperature (Figure 16), the temperature of cold winter days (Figure 20) and the number of cold and intense cold spells (Figure 36) in the present-day (noting that some members of CPM-PPE also have large biases). As a result of these biases, CPM-MRI still has lower winter temperatures, and more cold and intense cold spells, in the future than CPM-ACCESS and CPM-MPI, even with greater warming. This is consistent with CPM-MRI having the most lying snow of any model in the future (see Section 5.4.4 below).

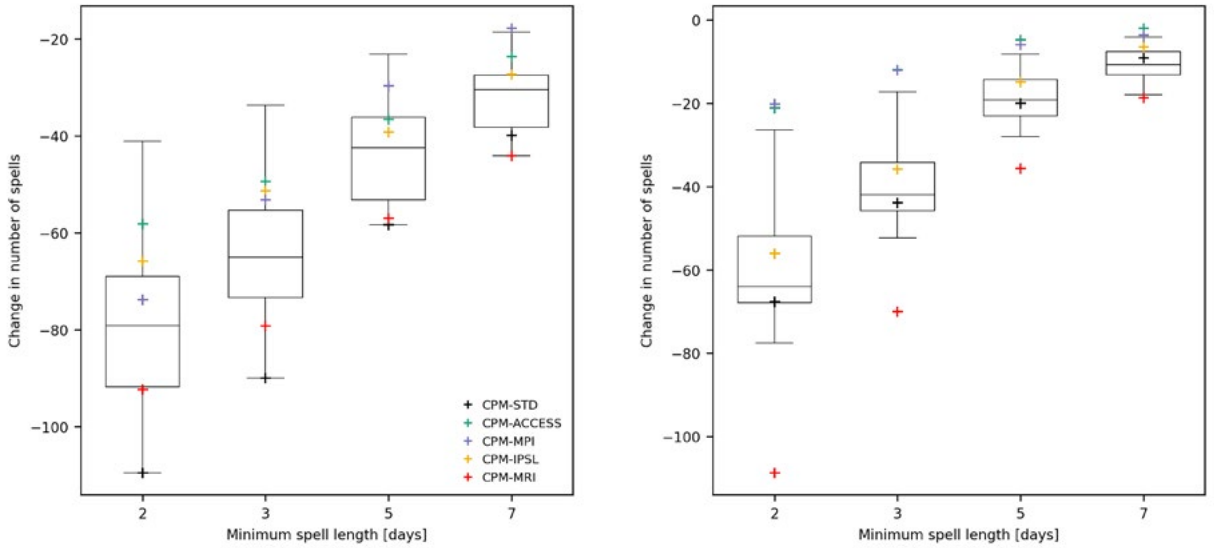

Figure 59. Future changes in the frequency of cold spells (left) and intense cold spells (right) over Scotland. The layout of the plots is the same as in Figure 58.

5.4.3 **Soil moisture**

Future changes in the annual cycle of soil moisture are shown in Figure 60, averaged over England and Scotland, along with the resulting soil moisture in the future period. As in Section 3.2.4.3, only moisture in the top 1m of soil is considered, and only the RCMs and CPMs are compared.

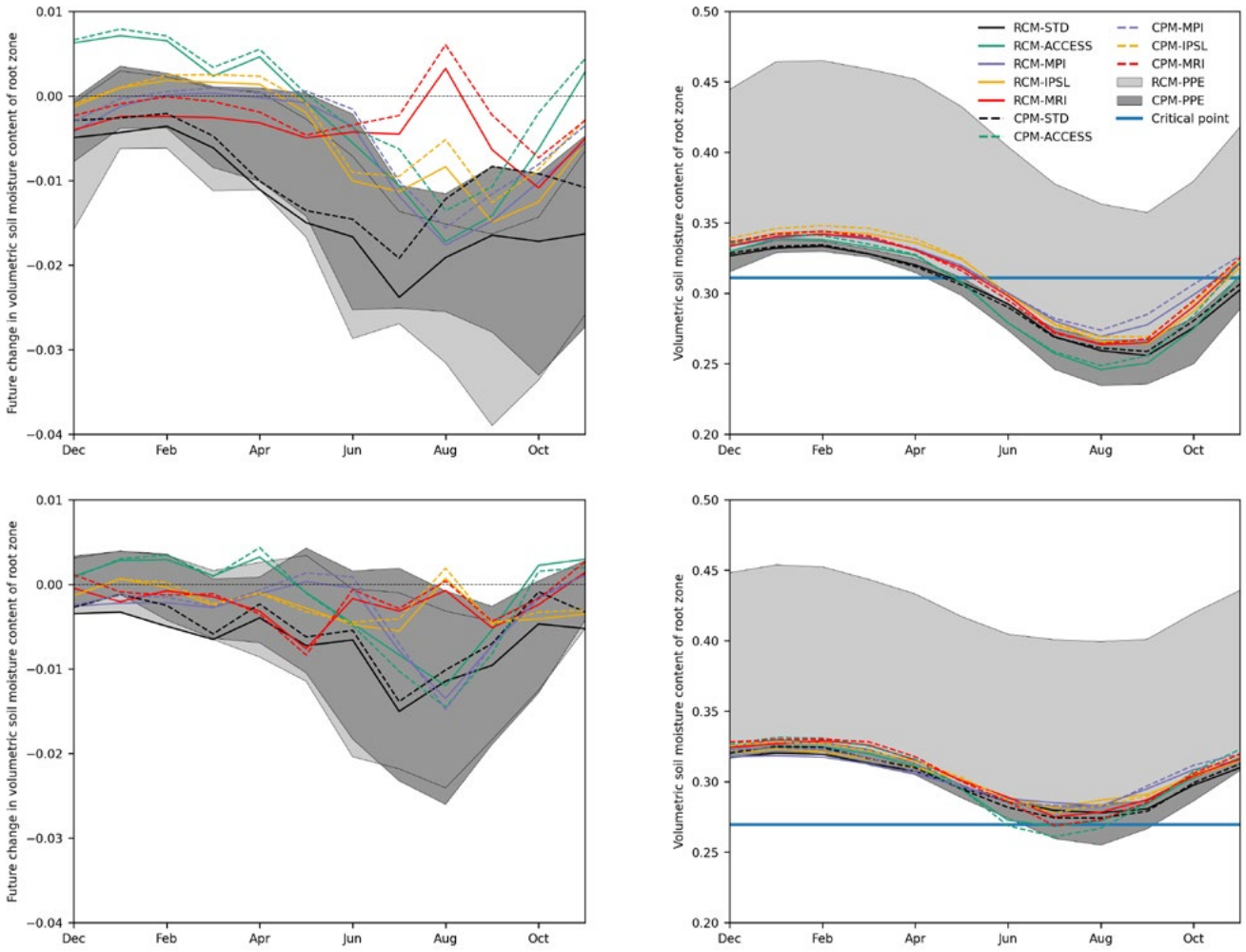

Figure 60. Future changes in the annual cycle of soil moisture (left column) and the annual cycle of soil moisture in the future period (right column), averaged over England (top row) and Scotland (bottom row). Only the top 1m of soil is considered (the root zone). Future changes are defined as differences between a 21-year future period, centred on the year when the global mean surface temperature reaches 3ºC above pre-industrial (see Table 5), and baseline period (1980 – 2000). Results from the RCMs and CPMs are shown, and all CPM data has been regridded onto the 12 km RCM grid before spatial averaging. The horizontal blue line indicates the critical level below which transpiration from vegetation becomes limited by the available soil moisture.

In summer months, the RCMs and CPMs driven by ACCESS, MPI and IPSL all show a future decrease in root-zone soil moisture for England, whereas the regional models driven by MRI show little overall change. The CMIP5-driven models behave similarly for Scotland, except those driven by IPSL which show little future change in soil moisture in this region. These signals are consistent with the projections for changes in summer mean precipitation from these models (Figure 44). Interestingly, RCM-STD and CPM-STD project larger future decreases in soil moisture in summer than any of the CMIP5-driven models, in both England and Scotland, yet display little future change in summer precipitation (Figure 44). Greater evaporative losses associated with larger future increases in summer mean temperature in these models (Figure 42) could be a factor here. Another contributing factor, at least in CPM-STD, could be the more pronounced intensification of short-duration rainfall in the future (Figure 55), which is less effective at wetting the soil (e.g. Berthou et al. 2020, Halladay et al. 2024).

In winter, the regional models driven by ACCESS show an increase in soil moisture across the UK, which is consistent with the projected increases in winter precipitation in this model (Figure 43). Likewise for the IPSL-driven models over England.

In the present-day, evapotranspiration becomes soil-moisture limited in England in summer months in all CMIP5-driven RCMs and CPMs, all members of CPM-PPE, and five members of RCM-PPE (Figure 37). As soils dry out in the future, models tend to enter the moisture-limited regime earlier in the year and move further into this regime in summer. This has the potential to amplify positive soil moisture-precipitation feedback effects, increasing the frequency, intensity and duration of temperature extremes such as hot spells. However, understanding how soil moisture influences the number of hot spells would require a more detailed analysis than possible with simple regional monthly mean data. Note that some models (CPM-ACCESS and three members of CPM-PPE) also move into the moisture-limited regime of evapotranspiration in Scotland in summer in the future (none are in this regime in the present-day).

5.4.4 **Snowfall and lying snow**

In a warming climate, one would expect snowfall and lying snow to decrease. From Figure 61 we see this is indeed the case: all models project less snowfall and snow on the ground in Scotland in the future. The decrease in winter snowfall is larger in the RCMs than the CPMs, consistent with more of a future increase (or less of a decrease) in winter mean precipitation in CPMs (Figure 43). In addition, the fraction of precipitation falling as snow decreases more in the future in the RCMs compared to the CPMs (not shown).

As in the present-day, the regional models driven by MRI produce more snowfall and snow on the ground in the future than any other model. The other CMIP5-driven RCMs and CPMs typically lie within the RCM-PPE and CPM-PPE range, respectively, apart from CPM-IPSL which also has considerably more snow on the ground in Scotland in the future than any member of CPM-PPE (as it did in the present-day; Figure 38). However, if we consider the fraction of Scotland covered by snow in the future, which is also reduced compared to the present-day, then the MRI-driven models are again similar to some of the more extreme members of the UKCP18 regional PPEs, and CPM-IPSL is within the CPM-PPE spread.

The presence of substantial snow on the ground in the future in RCM-MRI and CPM-MRI is potentially the reason why winter temperature projections from these models are comparable to those from their driving GCM (Figure 41). If the snow had all melted (i.e. if we were considering a more extreme global warming level), then we would likely have seen an enhanced warming in the MRI-driven regional models compared to MRI itself, due to a larger reduction of the surface albedo. Such an effect could be operating in summer in the MRI-driven regional models since they both have some snow over Scottish mountains in early summer in the present-day (recall Figure 38), but this has all melted when the global warming level reaches 3ºC above pre-industrial. However, the effect must be small since MRI, RCM-MRI and CPM-MRI all project similar future changes in summer mean temperatures (Figure 42), likely because the fraction of Scotland covered by snow in present-day summer is small, restricted to mountainous regions (Figures 38 and 39).

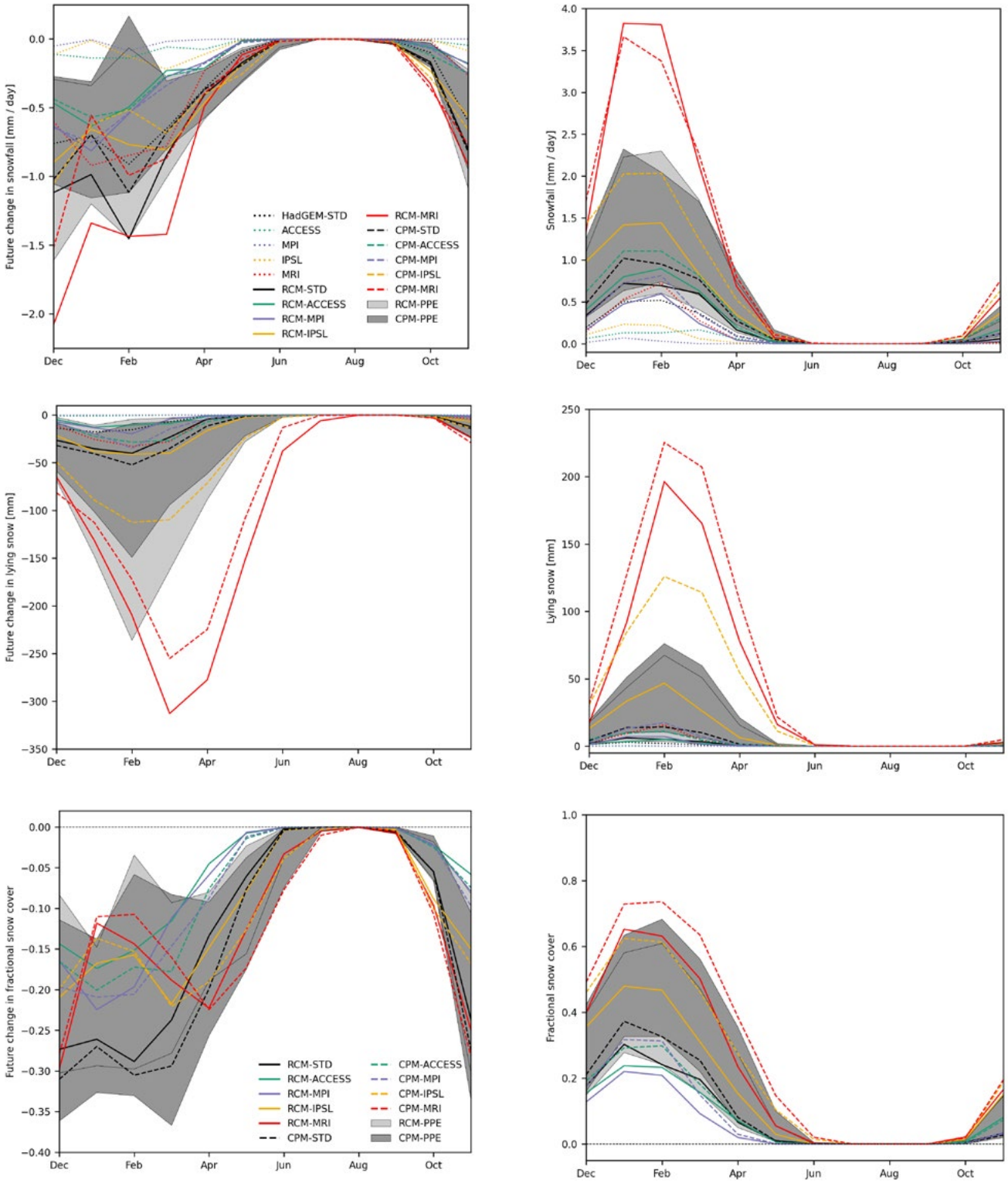

Figure 61. Future changes in the annual cycle of snowfall (top left) and lying snow (centre left), and the annual cycle of snowfall (top right) and lying snow (centre right) in the future period, averaged over Scotland. Results from GCMs, RCMs and CPMs are shown (although note that the lying snow diagnostic is not available from IPSL) and all data has been regridded onto a common n96 grid (with spacings of 1.875° and 1.25° in the longitudinal and latitudinal directions, respectively) before spatial averaging. Note that a snow density of 250 kg/m^3 has been assumed to convert the units of lying snow to mm. The bottom left panel shows future changes in the annual cycle of the fraction of Scotland covered by snow, and the bottom right panel shows the annual cycle of the fraction of Scotland covered by snow in the future period. The fractional coverage has been computed by applying a threshold of 0.02 mm to decide whether grid boxes are snow covered or not on each day, where all CPM data was first regridded onto the 12 km RCM grid. Only results from the RCMs and CPMs are shown since the required daily data is not available from the CMIP5-4 GCMs. Future changes are defined as differences between a 21-year future period, centred on the year when the global mean surface temperature reaches 3ºC above pre-industrial (see Table 5), and baseline period (1980 – 2000).

6 Summary of future changes

Model projections for a wide range of metrics related to temperature and precipitation have been presented in the preceding section. To condense all this information, we now construct a summary scorecard, similar to that in Section 4. The main aim is to help easily identify any situations where down-scaling the CMIP5-4 GCMs has broadened the range of future outcomes available from UKCP18, and whether these are to be considered plausible or not, based on present-day model performance (Section 3).

Given a CMIP5-driven model response, R, for a particular metric, we compare it with the range of responses from the corresponding PPE, and classify it using the following colour-coding system:

- Blue. The response lies below the minimum response in the PPE, $R < R_{min}$, and is thus a new future outcome.
- Grey. The response lies within the PPE range.
- Purple. The response lies above the maximum response in the PPE, $R > R_{max}$, and is thus a new future outcome.

In cases where a CMIP5-driven regional model has a warning flag for a present-day bias in a particular metric (Figure 40), we outline the response on the scorecard using the same colour as the warning flag, which gives an indication of its plausibility. If the outline is yellow or orange, caution is to be exercised when using projections from this model for this metric, and if the outline is red, projections from this model for this metric are to be considered unreliable.

Stippling is added to the scorecard to highlight situations where a regional model response is largely inherited from the driving global model. This is judged using a condition similar to Eq. 1 but with biases, B, replaced by responses, R. Note that a CPM response can only be stippled if the response of its parent RCM was also stippled, because we are aiming to trace the origin of the response back to the source GCM. The stippling is for information only; a large difference between the response of a nested model and its driving model is not necessarily a cause for concern, if there is a well-understood physical mechanism driving it (a good example is the larger future increase in winter precipitation in CPM-PPE compared to RCM-PPE, attributed to the improved representation of convection in the CPM, specifically its ability to advect winter showers inland from over the sea, Kendon et al. 2020).

Figure 62 shows the scorecard for future changes projected by the CMIP5-driven RCMs and CPMs. As before, only metrics on daily timescales and longer are included so that we have information from all GCMs, RCMs and CPMs available. The main points to note are as follows.

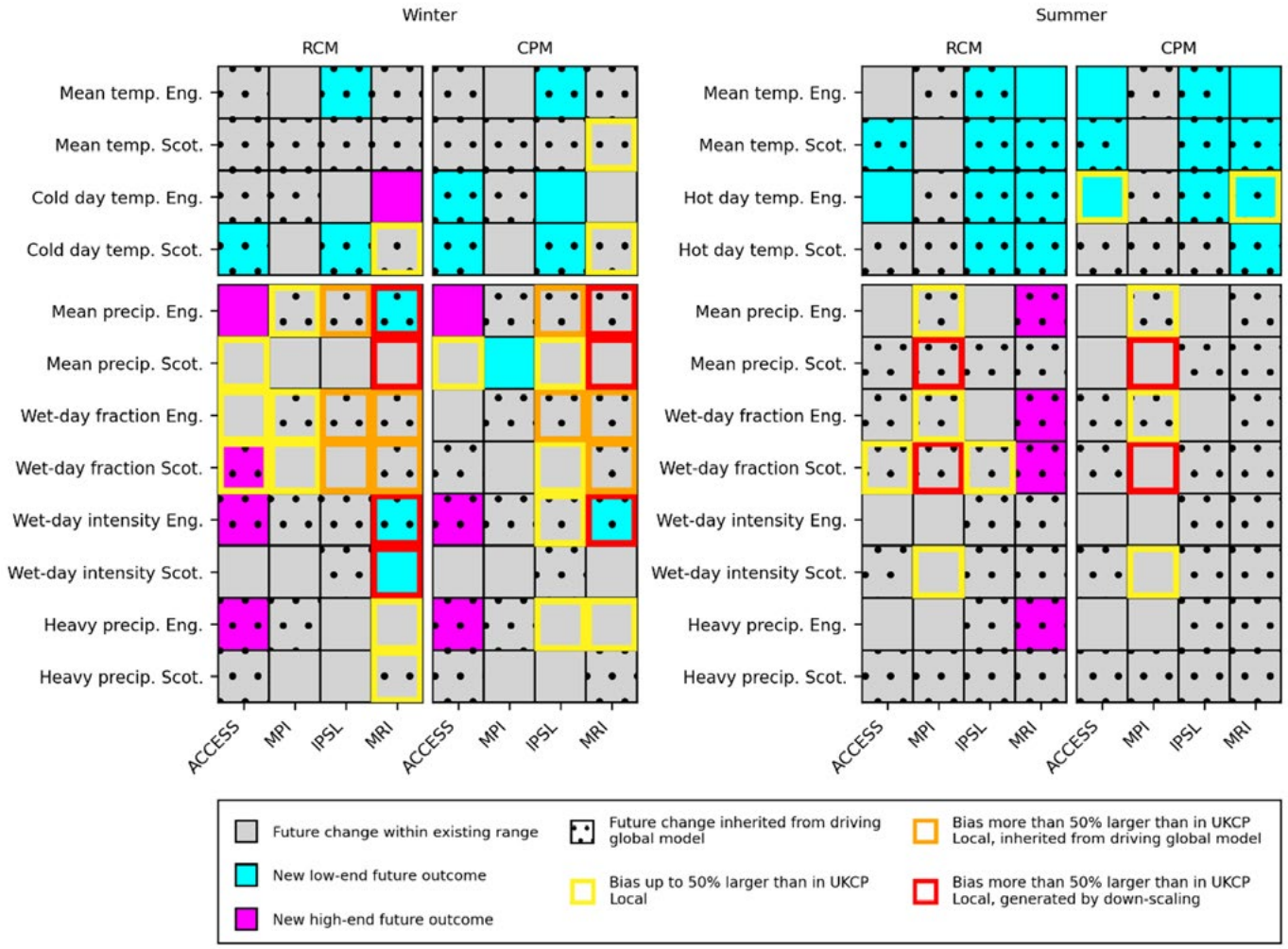

Figure 62. Summary of future changes in regionally averaged temperature and precipitation metrics (on daily timescales and longer) from the CMIP5-driven regional models, for winter (left panels) and summer (right panels). Future changes are defined as differences between a 21-year future period, centred on the year when the global mean surface temperature reaches 3°C above pre-industrial (see Table 5), and baseline period (1980 – 2000). All model data has been regridded onto a common n96 grid with spacings of 1.875° and 1.25° in the longitudinal and latitudinal directions, respectively, and spatial averaging of metrics was performed before computing future changes. The meaning of the various colours is briefly described in the legend; see the text for full details.

Winter

- The regional models driven by ACCESS, MPI and IPSL generally project smaller future increases in winter mean temperature (Figure 41) and the temperature of cold winter days (Figure 45) than most members of the regional PPEs. Responses from the regional models driven by ACCESS and IPSL (especially the CPMs) can be smaller than any in RCM-PPE or CPM-PPE (blue flags), largely inherited from their driving GCMs. There is nothing in the present-day performance of these models that would lead us to doubt the plausibility of these projections. Future increases in the temperature of cold winter days in the MRI-driven regional models lie at the upper end of the PPE distributions, but it should be remembered that we have less confidence in winter temperature projections from these models over Scotland due to large cold biases in the present-day (Figure 20) and too many cold spells (Figure 36), consistent with excessive snow on the ground (Figure 38).
- Future increases in winter mean precipitation over England are larger in RCM-ACCESS and CPM-ACCESS than any member of RCM-PPE and CPM-PPE (purple flags), respectively, particularly in the

south (Figure 43). The dominant contribution to this signal comes from future increases in precipitation intensity (Figures 48 and 49), rather than increases in wet-day frequency (Figure 47). This new future outcome is potentially high impact and, based on the present-day performance of the ACCESS-driven models (Figure 40), we have no reason to doubt its plausibility. Note that CPM-ACCESS also projects a greater future intensification of heavy hourly precipitation (99.95th percentile; Figure 53) and precipitation extremes (30-year return level; Figure 56) over England than any member of CPM-PPE.

- RCM-MPI and CPM-MPI project future decreases in winter mean precipitation over Scotland (Figure 43), which is driven by future decreases in wet day fraction (Figure 47) since there is little change in wet-day intensity (Figure 48). Winter mean precipitation responses from the MPI-driven models lie at the lower end of the respective RCM-PPE and CPM-PPE distributions (blue flag for CPM-MPI), both of which favour a future increase in winter precipitation over Scotland. Based on present-day performance (Figure 40), we believe the MPI-driven regional models offer plausible low-end future outcomes for Scotland.
- RCM-IPSL and CPM-IPSL also provide low-end outcomes for Scotland, with little future change in winter mean precipitation (Figure 43), the result of an increase in wet-day intensity (Figure 48) being balanced by a decrease in wet-day fraction (Figure 47). However, recall that RCM-IPSL and CPM-IPSL have orange/yellow warning flags for wet-day frequency (Figure 40), with biases largely inherited from the IPSL GCM (Figure 22). Therefore, we have lower confidence in the projected change in winter precipitation from the IPSL-driven regional models.
- Projections for metrics related to winter precipitation from the MRI-driven regional models are not considered reliable due to red flags for biases in the present-day (Figure 40).

Summer

- The regional models driven by IPSL and MRI project notably less of a future increase in summer mean temperature across the UK than any members of the regional PPEs (blue flags). The models driven by ACCESS and MPI also offer low-end outcomes for UK summer mean temperatures, with responses lying close to the lower bound of the PPE ranges. The responses of the CMIP5-driven models largely follow their driving GCMs (Figure 42). Future changes in the temperature of hot summer days are more mixed. Again, the models driven by IPSL and MRI project smaller future increases than any member of the PPEs (blue flags), as do RCM-ACCESS and CPM-ACCESS over England (Figure 46). We consider these projections to be equally as plausible as those from the existing regional PPEs, although it should be noted that both CPM-MRI and CPM-ACCESS have large biases in the 99th percentile of daily temperatures over England in the present-day (Figure 21), and considerably over-estimate the frequency of hot spells (Figure 35).
- RCM-MRI and CPM-MRI exhibit little future change in summer mean precipitation across the UK, following MRI GCM, whereas most PPE members favour a substantial decrease (Figure 44). The responses of RCM-MRI and CPM-MRI either lie in the upper quartile of the distribution of responses from the corresponding PPEs, or above the ensemble maxima (purple flag for RCM-MRI over England). The main reason for this is that MRI and its nested regional models show little future change in wet-day frequency in summer, whereas there is typically a decrease in the various PPEs (Figure 50). Similarly, the regional models driven by IPSL also suggest little future change in summer mean precipitation, following the IPSL GCM itself, but for Scotland only (Figure 44). Based on present-day performance (Figure 40),

there is no reason to doubt the plausibility of projections for summer precipitation from the regional models driven by MRI and IPSL.

- Projections for metrics related to summer precipitation from the MPI-driven regional models are not considered reliable due to red flags for biases in the present-day (Figure 40).

In summary, by down-scaling alternative GCMs from CMIP5 we have been able to sample new future outcomes for the UK with the RCM and CPM. In summer, the regional models driven by IPSL and MRI project less of a future increase in temperature than any member of the existing UKCP18 regional ensembles. The MRI-driven models also project little future change in summer precipitation – as do the IPSL-driven models over Scotland - whereas the existing UKCP18 PPEs favour a future decrease. Sampling a wider range of potential outcomes for summer was a key motivation for this work. In winter, future increases in precipitation over England are larger in RCM-ACCESS and CPM-ACCESS than in any member of RCM-PPE and CPM-PPE, respectively, which would have implications for increased flooding. At the other end of the scale, RCM-MPI and CPM-MPI project a decrease in winter precipitation over Scotland whereas most PPE members project future increases. Finally, future increases in temperature in winter in the models driven by ACCESS, MPI and IPSL are smaller than in most PPE members. Based on our assessment of present-day biases, we believe these are all plausible future outcomes.

As a final comment, we have demonstrated that down-scaling other GCMs works well for the UK, in the sense that future changes in the nested regional models largely follow their driving global model. The location of the UK is likely to be a key factor here: the jet stream influences the formation and movement of low-pressure systems affecting the UK, which enter through the western boundary of the RCM domain and travel eastwards towards the UK over open ocean. For more complex European regions (e.g. the Mediterranean area), there may be less consistency between the projections of the regional models and their driving global models. This needs further investigation, but users of the new CMIP5-driven UKCP Regional projections for regions other than the UK should bear this in mind.

Acknowledgments

We thank Dr Geert Lenderink and Dr Erasmo Buonomo for reviewing this report and providing valuable comments that helped to improve it. This UKCP18 project is part of the Hadley Centre Climate Programme which is funded by the Department for Science, Innovation and Technology (DSIT) as well as through the UKCP Climate Service which is funded by the Department for Environment, Food and Rural Affairs (Defra).

References

Andrews, T., Andrews, M. B., Bodas-Salcedo, A., Jones, G. S., Kuhlbrodt, T., Manners, J., et al. (2019). Forcings, feedbacks, and climate sensitivity in HadGEM3-GC3.1 and UKESM1. Journal of Advances in Modeling Earth Systems, 11, 4377–4394. https://doi.org/10.1029/2019MS001866

Ansell, T. J., and Coauthors, 2006: Daily Mean Sea Level Pressure Reconstructions for the European–North Atlantic Region for the Period 1850–2003. J. Climate, 19, 2717–2742, https://doi.org/10.1175/JCLI3775.1

Antic, S., Laprise, R., Denis, B. et al. Testing the downscaling ability of a one-way nested regional climate model in regions of complex topography. Clim Dyn 26, 305–325 (2006). https://doi.org/10.1007/s00382-005-0046-z

Ban, N., Caillaud, C., Coppola, E. et al. The first multi-model ensemble of regional climate simulations at kilometer-scale resolution, part I: evaluation of precipitation. Clim Dyn 57, 275–302 (2021). https://doi.org/10.1007/s00382-021-05708-w

Barnes, C.R., R.E. Chandler and C.M. Brierley: Comparison of EuroCORDEX output with UKCP18 regional ensemble. Technical report, UK Climate Resilience Programme project CR20-3 Enabling the use and producing improved understanding of EuroCORDEX data over the UK, January 2022 (revised July 2022), https://www.ucl.ac.uk/statistics/sites/statistics/files/evaluation_of_ukcordex_vs_ukcp18_v2.pdf

Berthou, S., Kendon, E.J., Chan, S.C. et al. Pan-European climate at convection-permitting scale: a model intercomparison study. Clim Dyn 55, 35–59 (2020). https://doi.org/10.1007/s00382-018-4114-6

Best, M. J., Pryor, M., Clark, D. B., Rooney, G. G., Essery, R. L. H., Ménard, C. B., Edwards, J. M., Hendry, M. A., Porson, A., Gedney, N., Mercado, L. M., Sitch, S., Blyth, E., Boucher, O., Cox, P. M., Grimmond, C. S. B., and Harding, R. J.: The Joint UK Land Environment Simulator (JULES), model description – Part 1: Energy and water fluxes, Geosci. Model Dev., 4, 677–699, https://doi.org/10.5194/gmd-4-677-2011, 2011

Caillaud, C., Somot, S., Alias, A. et al. Modelling Mediterranean heavy precipitation events at climate scale: an object-oriented evaluation of the CNRM-AROME convection-permitting regional climate model. Clim Dyn 56, 1717–1752 (2021). https://doi.org/10.1007/s00382-020-05558-y

Chan, S. C., E. J. Kendon, H. J. Fowler, S. Blenkinsop, N. M. Roberts, and C. A. T. Ferro, 2014: The Value of High-Resolution Met Office Regional Climate Models in the Simulation of Multihourly Precipitation Extremes. J. Climate, 27, 6155–6174, https://doi.org/10.1175/JCLI-D-13-00723.1

Coppola, E, S. Sobolowski, E. Pichelli, F. Raffaele, B. Ahrens, I. Anders, N. Ban, S. Bastin, M. Belda, D. Belusic, A. Caldas Alvarez, R. M. Cardoso, S. Davolio, A. Dobler, J. Fernandez, L. Fita, Q. Fumiere, F. Giorgi, K. Goergen, I. Güttler, T. Halenka, D. Heinzeller, Ø. Hodnebrog, D. Jacob, S. Kartsios, E. Katragkou, E. Kendon, S. Khodayar, H. Kunstmann, S. Knist, A. Lavín Gullón, P. Lind, T. Lorenz, D. Maraun, L. Marelle, E. van Meijgaard, J. Milovac, G. Myhre, H. J. Panitz, M. Piazza, M. Raffa, T. Raub, B. Rockel, C. Schär, K. Sieck, P. M. M. Soares, S. Somot, L. Srnec, P. Stocchi, M. H. Tölle, H. Truhetz, R. Vautard, H. de Vries, K. Warrach Sagi (2018) A first-of-its-kind multi-model convection permitting ensemble for investigating convective phenomena over Europe and the Mediterranean. Climate Dynamics. doi: https://doi.org/10.1007/s00382-018-4521-8

Dawson, A., T. N. Palmer, and S. Corti (2012), Simulating regime structures in weather and climate prediction models, Geophys. Res. Lett., 39, L21805, doi:10.1029/2012GL053284

Fabiano, F., Christensen, H.M., Strommen, K. et al. Euro-Atlantic weather Regimes in the PRIMAVERA coupled climate simulations: impact of resolution and mean state biases on model performance. Clim Dyn 54, 5031–5048 (2020). https://doi.org/10.1007/s00382-020-05271-w

Fabiano, F., Meccia, V. L., Davini, P., Ghinassi, P., and Corti, S.: A regime view of future atmospheric circulation changes in northern mid-latitudes, Weather Clim. Dynam., 2, 163–180, https://doi.org/10.5194/wcd-2-163-2021, 2021

Fereday, D., & Knight, J. (2023). The roles of atmospheric circulation and sea surface temperature in UK surface climate. Atmospheric Science Letters, 24(3), e1139. https://doi.org/10.1002/asl.1139

Fiedler, S., Stevens, B., Gidden, M., Smith, S. J., Riahi, K., and van Vuuren, D.: First forcing estimates from the future CMIP6 scenarios of anthropogenic aerosol optical properties and an associated Twomey effect, Geosci. Model Dev., 12, 989–1007, https://doi.org/10.5194/gmd-12-989-2019, 2019

Fung, F (2018). How to Bias Correct, UKCP18 Guidance, Met Office, https://www.metoffice.gov.uk/binaries/content/assets/metofficegovuk/pdf/research/ukcp/ukcp18-guidance---how-to-bias-correct.pdf

Halladay, K., Berthou, S. & Kendon, E. Improving land surface feedbacks to the atmosphere in convection-permitting climate simulations for Europe. Clim Dyn 62, 6079–6096 (2024). https://doi.org/10.1007/s00382-024-07192-4

Hanlon, H.M., Bernie, D., Carigi, G. et al. Future changes to high impact weather in the UK. Climatic Change 166, 50 (2021). https://doi.org/10.1007/s10584-021-03100-5

Harrison D.L., S. J. Driscoll and M. Kitchen (2000) Improving precipitation estimates from weather radar using quality control and correction techniques, Meteorol. Appl. 6, 135–144, doi: 10.1017/S1350482700001468

Hersbach H, Bell B, Berrisford P, et al. The ERA5 global reanalysis. Q J R Meteorol Soc. 2020; 146: 1999–2049. https://doi.org/10.1002/qj.3803

Hewitt C.D. and J.A. Lowe (2018) Toward a European Climate Prediction System, BAMS, doi: 10.1175/BAMS-D-18-0022.1

Jacob, D., J. Petersen, B. Eggert, A. Alias, O. B. Christensen, L. M. Bouwer, A. Braun, A. Colette, M. Déqué, G. Georgievski, E. Georgopoulou, A. Gobiet, L. Menut, G. Nikulin, A. Haensler, N. Hempelmann, C. Jones, K. Keuler, S. Kovats, N. Kröner, S. Kotlarski, A. Kriegsmann, E. Martin, E. van Meijgaard, C. Moseley, S. Pfeifer, S. Preuschmann, C. Radermacher, K. Radtke, D. Rechid, M. Rounsevell, P. Samuelsson, S. Somot, J-F. Soussana, C. Teichmann, R. Valentini, R. Vautard, B. Weber and P. Yiou (2014) EURO-CORDEX: new high-resolution climate change projections for European impact research, Regional Environmental Change, 14, 2, 563-578, https://doi.org/10.1007/s10113-013-0499-2

Jones, R.G., Murphy, J.M. and Noguer, M. (1995), Simulation of climate change over Europe using a nested regional-climate model. I: Assessment of control climate, including sensitivity to location of lateral boundaries. Q.J.R. Meteorol. Soc., 121: 1413-1449. https://doi.org/10.1002/qj.49712152610

Jury, M.W., Herrera, S., Gutiérrez, J.M. et al. Blocking representation in the ERA-Interim driven EURO-CORDEX RCMs. Clim Dyn 52, 3291–3306 (2019). https://doi.org/10.1007/s00382-018-4335-8

Kendon, E. J., and Coauthors, 2017: Do Convection-Permitting Regional Climate Models Improve Projections of Future Precipitation Change?. Bull. Amer. Meteor. Soc., 98, 79–93, https://doi.org/10.1175/BAMS-D-15-0004.1

Kendon, E. J., et al (2019) UKCP Convection-permitting model projections: Science Report, Met Office Hadley Centre, Exeter, September 2019, https://www.metoffice.gov.uk/pub/data/weather/uk/ukcp18/science-reports/UKCP-Convection-permitting-model-projections-report.pdf

Kendon, E. J., et al (2020) Greater future UK winter precipitation increase in new convection-permitting scenarios. J Climate. DOI: 10.1175/JCLI-D-20-0089.1

Kendon, E.J. et al (2021) Update to UKCP Local (2.2km) projections, Met Office Hadley Centre, Exeter, July 2021, https://www.metoffice.gov.uk/pub/data/weather/uk/ukcp18/science-reports/ukcp18_local_update_report_2021.pdf

Kendon, E.J., E.M. Fischer and C.J. Short (2023a) Variability conceals emerging trend in 100yr projections of UK local hourly rainfall extremes, Nature Comms, doi: 10.1038/s41467-023-36499-9

Kendon, E.J. et al (2023b) UKCP Local (2.2km) transient projections, Met Office Hadley Centre, Exeter, March 2023, https://www.metoffice.gov.uk/binaries/content/assets/metofficegovuk/pdf/research/ukcp/ukcp_local_report_2023.pdf

Leduc, M., Laprise, R. Regional climate model sensitivity to domain size. Clim Dyn 32, 833–854 (2009). https://doi.org/10.1007/s00382-008-0400-z

Lewis, E., N. Quinn, S. Blenkinsop, H. J. Fowler, J. Freer, M. Tanguy, O. Hitt, G. Coxon, P. Bates, R. Woods (2018) A rule based quality control method for hourly rainfall data and a 1 km resolution gridded hourly rainfall dataset for Great Britain: CEH-GEAR1hr, Journal of Hydrology, 564, 930–943

Matte, D., Laprise, R., Thériault, J.M. et al. Spatial spin-up of fine scales in a regional climate model simulation driven by low-resolution boundary conditions. Clim Dyn 49, 563–574 (2017). https://doi.org/10.1007/s00382-016-3358-2

McSweeney CF, Murphy J, Sexton D, Rostron J, Yamazaki K, Harris G (2018). Selection of CMIP5 members to augment a perturbed–parameter ensemble of global realisations of 21st century climate for the UKCP18 scenarios. Hadley Centre Technical Note No. 102, Met Office, Exeter, UK, https://digital.nmla.metoffice.gov.uk/IO_28f93601-3178-4c48-8621-fb4388ec66a1

Morice, C. P., J. J. Kennedy, N. A. Rayner, and P. D. Jones (2012), Quantifying uncertainties in global and regional temperature change using an ensemble of observational estimates: The HadCRUT4 data set, J. Geophys. Res., 117, D08101, doi:10.1029/2011JD017187

Moss, R., Edmonds, J., Hibbard, K. et al. The next generation of scenarios for climate change research and assessment. Nature 463, 747–756 (2010). https://doi.org/10.1038/nature08823

Murphy, J.M., et al (2018) UKCP18 Land Projections: Science Report, Met Office Hadley Centre, Exeter, November 2018 (revised March 2019), https://www.metoffice.gov.uk/pub/data/weather/uk/ukcp18/science-reports/UKCP18-Land-report.pdf

Neal, R., Fereday, D., Crocker, R. and Comer, R.E. (2016), A flexible approach to defining weather patterns and their application in weather forecasting over Europe. Met. Apps, 23: 389-400. https://doi.org/10.1002/met.1563

Perkins, S. E., A. J. Pitman, N. J. Holbrook, and J. McAneney, 2007: Evaluation of the AR4 Climate Models' Simulated Daily Maximum Temperature, Minimum Temperature, and Precipitation over Australia Using Probability Density Functions. J. Climate, 20, 4356–4376, https://doi.org/10.1175/JCLI4253.1

Perry, M.C., Hollis, D.M., and Elms, M.I. (2009) The generation of daily gridded data sets of temperature and rainfall for the UK, NCIC Climate Memorandum No. 24. Met Office: Exeter, UK

Pope, J.O., Brown, K., Fung, F. et al. Investigation of future climate change over the British Isles using weather patterns. Clim Dyn 58, 2405–2419 (2022). https://doi.org/10.1007/s00382-021-06031-0

Rayner, N. A., D. E. Parker, E. B. Horton, C. K. Folland, L. V. Alexander, D. P. Rowell, E. C. Kent, and A. Kaplan (2003), Global analyses of sea surface temperature, sea ice, and night marine air temperature since the late nineteenth century, J. Geophys. Res., 108, 4407, doi:10.1029/2002JD002670, D14

Reynolds, R. W., N. A. Rayner, T. M. Smith, D. C. Stokes, and W. Wang, 2002: An Improved In Situ and Satellite SST Analysis for Climate. J. Climate, 15, 1609–1625, https://doi.org/10.1175/1520-0442(2002)015<1609:AIISAS>2.0.CO;2

Sanchez-Gomez, E., Somot, S. & Déqué, M. Ability of an ensemble of regional climate models to reproduce weather regimes over Europe-Atlantic during the period 1961–2000. Clim Dyn 33, 723–736 (2009). https://doi.org/10.1007/s00382-008-0502-7

Schlund, M., Lauer, A., Gentine, P., Sherwood, S. C., and Eyring, V.: Emergent constraints on equilibrium climate sensitivity in CMIP5: do they hold for CMIP6?, Earth Syst. Dynam., 11, 1233–1258, https://doi.org/10.5194/esd-11-1233-2020, 2020.

Shooter R and Brown SJ, 2024. High-resolution estimation of daily precipitation extremes in the United Kingdom using a generalised additive model framework. In review.

Stevens B, Fiedler S, Kinne S, Peters K, Rast S, Müsse J, Smith SJ, Mauritsen T (2017) MACv2-SP: a parameterization of anthropogenic aerosol optical properties and an associated Twomey effect for use in CMIP6. Geosci Model Dev 10(1):433–452. https://doi.org/10.5194/gmd-10-433-2017

Taylor, K. E., R. J. Stouffer, and G. A. Meehl, 2012: An Overview of CMIP5 and the Experiment Design. Bull. Amer. Meteor. Soc., 93, 485–498, https://doi.org/10.1175/BAMS-D-11-00094.1

Vanden Broucke, S., Wouters, H., Demuzere, M. et al. The influence of convection-permitting regional climate modeling on future projections of extreme precipitation: dependency on topography and timescale. Clim Dyn 52, 5303–5324 (2019). https://doi.org/10.1007/s00382-018-4454-2

Voigt, A., Stevens, B., Bony, S., and Boucher, O.: Easy Aerosol – a modeling framework to study robustness and sources of uncertainties in aerosol-induced changes of the large-scale atmospheric circulation, WCRP, available at: https://www.wcrp-climate.org/images/grand_challenges/clouds/documents/easyaerosol_projectdescription_expprotocol.pdf, 2014

Weedon, G. P., G. Balsamo, N. Bellouin, S. Gomes, M. J. Best, P. Viterbo (2014) The WFDEI meteorological forcing data set: WATCH Forcing Data methodology applied to ERA-Interim reanalysis data, Water Resources Research, doi: 10.1002/2014WR015638

Yamazaki, K., Sexton, D.M.H., Rostron, J.W. et al. A perturbed parameter ensemble of HadGEM3-GC3.05 coupled model projections: part 2: global performance and future changes. Clim Dyn 56, 3437–3471 (2021). https://doi.org/10.1007/s00382-020-05608-5

Youngman, B.D., 2018. Generalized additive models for exceedances of high thresholds with an application to return level estimation for US wind gusts. J. Am. Stat. Assoc. https://doi.org/10.1080/01621459.2018.1529596.